Theses and Dissertations   1. Thesis and Dissertation Collection, all items

2019-12

MODELING A MEGACITY CHALLENGE TO DOCTRINE: HOW SENSORS IN URBAN MUNICIPAL INFRASTRUCTURE INFLUENCE FUTURE FIGHTS

Smith, Shane K.

Monterey, CA; Naval Postgraduate School

https://hdl.handle.net/10945/64071

NAVAL POSTGRADUATE SCHOOL

MONTEREY, CALIFORNIA

THESIS

MODELING A MEGACITY CHALLENGE TO DOCTRINE: HOW SENSORS IN URBAN MUNICIPAL INFRASTRUCTURE INFLUENCE FUTURE FIGHTS

by

Shane K. Smith

December 2019

Thesis Advisor: Hong Zhou
Second Reader: Carlos F. Borges

Approved for public release. Distribution is unlimited.

THIS PAGE INTENTIONALLY LEFT BLANK

REPORT DOCUMENTATION PAGE		*Form Approved OMB No. 0704-0188*

Public reporting burden for this collection of information is estimated to average 1 hour per response, including the time for reviewing instruction, searching existing data sources, gathering and maintaining the data needed, and completing and reviewing the collection of information. Send comments regarding this burden estimate or any other aspect of this collection of information, including suggestions for reducing this burden, to Washington headquarters Services, Directorate for Information Operations and Reports, 1215 Jefferson Davis Highway, Suite 1204, Arlington, VA 22202-4302, and to the Office of Management and Budget, Paperwork Reduction Project (0704-0188) Washington, DC 20503.

1. AGENCY USE ONLY *(Leave blank)*	2. REPORT DATE December 2019	3. REPORT TYPE AND DATES COVERED Master's thesis	
4. TITLE AND SUBTITLE MODELING A MEGACITY CHALLENGE TO DOCTRINE: HOW SENSORS IN URBAN MUNICIPAL INFRASTRUCTURE INFLUENCE FUTURE FIGHTS		5. FUNDING NUMBERS	
6. AUTHOR(S) Shane K. Smith			
7. PERFORMING ORGANIZATION NAME(S) AND ADDRESS(ES) Naval Postgraduate School Monterey, CA 93943-5000		8. PERFORMING ORGANIZATION REPORT NUMBER	
9. SPONSORING / MONITORING AGENCY NAME(S) AND ADDRESS(ES) N/A		10. SPONSORING / MONITORING AGENCY REPORT NUMBER	

11. SUPPLEMENTARY NOTES The views expressed in this thesis are those of the author and do not reflect the official policy or position of the Department of Defense or the U.S. Government.

12a. DISTRIBUTION / AVAILABILITY STATEMENT Approved for public release. Distribution is unlimited.	12b. DISTRIBUTION CODE A

13. ABSTRACT (maximum 200 words)

During the last century, U.S. military doctrine instructed commanders to bypass dense urban areas at all costs. This train of thought is now obsolete, as senior U.S. military leaders predict the military will fight the next major war in a megacity. This research models sensor detection of subsurface adversary movements in urban municipal infrastructure to provide early warning to U.S. troops in the defense. Our model assesses whether tactics used on the ground can be applied underground. Results show that some tactics do not perform the same in the subsurface; however, the tactics that perform well in an urban subterranean environment may have negative consequences on the civilian population.

14. SUBJECT TERMS unattended ground sensors, subterranean, subsurface, underground, municipal infrastructure, megacity, sewer, storm drainage, U.S. Army, U.S. Marines, United States Corps of Engineers, future wars, urban warfare, underground warfare	15. NUMBER OF PAGES 181
	16. PRICE CODE

17. SECURITY CLASSIFICATION OF REPORT Unclassified	18. SECURITY CLASSIFICATION OF THIS PAGE Unclassified	19. SECURITY CLASSIFICATION OF ABSTRACT Unclassified	20. LIMITATION OF ABSTRACT UU

THIS PAGE INTENTIONALLY LEFT BLANK

MODELING A MEGACITY CHALLENGE TO DOCTRINE: HOW SENSORS IN URBAN MUNICIPAL INFRASTRUCTURE INFLUENCE FUTURE FIGHTS

Shane K. Smith
Captain, United States Army
BS, U.S. Military Academy, 2011

Submitted in partial fulfillment of the
requirements for the degree of

MASTER OF SCIENCE IN APPLIED MATHEMATICS

from the

NAVAL POSTGRADUATE SCHOOL
December 2019

Approved by: Hong Zhou
                Advisor

                Carlos F. Borges
                Second Reader

                Wei Kang
                Chair, Department of Applied Mathematics

THIS PAGE INTENTIONALLY LEFT BLANK

ABSTRACT

During the last century, U.S. military doctrine instructed commanders to bypass dense urban areas at all costs. This train of thought is now obsolete, as senior U.S. military leaders predict the military will fight the next major war in a megacity. This research models sensor detection of subsurface adversary movements in urban municipal infrastructure to provide early warning to U.S. troops in the defense. Our model assesses whether tactics used on the ground can be applied underground. Results show that some tactics do not perform the same in the subsurface; however, the tactics that perform well in an urban subterranean environment may have negative consequences on the civilian population.

THIS PAGE INTENTIONALLY LEFT BLANK

Contents

List of Figures

List of Tables

THIS PAGE INTENTIONALLY LEFT BLANK

List of Acronyms and Abbreviations

BCT   Brigade Combat Team

DoD   Department of Defense

ERDC   Engineer Research and Development Center

IPB   Intelligence Preparation of the Battlefield

NPS   Naval Postgraduate School

TRADOC Training and Doctrine Command

UMI   Urban Municipal Infrastructure

USG   United States Government

USMC   U.S. Marine Corps

USA   U.S. Army

USACE   United States Army Corps of Engineers

THIS PAGE INTENTIONALLY LEFT BLANK

Executive Summary

Sewers, drainage systems, communication conduits and other urban municipal infrastructure are defensively advantageous for foes to escape the U.S. military's might, evade intelligence, surveillance, and reconnaissance detection, and engage occupying forces. Occupying forces may have limited intelligence to thwart surprise attacks due to underwhelming knowledge of operational environment and detection capabilities in the urban subterranean environment.

The ABC model utilizes Markov chains and differential equations to model targets flowing into and out of hiding area(s) and operating area(s) through urban municipal infrastructure (sewers, storm drainage, and communication conduits). The model parallels U.S. military doctrine as best as possible to assess a platoon's subsurface performance upon occupation of a city block. Sensors are placed on routes to detect target movement with a probability of detection. Detection provides units early warning to nearby target movement and aids leadership to understand the operational environment.

Research concludes some of the tactics and principles executed by the U.S. military on land are not an effective approach to engage foes in urban municipal infrastructure. Obstacle effects of fixing, disrupting, and turning enemy movement and maneuver lowers the probability of detection. While blocking a corridor increases model performance in the subterranean environment, the principle of obstacle over watch is severely limited, and the obstacle can be breached without resistance. Moreover, blocked urban municipal infrastructure may have negative effects on a population's public service.

The most important, non-mathematical recommendation drawn from this research emphasizes knowledge of the operating environment before entering an urban environment. Open-source documentation offers very beneficial information when researching a megacity's urban municipal infrastructure. Data must be complied before the conflict begins. The most effective mathematical way to increase the probability of detection, with minimal physical impact to the environment, is to influence an enemy's selection of which route they will select to travel between the hiding area to operating area.

THIS PAGE INTENTIONALLY LEFT BLANK

Acknowledgments

THIS PAGE INTENTIONALLY LEFT BLANK

CHAPTER 1:
Research Question and Objectives

1.1 Research Question

How might sensor technology shape the ability of the U.S. Department of Defense to fight in an urban, subterranean environment during defensive (force protection) operations?

1.2 Research Objectives

Assess detectability: What is the probability of detecting (providing early warning) moving targets in subterranean urban municipal infrastructure?

Improve readiness: Do probability results affect the Department of Defense and Department of Homeland Security efforts to combat current and future subterranean operations?

THIS PAGE INTENTIONALLY LEFT BLANK

CHAPTER 2:
Introduction

2.1 Vignette

Consider a future military conflict in a megacity with a population of at least ten million. Soon after its arrival, the U.S. military races to secure urban blocks to deny enemy access to key terrain. Commanders must select the location of command posts, assembly areas, and establish lines of communication. Subordinate units establish a basis of operations. In a short time, buildings are cleared and secured, and the skies above are friendly. Soldiers routinely work, rest, eat, and sleep. In the following days, the enemy conducts massive, coordinated, dismounted attacks without warning. The losses are significant. The intelligence community is perplexed, but soon realizes the enemy exploited the U.S. military's inability to address the subterranean fight.

Now, imagine a conflict where the U.S. military utilizes subterranean sensors in a megacity to detect movement of enemy presence in underground municipal infrastructure (UMI) or rudimentary passageways. Soldiers use commercial sensors like the ones used in homes to provide early warning to their units during defensive operations. Ultimately, the U.S. military would be able to ward off enemy attacks and employ the same sensors in the offense to target enemy hiding areas or underground facilities. The possibilities are many.

2.2 Historical Significance

2.2.1 U.S. History

While U.S. military's history contains many examples of subterranean challenges, the Department of Defense has recently begun to address these challenges. During the American Civil War, Union troops tunneled under Confederate positions to break the stalemate at the Battle of Petersburg. As a countermeasure, the Confederates dug their own tunnel to block Union advancement [1].

During the Vietnam War, the Vietcong effectively supported thousands of troops through

elaborate tunnel systems to elude U.S. ground forces while setting conditions for campaigns such as the Tet Offensive in 1968. Tunnels provided cover and concealment from ground patrols and aerial assets while enhancing protection from artillery, aerial bombardment, and close combat aviation. In response to the Vietcong's underground tactics, the U.S. military employed "Tunnel Rats" who were tasked to find, explore, and destroy subterranean threats. With primitive equipment, ad hoc training, and constant fear during each mission, these Soldiers accomplished what they could with the resources at hand [1].

Throughout the past two decades in Iraq and Afghanistan, adversaries consistently sought protection in caves and urban areas to evade detection. Robots, military working dogs, and infrared systems fare well in minimizing risks to Soldiers during insurgencies, but have yet to be tested in high-intensity decisive operation conflicts. Even the Massive Ordnance Aerial Blast, dropped on a tunnel system in Afghanistan, had limited effects on destroying rudimentary underground infrastructure [2].

Adversary utilization of subterranean environment significantly degrades or neutralizes one or more Warfighting Functions of U.S. military's superior "technological might" [1]. Combatant use of the subterranean environment drove the U.S. military to execute a mission it usually would not do nor is prepared to do. Once underground, adversaries seek to maximize survivability [1] with a goal of prolonging conflicts past the threshold of U.S. public and political support.

2.2.2 International History

The previous examples focus on rudimentary tunnels used against the U.S. military. This research paper concentrates efforts on usage of established tunnels, pipes, conduit, lines of communication systems, also known as urban municipal infrastructure, or subsurface area. While there are no notable U.S military battles in which UMI plays a pivotal role, the following World War II example highlights how an overwhelmed force maximized survivability in the face of a dominant force.

During the Nazi occupation of Warsaw, Poland, in 1944, the Polish military and civilians used the Warsaw's sewer system to evade the German military while simultaneously mounting an insurgency called the Warsaw Uprising. The Polish used Warsaw sewer systems to move civilians, military personnel, weapons, equipment, and supplies [3]. Initially, the

4

resistance was projected to last three to four days. However, it lasted two months and approximately 6,000 Poles retreated to safety through thousands of meters of sewer [4], as seen in Figure 2.1 and Figure 2.2.

Liaison sewer route from Zoliborz to Stare Miasto

Figure 2.1. A segment of Warsaw's sewer system used during the Warsaw Uprising. Source: [3].

Once German units discovered the operational importance of the sewer system to the Poles, German officers ordered the damming sewer lines, release of poisonous gas into the sewers, and lowering listening devices down into the sewer. When voices were confirmed, the Germans threw grenades into the sewers. In response, Polish demolition units destroyed the dams, and all travel in the sewers required absolute silence [4].

0,60 x 1,10 m

Adult insurgent at the lowest canal
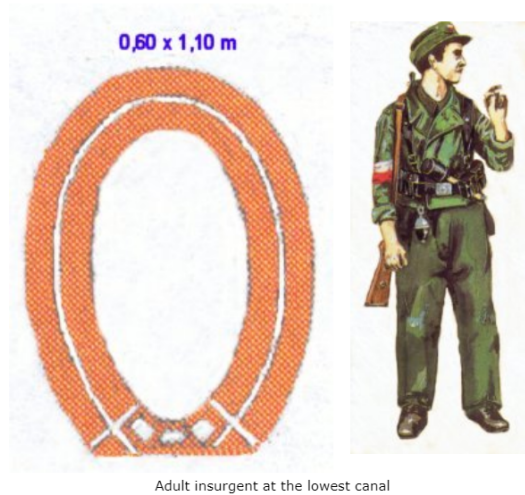
Figure 2.2. Image compares the height of Warsaw's sewers to a Polish Soldier. Source: [3].

Although Warsaw fell to the Nazis in early October 1944, German leadership underestimated the importance of Warsaw's sewer systems. "General von dem Bach admitted during the capitulation talks that initially he did not recognize the role of the municipal sewer system and its usefulness as a means of transportation and communication between Warsaw's city districts" [4]. Moreover, German Soldiers were afraid of the sewers. General von dem Bach "never managed to convince his soldiers to descend into the sewers and carry on the struggle there" [4].

In the end, Nazi units failed to control the subsurface zone, and as a result, they accrued additional costs by entering a prolonged fight. Although not a megacity fight, the Battle of Warsaw is an excellent example of how UMI can play a role in future urban warfare. One could imagine the cost of war if a dug-in, well trained, and supplied force occupied a megacity, ready to fight.

2.3 Benefit of Study

The United States Army budgeted over \$571,000,000 in fiscal year 2019 to man, equip, and train units to deploy into a hostile subterranean environments. This study applies a mathematical model to an important challenge facing the U.S. Army and Customs and

Border Patrol domestically, but also abroad for our international allies in Israel and the Republic of Korea, as well as coalition partners in Iraq and Afghanistan [5].

The United States Corps of Engineers Engineer Research and Development Center's Geotechnical and Structures Laboratory continues to seek and develop technologies vital to Warfighters' future fights, especially in the complex urban terrain. This study aids Engineer Research and Development Center (ERDC) research efforts, in theoretical scenarios, to gain feedback as to how and where to best employ military equipment in future fights.

2.4 Related Work

In addition to ERDC's current efforts, there are dozens of open-source references describing the urban subterranean environment. This section summarizes publications related to military operations in urban subterranean environments.

In "Underground Warfare," Richemond-Barak takes an in-depth look at the subterranean challenge through many lenses. From her vantage point in Israel, the subterranean challenge is a constant threat affecting the government, military, and civilians alike [6].

She begins her dialogue by providing a historical context to subterranean operations. Next, she describes and gives examples of why the subterranean problem set is a global threat. Later, she explains how international laws should be applied to subterranean operations and should address tunnel detection technology. The variety of tunnel detection technology offers unique capabilities when governments are faced with different types of tunnel construction and usage [7].

While her recommendations seem Israeli Defense Force centric, destroying tunnel systems [6] used by targets may not be effective for urban municipal infrastructure used by civilians.

The Mitre Corporation published an article on behalf of the U.S. Army Training and Doctrine Command Training and Doctrine Command (TRADOC) titled "U.S. Army TRADOC G-2 Mad Scientist Megacities and Dense Urban Areas Initiative: Data Collection and Analysis." TRADOC's G-2 envisions a world, by 2050, where nearly two-thirds of the world's population resides in cities. Due to the population increase, social unrest ensues resulting in governance tasking the military to restore order in urban environment [8]. Out of

the four Army Warfighting Challenges addressed in the study, two challenges are applicable when the U.S. military operates in the subterranean environment [8].

The first challenge is to know the operating environment before deploying into an urban environment. During the Military Decision-Making Process, or the Joint Operations Planning Process, gathering the most current information available, before deploying to a conflict, is critical. The authors point out "awareness of 'invisible geographies' where seen and unseen features (ex: cultural forces, religious systems, old and new infrastructure) intersect" [8] can be decisive when establishing operational objectives and projecting forces, especially when subterranean changes are not easily tracked from satellite imaginary.

The article addresses the technological challenges with commercial off-the-shelf equipment that will aid in intelligence gathering and situation understanding. The article also notes, "Commercial approaches can inform military unmanned system development but will not completely meet military needs because commercial devices are not created for or working in unstructured, austere environments (e.g., rubble, underground, hostile environments)" [8].

In "Reimagining the Character of Urban Operations for the U.S. Army," the RAND Corporation arrives at similar conclusions as the Mitre Corporation report. In addition to emphasizing intelligence as a significant enabler before and during urban operations, the RAND report argues for a need to use light and armored formations within an urban environment [9]. If future urban environments warrant light and armored formations, then all Brigade Combat Teams may benefit from subterranean sensor use.

The Deputy Director of the Modern Warfare Institute, John Spencer, U.S. Army Major (retired), also acknowledges U.S. Army subterranean gaps. He mentions a "Subterranean Wishlist" which includes robots, canary birds, ground-penetrating radar, and sensors such as sound echolocation devices called "bat vision" and thermal sights. The concept of using sensors to enhance movement and maneuver, and survivability is vital to subterranean operations [10].

In March 2019, the *Army Times* published an article titled "The Subterranean Battlefield." The article touches on a broad spectrum of ongoing efforts such as historical significance, current training opportunities, opinions on the environment from field experts, and a list of future technologies developed to address subterranean challenges. According to the article,

the cost to equip a Brigade Combat Team with a subterranean equipment package runs about $15.3 million [11].

Whether advocating the integration of light and armored formations in an urban environment, stressing the importance of intelligence, or discussing technologies to close gaps, most authors emphasize the importance and urgent need to address some sort of urban warfare challenge. Some experts offer a list of sensor technologies to aid in the subterranean fight.

However, none of the articles addresses deployment of new technology in the subsurface operations within a doctrinal approach. Moreover, no researched article applied a qualitative model to sensor detection in a subterranean environment. Creating and testing a mathematical model is the focus of this work. The next section introduces a variety of sensors technologies that may aid in the subterranean fight.

THIS PAGE INTENTIONALLY LEFT BLANK

CHAPTER 3:
Sensors

3.1 Sensor Technology

Before immediately exploring sensor options, note there are currently no Department of Defense fielded sensors designed and tested for subterranean use. There are many factors of the subterranean environment that are known to significantly degrade or even prevent unattended ground sensor performance.

As reported by Sandia National Laboratories, "it is apparent that no one sensor is capable of robustly detecting all types of tunnels in varying environments, which in turn has led to strategies of employing suites of sensors for detection" [12]. This logic holds for detecting targets in the same tunnels, once discovered. Detecting movement of a target is not limited to line of sight. Detecting magnetic, heat, or sound signatures are sometimes more effective than detecting motion. This research paper assumes the following are future sensor technologies able to impact the subterranean operations. Moreover, our work focuses on the mathematical model, not sensor performance. For example, addressing a sensor's effective range, frequency thresholds, or probability of false alarms is outside our scope. Below is a list of different sensor technology.

3.1.1 Passive Infrared Detection

Passive Infrared Detection detects movements. Passive Infrared Detection does not take a picture or video of the target. It simply alerts users of a change in the location of an object. Passive Infrared technology would provide early warning of unexpected movement underground. Although simple, its employment must be thought out to maximize effectiveness.

3.1.2 Magnetic Detection

Magnetic Detection recognizes the presence of a metal target crossing or intersecting sensor receivers. It's adaptable to the subterranean environments to alert sensors to a change of

magnetic signatures in an area. Magnetic detection sensors would be highly effective underground by "drowning out" magnetic noise from surface movement signatures.

3.1.3   Magnetic Switch Detection

Magnetic Switch Detection identifies a change in the position of two adjacent or joined surfaces. Much like a door alarm in a residential house, a magnetic switch would alert users to the disconnection of two sensors. Magnetic switch detection would be used to detect the opening of a portal separating rooms or passageways. Employment of Magnetic switches may require a bit of innovation and creative thinking for subterranean use.

3.1.4   Ultrasonic Sound

Ultrasonic Sound sensors expose targets by releasing and receiving inaudible frequencies. A change in the 'release' and 'receive' interval alerts users to a moving object traveling toward or away from the sensor. In nature, ultrasonic sound is known as echolocation. Ultrasonic sound sensors would be highly effective underground, but like Passive Infrared, emplacement would require a degree of planning.

3.1.5   Acoustic Detection

Acoustic Detection uses sound waves to detect movement. Acoustic detection is highly vulnerable to cultural and vehicular noise. Predetermined frequency thresholds would focus detection on a limited frequency range to employ acoustic detection effectively. Once operational, acoustic detection could provide users with an effective way to detect unexpected noise at certain times to establish target patterns.

3.1.6   Night Vision Infrared Detection

Night Vision Infrared Detection reveals and records a picture of a target once the target enters predetermined range of the sensor. Once the sensor detects motion, the embedded camera records a picture of the target. The picture is sent to the user for identification. Some might relate this technology to a recreational hunter's night vision infrared camera. In a surface environment, identifying friendly movement versus hostiles is important. In a subsurface environment, limited use of infrastructure allows units to determine friend or foe simply by knowing the time of day or concurrent missions. Moreover, like a few

of the sensors mentioned, the night vision infrared camera requires a specific degree of technical installation to collect the desired effects. Night Vision Infrared Detection Camera technology may benefit intelligence operations.

3.2 Definition of Layer 1a and Layer 1b Sensors

3.2.1 Layer 1a Sensor

Sensors initially placed are called "Layer 1a" sensors. In theory, Layer 1a sensors are elementary to place, are for temporary use, and are designed to be expendable. These sensors function long enough to provide unit leadership the data to make initial decisions about the subterranean environment.

3.2.2 Layer 1b Sensor

If time allows, "Layer 1b" sensors replace Layer 1a sensors, or are placed near Layer 1a sensors to provide redundancy. Like Layer 1a sensors, Layer 1b sensors are also easy to place but may require certain positioning to optimize capabilities. The designs are discrete, durable, and semi-permanent only to the extent that they are still easily recoverable as units move. These sensors are effective and provide early warning of enemy movement in UMI. Moreover, these future sensors operate as a network with other sensors in a designated area of operations. In theory, these sensors function long enough to provide leadership the data necessary to effectively operate in an area of operations for an extended time.

3.3 Sensor Probability of Detection

For operational security (OPSEC) measures, the sensors will be referred to as Sensor 1, through Sensor 6 and the probabilities of sensor target detection will not be disclosed. Distribution of this information is a need-to-know basis only. The Results and Analysis Chapter provides the reader with an increase or decrease value of how the sensors performed.

THIS PAGE INTENTIONALLY LEFT BLANK

CHAPTER 4:
Methodology

This thesis approaches the problem of adversaries moving undetected in UMI to conduct operations. The baseline for the methodology is Wang and Zhou's ABC search problem. In ABC search problem,

> consider a search problem as depicted in Figure [4.1] where a target follows constrained pathways, moving between a hiding area and an operating area. The target can stay in the hiding area where the sensors cannot penetrate, and consequently the target is not detectable; it can travel along one of the routes connecting the hiding area and the operating area; and it can spend time in the operating area to carry out certain activities/tasks before returning to the hiding area via one of the routes. [13]

Again, "in Figure [4.1], the hiding area is denoted by 'A'; the collection of all routes is represented by 'B'; and the operating area is marked by 'C'. The target is detectable by a sensor both along the set of routes B and in the operating area C. In the hiding area A, the target is not detectable" [13]. Assume hiding area A is an underground facility or a building of cultural importance unable to be disrupted. For this model, detection in the operating area C is insignificant to the problem. Targets detected in operating area C are on or above ground level. Only targets in the subterranean environment are of interest. This search problem is relevant to homeland security, military, counter-drug, counter-trafficking, and law enforcement operations.
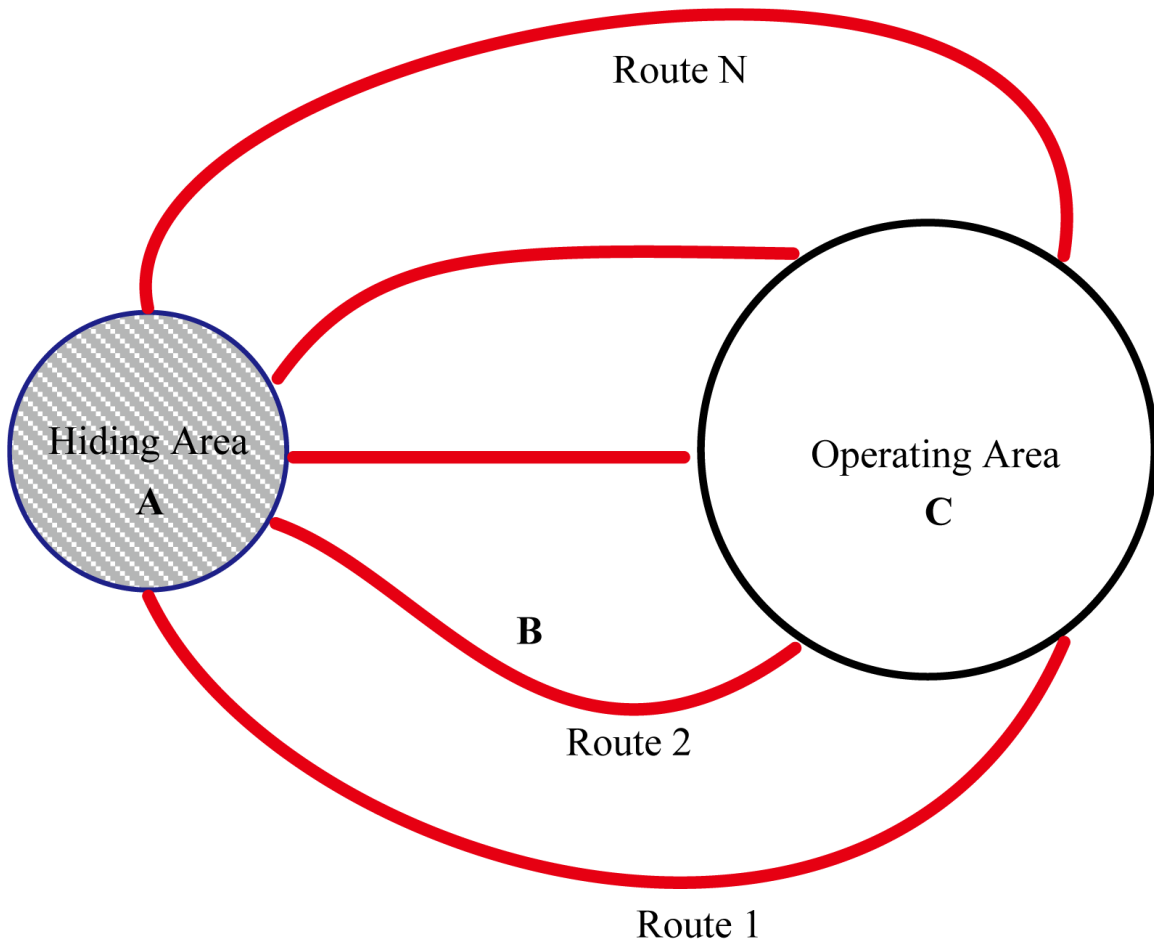
Figure 4.1. This figure visually depicts the ABC model with each element: hiding area, operating area and multiple (n) routes k. Source: [13].

This ABC model uses Markov chains, first order differential equations, sensors with varying probabilities of detection, all within a U.S. Army doctrinal framework to model flow and probabilities of target detection. The current doctrinal framework approaches the problem in Training Circular (TC) 3-21.50 "Small Unit Training in Subterranean Environments" and Army Techniques Publication (ATP) 3-21.50 "Subterranean Operations" with an offensive mindset. Troops enter subterranean environments and conduct a series of battle drills to secure subsurface terrain or engage combatants in tunnels or underground facilities [14] [15]. One shortfall of the current doctrine is the lack of a defensive or force protection posture when conducting operations in an urban subterranean environment. To address the current

gap, this thesis' methodology takes an incremental, layered approach, using additional U.S. Army publications to model different scenarios.

First in Figure 4.2, a simple model depicts a UMI route with the presence of no military action. The subterranean environment is in a steady-state, and targets can move freely [13] in the subterranean environment. In this state, the model represents an underground UMI from one point to another. There are no sensors to detect target movement.
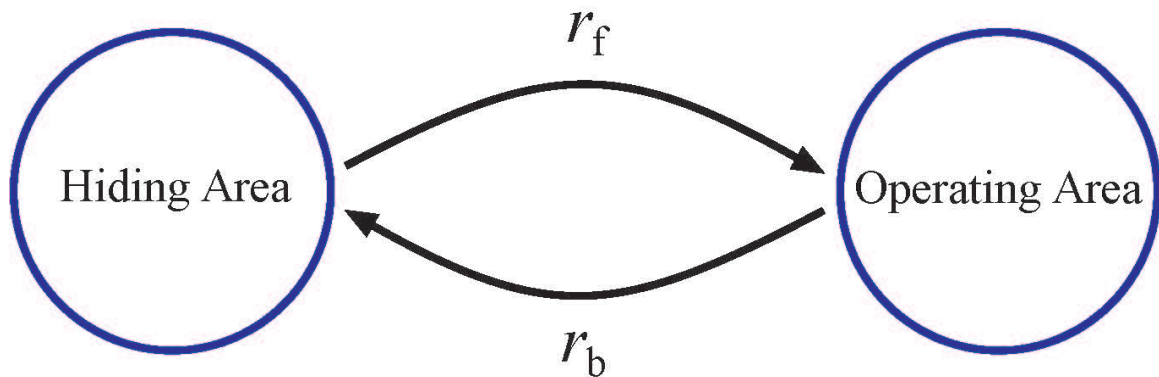
Figure 4.2. Diagram of the steady state. Source: [13].

Next, the model adds a sensor to the single route in Figure 4.3. With the introduction of a sensor, there exists a probability of detection [13]. Detection provides early warning to troops of target activity in the UMI.
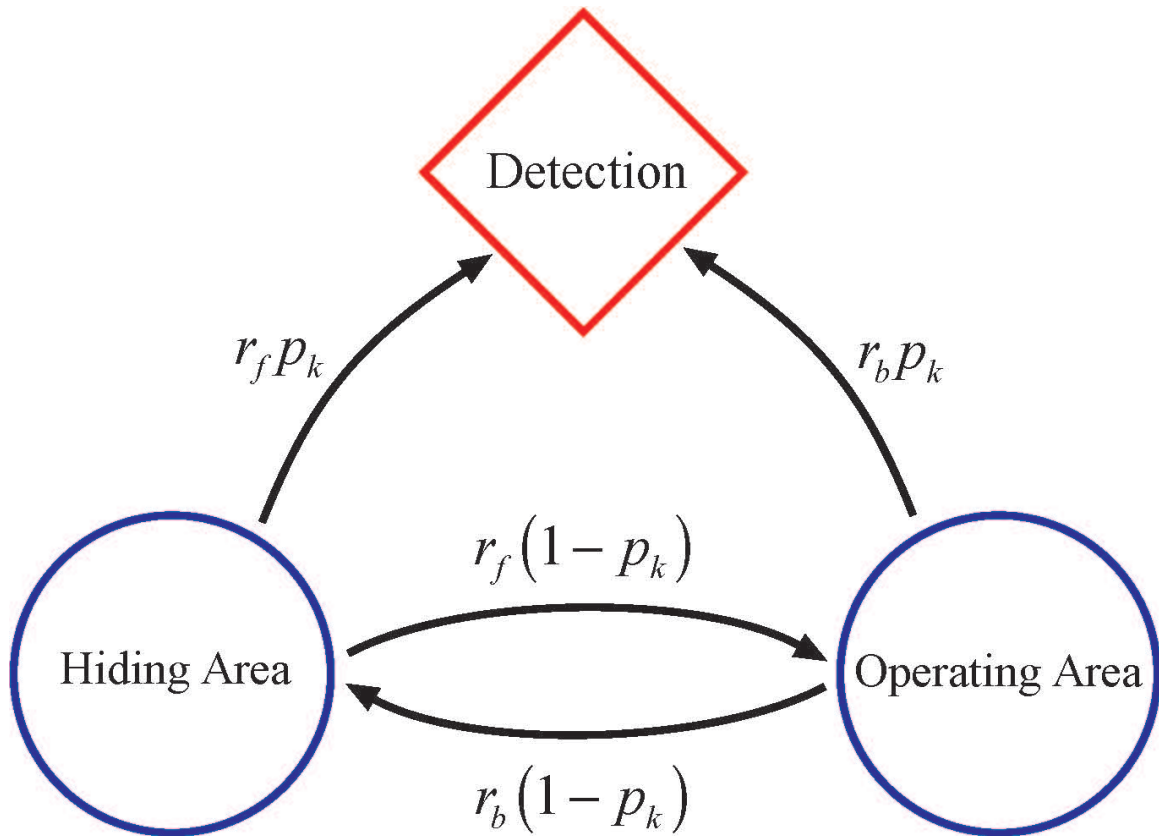
Figure 4.3. Diagram of the Markov chain after the sensor is introduced.
Source: [13].

The model gradually increases in complexity. Additional routes and sensors replicate a force occupying and defending a city block against targets moving through multiple subsurface avenues of approach to their operating area.

Covering every subsurface avenue of approach with a sensor is unreasonable. A critical step in the models' results is determining the probability of detection when a sensor does not cover every UMI corridor. In theory, this limitation forces leaders to select effective locations to maximize early detection. A model with all routes covered by a sensor offers an opportunity to compare results to models with only limited coverage.

With security as the top priority, allotting additional time in an area allows for the placement of multiple Layer 1a or Layer 1b sensors. The model with Layer 1a and Layer 1b sensors

on a single route assesses how much redundancy increases the probability of detection.

The model expands to represent a subsurface city block with a unit defending the operating area from targets leaving multiple hiding areas through UMI to carryout activities in the operating area. This model is adaptable and scalable to compare the probability of detecting targets after placing sensors on every route, or on a limited number of important routes, or randomly on routes throughout the subsurface.

Tactically, each model addresses how current doctrine might perform in UMI. Models aim to replicate a U.S. Army unit a defending a block. Since TC 3-21.50 focuses on squad level tactics, assume the same for the models. Figure 4.4 below from ATP 3-06 gives size unit requirements to defend an urban area. A platoon leads and directs squads to place sensors and defend against enemy targets.

Table 5-1. Approximate defensive frontages and depths

Unit	Frontage (Blocks*)	Depth (Blocks*)
Battalion	4 – 8	3 – 6
Company	3 – 4	2 – 3
Platoon	1 – 2	1
*Average block is 175 meters (191 yards)		

Figure 4.4. ATP 3-06 Urban Operations Table 5-1. Source: [16]

.

In ATP 3-06, "Urban Operations," an engineer's countermobility or obstacle plan is essential to unit defense in a megacity [16]. Units place obstacles to gain an advantage against enemy movement. ATP 3-06 explains, "countermobility operations in urban terrain drastically increase the defense's ability to shape the attacker's approach and to increase the combat power ratios in favor of the defense" [16]. There are four types of obstacle effects evaluated: disrupt, turn, fix, and block, see Figure 4.5.
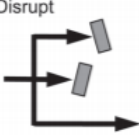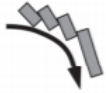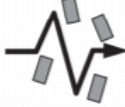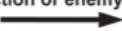
Application	Description
Disrupt	The arrows indicate the direction of enemy advance. The length of the arrows indicate where the enemy is slowed or allowed to bypass.
Turn	The heel of the arrow is the anchor point. The direction of the arrow indicates the desired direction of the turn.
Fix	The arrow indicates the direction of enemy advance. The irregular part of the arrow indicates where enemy advance is slowed by obstacles.
Block	The vertical line indicates the limit of enemy advance and where the obstacle ties into severely restricted terrain. The horizontal line shows the depth of the obstacle effort.

Direction of enemy attack

Figure 4.5. ATP 3-90.8 Combined Arms Countermobility Operations' Obstacle Effects. Source: [17]

.

ATP 3-90.8 defines each obstacle effect.

Disrupt: "An obstacle effect focuses fire planning and obstacle effort to cause the enemy to break up its formation and tempo, interrupt its timetable, commit breaching assets prematurely, and attack in a piecemeal effort" [17].

Turn: An "obstacle effect that integrates fire planning and obstacle effort to divert an enemy formation from one avenue of approach to an adjacent avenue of approach into an engagement area" [17].

Fix: "An obstacle effect that focuses fire planning and obstacle effort to slow an attacker's movement within a specified area, normally an engagement area" [17].

Block: "An obstacle effect that integrates fire planning and obstacle efforts to stop an

attacker along a specific avenue of approach or to prevent the attacking force from passing through an engagement area" [17].

By increasing or decreasing a model's parameter values, one can assess each obstacle effect's quantitative performance and the probability of detection. In addition to numerical results, a qualitative assessment "considers collateral damage and the second- and third-order effects of obstacle construction" [16].

Lastly, the conclusion references survey responses by U.S. Army officers who share their unit's experience with urban operations subterranean training and sensor utilization. The intent of the survey aims to discover any doctrine or lessons learned about subterranean operation not already researched, in an effort to improve the ABC model and better reflect a possible urban subterranean environment to yield impactful results.

THIS PAGE INTENTIONALLY LEFT BLANK

CHAPTER 5:
Experimental Setup

5.1 Definition of Parameters

To maintain consistency, the definition of parameters is identical to Wang and Zhou's initial definitions and situational assumptions.

"The dwell time of the target in the hiding area is exponentially distributed with rate r_f the forward rate of traveling from the hiding area to the operating area" [13]. "The dwell time of the target in the operating area is exponentially distributed with rate r_b the backward rate of traveling from the operating area back to the hiding area" [13]. "The probability of [the target] being in the hiding area and that of being in the operating area at time t" [13] is $p_h(t)$ and $p_o(t)$, respectively.

"On its travels between the hiding area and the operating area, the target takes route k, k is a numbered route in the ABC model with probability p_k. In particular, the probability of choosing route k is the same for both directions. This assumption will be relaxed in the later discussion and models" [13].

Models express sensor probability of detection as ps_i. For example, Sensor 1 is ps_1, Sensor 2 is ps_2, ... and Sensor 6 is ps_6. Assume that each ps_i can be different or the same than another ps_i in each model. In order to evaluate the performance of sensors, Layer 1a sensors have lower probabilities of detection than Layer 1b sensors. Otherwise, the actual sensor's probability of defection is not disclosed.

"The travel time between the operating area and the hiding area is negligible in comparison with the dwell times in the hiding area and the operating area. Mathematically, we treat the travel time along a route as zero" [13].

5.2 Key Assumptions

In this model, self-loops do not exist such that the summation of $p_h + p_o = 1$. If one wanted to model self-loops, the summation of p_k would not equal one, meaning some of the targets

do not travel from one location to the next. The targets are bound to move within the UMI routes between hiding areas to operating areas.

Lastly, the percentage of targets beginning in hiding and operating area fluctuates, the percentages could either be equal or not equal. Targets will likely concentrate in a "safe" hiding area before traveling to an operating area. However, there is a chance that targets can start in the operating area. The initial conditions of targets are the least predictable parameter to model. Since targets also have the ability to influence the outcome in real conflicts, unpredictable behavior adds value to results.

5.3   Numeric and Analytic Solutions

For 2x2 matrices, numerical and an analytic solutions are achievable. For complex 3x3 or 4x4 size matrices in Section 5.11, it is too difficult to find analytical solutions. However, Chapter 6 details numerical solutions to 3x3 and 4x4 matrices.

From the conservation law, in-flow equals out-flow. The following in-flow/out-flow equations result for hiding area A and operating area C.

The rate of change over time in "A" can be written

$$\frac{dp_h}{dt} = ap_h + bp_o, \tag{5.1}$$

while the rate of change over time in "C" is written

$$\frac{dp_o}{dt} = dp_h + cp_o. \tag{5.2}$$

Together, a 2x2 matrix represents the rate of change over A and C over time t where,

$$\frac{d}{dt}\begin{bmatrix} p_h \\ p_o \end{bmatrix} = \begin{bmatrix} a & b \\ d & c \end{bmatrix}\begin{bmatrix} p_h \\ p_o \end{bmatrix} = A\begin{bmatrix} x_1 \\ x_2 \end{bmatrix} \tag{5.3}$$

and

$$A = \begin{bmatrix} a & b \\ d & c \end{bmatrix}, \begin{bmatrix} x_1 \\ x_2 \end{bmatrix} = \begin{bmatrix} p_h \\ p_o \end{bmatrix} \tag{5.4}$$

24

The general solution of Equation 5.3, $\frac{d\vec{x}}{dt} = A\vec{x}$, is

$$\vec{x}(t) = c_1 \vec{V_1} e^{\lambda_1 t} + c_2 \vec{V_2} e^{\lambda_2 t} \tag{5.5}$$

where λ_1 and λ_2, $(\lambda_1 \neq \lambda_2)$ are the eigenvalues of A with corresponding eigenvectors $\vec{V_1}$ and $\vec{V_2}$, respectively. .

To find for the eigenvalues, we solve the characteristic equation

$$det(\lambda I - A) = \begin{vmatrix} \lambda - a & -b \\ -d & \lambda - c \end{vmatrix} = 0. \tag{5.6}$$

After expanding, we have the following quadratic equation:

$$\lambda^2 - (a + c)\lambda + ac - bd = 0 \tag{5.7}$$

The quadratic formula yields two routes, λ_1 and λ_2.

$$\lambda_{1,2} = \frac{(a + c) \pm \sqrt{(a + c)^2 - 4(ac - bd)}}{2}, \lambda_1 \neq \lambda_2 \tag{5.8}$$

After finding the eigenvalues, one can solve

$$(A - \lambda I)\vec{V} = \vec{0}. \tag{5.9}$$

to find the corresponding eigenvector for each eigenvalue. The coefficients c_1 and c_2 in Equation 5.5 are found by imposing initial conditions $P_h(0)$ and $P_o(0)$. However, we can find the sum $P_h(0) + P_o(0)$ (escape probability or survival probability) directly without computing eigenvectors [13].

Assuming

$$p_h(t) + p_o(t) = C_1 e^{\lambda_1 t} + C_2 e^{\lambda_2 t}, \tag{5.10}$$

then

$$p'_h(t) + p'_o(t) = C_1 \lambda_1 e^{\lambda_1 t} + C_2 \lambda_2 e^{\lambda_2 t}, \tag{5.11}$$

From Equations 5.1 and 5.2, we have

$$p_h{}'(t) = ap_h(t) + bp_o(t), \tag{5.12}$$

$$p_o{}'(t) = dp_h(t) + cp_o(t), \tag{5.13}$$

Imposing known initial conditions, $p_o(0)$ and $p_h(0)$, we obtain

$$C_1 + C_2 = P_h(0) + P_o(0) \tag{5.14}$$

and

$$C_1\lambda_1 + C_2\lambda_2 = P'_h(0) + P'_o(0) = (a + d)P_h(0) + (b + c)P_o(0). \tag{5.15}$$

Multiplying Equation 5.14 by λ_2 yields

$$C_1\lambda_2 + C_2\lambda_2 = [P_h(0) + P_o(0)]\lambda_2. \tag{5.16}$$

To find C_1, subtract 5.16 and 5.15:

$$C_1(\lambda_1 - \lambda_2) = (a + d - \lambda_2)p_h(0) + (b + d - \lambda_2)p_o(0) \tag{5.17}$$

$$C_1 = \frac{(a + d - \lambda_2)p_h(0) + (b + d - \lambda_2)p_o(0)}{(\lambda_1 - \lambda_2)}. \tag{5.18}$$

Similarity, after multiplying Equation 5.14 by λ_1, we have

$$C_1\lambda_1 + C_2\lambda_1 = [P_h(0) + P_o(0)]\lambda_1. \tag{5.19}$$

Subtracting Equations 5.19 and 5.15 yields C2:

$$C_2(\lambda_2 - \lambda_1) = (a + d - \lambda_1)p_h(0) + (b + d - \lambda_1)p_o(0) \tag{5.20}$$

$$C_2 = \frac{(a + d - \lambda_1)p_h(0) + (b + d - \lambda_1)p_o(0)}{(\lambda_2 - \lambda_1)}. \tag{5.21}$$

Therefore,

$$p_h(t) + p_o(t) = C_1 e^{\lambda_1 t} + C_2 e^{\lambda_2 t}, \tag{5.22}$$

where C_1 and C_2 are given in Equations 5.18 and 5.21.

Chapter 6 will validate this analytic solution for $p_h(t) + p_o(t)$ against the ODE45 program solver solution for $p_h(t) + p_o(t)$.

5.3.1 Validating the Numerical Solution for a 3x3 or 4x4 System of Equations in MATLAB

Together, a 3x3, 4x4, ...ixi square matrix represents the rate of change over hiding area A and operating area C over time t.

$$\frac{d}{dt}\begin{bmatrix} x_1 \\ x_2 \\ . \\ . \\ . \\ x_i \end{bmatrix} = A \begin{bmatrix} x_1 \\ x_2 \\ . \\ . \\ . \\ x_i \end{bmatrix} \tag{5.23}$$

where,

$$A = \begin{bmatrix} a_{11} & ... & a_{1i} \\ . & & . \\ . & & . \\ . & & . \\ a_{i1} & ... & a_{ii} \end{bmatrix} \tag{5.24}$$

To find for the eigenvalues, we solve the characteristic equation

$$det(\lambda I - A) = \begin{vmatrix} \lambda - a_{11} & ... & a_{1i} \\ . & & . \\ . & & . \\ . & & . \\ a_{i1} & ... & \lambda - a_{ii} \end{vmatrix} = 0. \tag{5.25}$$

After expanding, solve for each eigenvalue (root) of the characteristic equation.

To find the eigenvector, one can solve

$$(A - \lambda I)\vec{V} = \vec{0}. \tag{5.26}$$

We can use MATLAB to numerically solve for eigenvalues and eigenvectors using the command "$[V, D] = eigen(A)$" [18]. The resulting columns in matrix V are eigenvectors, and the values along the main diagonal in matrix D are the eigenvalues.

When A has i distinct eigenvalues $\lambda_1,...,\lambda_i$, the general solution of Equation 5.25. can be written as

$$
\begin{bmatrix} x_1 \\ x_2 \\ . \\ . \\ . \\ x_i \end{bmatrix} = C_1 \vec{V}_1 e^{\lambda_1 t} + ... + C_i \vec{V}_i e^{\lambda_i t}. \tag{5.27}
$$

At time, $t = 0$

$$
\begin{bmatrix} x_1(0) \\ x_2(0) \\ . \\ . \\ . \\ x_i(0) \end{bmatrix} = C_1 \vec{V}_1 + ... + C_i \vec{V}_i = [\vec{V}_1...\vec{V}_i] \begin{bmatrix} C_1 \\ C_2 \\ . \\ . \\ . \\ C_i \end{bmatrix} = V_{ixi} \begin{bmatrix} C_1 \\ C_2 \\ . \\ . \\ . \\ C_i \end{bmatrix}_{ix1} \tag{5.28}
$$

Finally, solving the numerical solution's constant coefficients

$$
\begin{bmatrix} C_1 \\ C_2 \\ . \\ . \\ C_i \end{bmatrix} = V^{-1} * \begin{bmatrix} x_1(0) \\ x_2(0) \\ . \\ . \\ x_i(0) \end{bmatrix}. \tag{5.29}
$$

The general form is

$$\begin{bmatrix} x_1 \\ x_2 \\ . \\ . \\ . \\ x_i \end{bmatrix} = C_1 \vec{V_1} e^{\lambda_1 t} + C_2 \vec{V_2} e^{\lambda_2 t} + ... + C_i \vec{V_i} e^{\lambda_i t}. \tag{5.30}$$

The coefficients C_1, C_2,...,C_i can be found by imposing initial conditions.

In Chapter 6, the numerical solutions for 3x3 and 4x4 systems of equations are compared to MATLAB's ODE45 program to validate our solutions through a different approach.

5.4   Route without Sensor

In this model, the target's movement between the hiding area and operating area is critical. First, $\frac{dp_h}{dt}$ represents the rate of change of p_h, hiding area A. Secondly, $\frac{dp_o}{dt}$ represents the rate of change of p_o, operating area C. From the conservation law, the rates of change in both areas yield a system of in-flow, out-flow equations. The vector $\vec{x}$ is expressed as:

$$\vec{x} = \begin{bmatrix} p_h \\ p_o \end{bmatrix} = \begin{bmatrix} x_1 \\ x_2 \end{bmatrix} \tag{5.31}$$

The initial ABC model is simple. One hiding area, one route ($B = 1$) represent a sewage or drainage line running from a hidden area into an operating area (represented by a city block). Since no sensors are present, the probability of detection does not exist. Targets freely move between Hiding area and Operating area. Figure 5.1 illustrates the model.

One Route, No Sensor on Route

$r_f p_h$

Hiding Area

Operating Area

$r_b p_o$
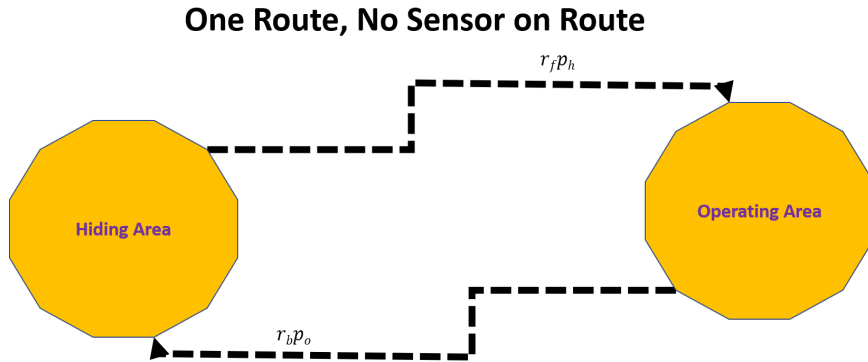
Figure 5.1. Diagram of Markov chain representing one route with no sensor

.

Below are the Markov chain's system of equations and parameters used to model the initial ABC scenario. Again, the percentage of targets beginning in hiding p_h and operating area p_o can fluctuate.

$$\frac{dp_h}{dt} = -r_f p_h + r_b p_o \tag{5.32}$$

$$\frac{dp_o}{dt} = -r_b p_o + r_f p_h \tag{5.33}$$

5.5 One Route, One Sensor on Route

Figure 5.2 depicts the addition of a senor to the route. Tactically, this model represents the presence of an opposing force interested in detecting target movement along Route 1.

One Route, One Sensor on Route 1

$r_f p_h p s_1$

Detection

$r_b p_o p s_1$

$r_{f(1-ps_1)} p_h$

Hiding Area

Operating Area

$r_b (1 - ps_1) p_o$
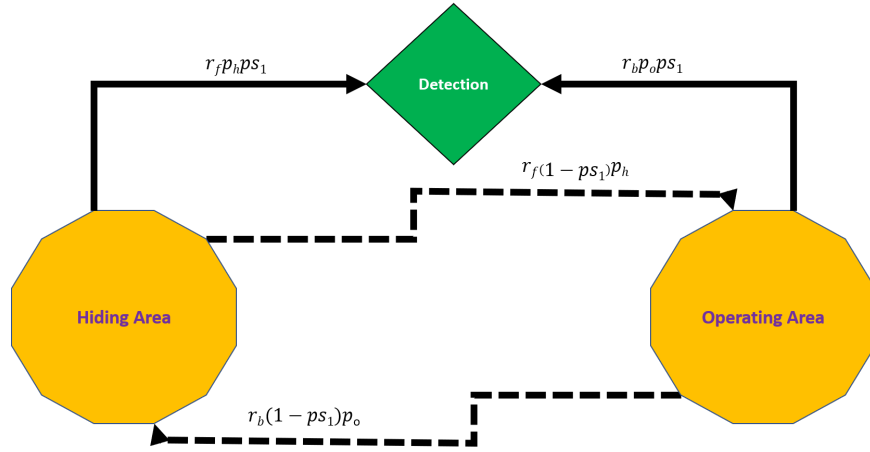
Figure 5.2. Diagram of Markov chain representing one route with one sensor

Here, we have the system of equations representing the in-flow and out-flow between hiding and operating areas. Note if the sensor's probability of detection is 0.0%, then the model is equivalent to the previous model without a sensor.

$$\frac{dp_h}{dt} = -r_f p_h + r_b[(1 - ps_1)]p_o \qquad (5.34)$$

$$\frac{dp_o}{dt} = -r_b p_o + r_f[(1 - ps_1)]p_h \qquad (5.35)$$

5.6   Two Routes, One Sensor on Route 1

Next, the initial ABC model includes additional UMI. In Figure 5.3, the ABC model grows to AB^2C size. There are now two routes ($B = 2$) connecting the hidden area to operating area. Below one sensor covers Route 1, while Route 2 remains uncovered. The model represents placing a very limited number of Layer 1a sensors in the UMI with a moderate probability of detection. Tactically, assume emplacement is hasty and it is unreasonable to cover every subterranean void.

Two Routes, One Sensor on Route 1
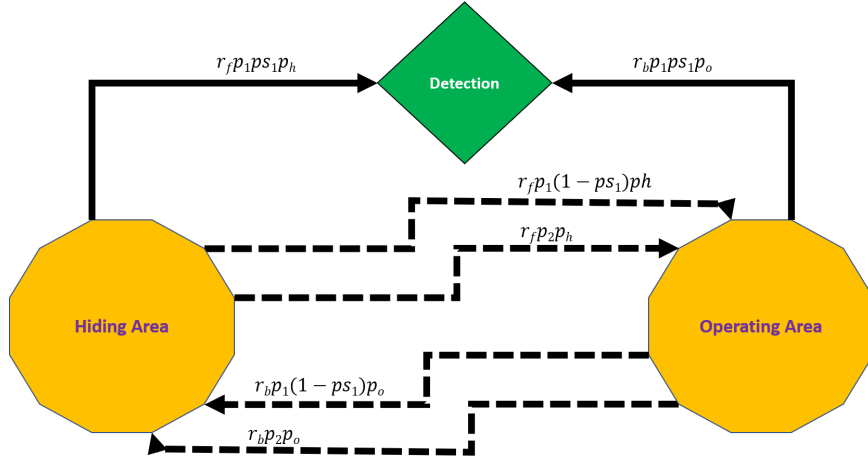
Figure 5.3. Diagram of Markov chain representing two routes with one sensor on Route 1

The Markov chain and parameter lists expand to include an additional route $p2$.

$$\frac{dp_h}{dt} = -r_f p_h + r_b[p_1(1 - ps_1) + p_2]p_o \tag{5.36}$$

$$\frac{dp_o}{dt} = -r_b p_o + r_f[p_1(1 - ps_1) + p_2]p_h \tag{5.37}$$

Now the probabilities of going forward and backward on respective routes are different. The target has two unique probabilities of selecting the route traveling forward to the operation area and two different probabilities selecting the route traveling back to the hiding area. Sensor ps_1 remains on Route 1.

$$\frac{dp_h}{dt} = -r_f p_h + r_b[p_3(1 - ps_1) + p_4]p_o \tag{5.38}$$

$$\frac{dp_o}{dt} = -r_b p_o + r_f[p_1(1 - ps_1) + p_2]p_h \tag{5.39}$$

The next section implements additional sensors along routes providing redundant detection capabilities.

5.7 Two Routes, Two Independent Sensors on Route 1

From the model above, when sensor emplacement is hasty. Now, additional time allows the emplacement of an additional sensor on a Route 1. In Figure 5.4, Sensor 1 (Layer 1a) with probability of detection ps_1 and Sensor 2 (Layer 1b) with probability of detection ps_2 cover Route 1, Route 2 remains undiscovered.

Two Routes, Two Independent Sensors on Route 1
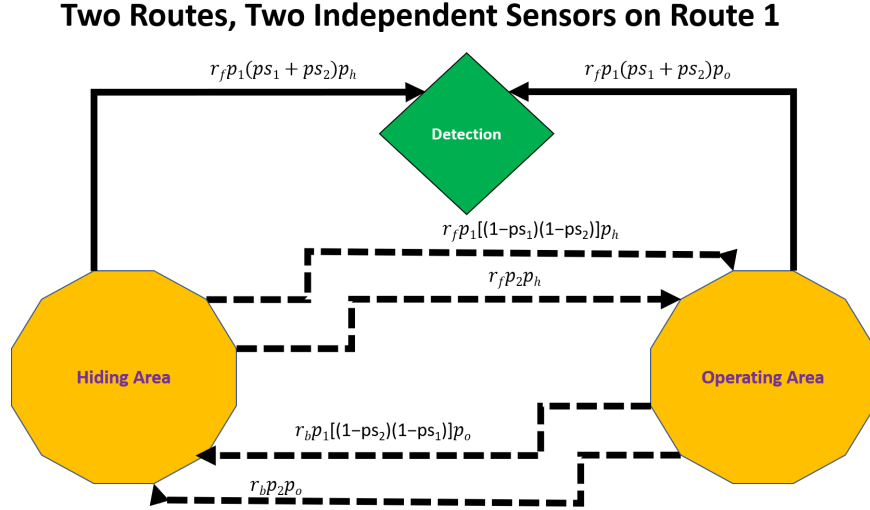
Figure 5.4. Diagram of Markov chain representing two routes with two independent sensors on Route 1

The probabilities of detection of ps_1 and ps_2 are different. The Markov chain's system of equation and parameter lists expands to include the following updated equations and parameters.

$$\frac{dp_h}{dt} = -r_f p_h + r_b [p_2 + p_1(1 - ps_2)(1 - ps_1)]p_o \tag{5.40}$$

$$\frac{dp_o}{dt} = -r_b p_o + r_f [p_2 + p_1(1 - ps_1)(1 - ps_2)]p_h \tag{5.41}$$

Similar to Equations 5.38 and 5.39, the probabilities of going forward and backward on respective routes are different. The target has two different probabilities of going forward to the operation area and two different probabilities returning to the hiding area. Different forward and backward probabilities can be modeled when there are more than two routes

between hiding and operating areas.

$$\frac{dp_h}{dt} = -r_f p_h + r_b [p_4 + p_3(1 - ps_2)(1 - ps_1)]p_o \tag{5.42}$$

$$\frac{dp_o}{dt} = -r_b p_o + r_f [p_2 + p_1(1 - ps_1)(1 - ps_2)]p_h \tag{5.43}$$

The next section implements models implementation of additional sensors covering all routes. In theory, with additional time, sensors will cover each route k.

5.8 Two Routes, One Sensor on each Route

Previous models depict a limited number of Layer 1a and Layer 1b sensors because of limited time available and hasty emplacement. With more time, placement of additional sensors can detect targets traveling along all routes k. In Figure 5.5 Route 1 and Route 2 are covered by Sensor 1 ps_1 and Sensor 2 ps_2. Again, the probabilities of detection of ps_1 and ps_2 are different.
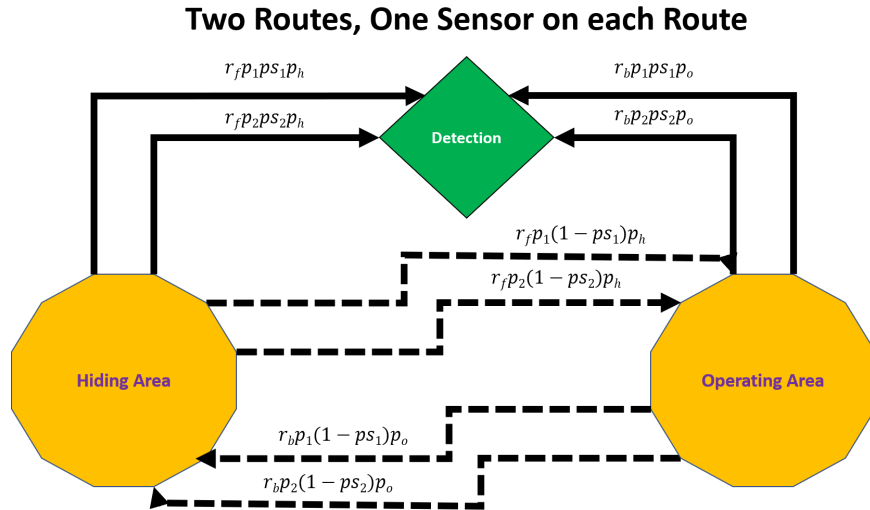
Figure 5.5. Diagram of Markov chain representing two routes with one sensor on each Route

The Markov chain's system of equations and parameter lists expand to include an additional sensor ps_i.

$$\frac{dp_h}{dt} = -r_f p_h + r_b[p_1(1 - ps_1) + p_2(1 - ps_2)]p_o \tag{5.44}$$

$$\frac{dp_o}{dt} = -r_b p_o + r_f[p_1(1 - ps_1) + p_2(1 - ps_2)]p_h \tag{5.45}$$

The next model increases the number of routes and sensors, the number of hiding and operating areas remains unchanged.

5.9   Twelve Routes, One Sensor on each Block Corner

The model represents an actual city block troops may operate throughout. Downtown Monterey, California's UMI network provides a visual representation of how sewers (Figure 5.6) and storm (Figure 5.7) systems form a network of connected voids capable of supporting dismounted movement of formations, equipment, and supplies.
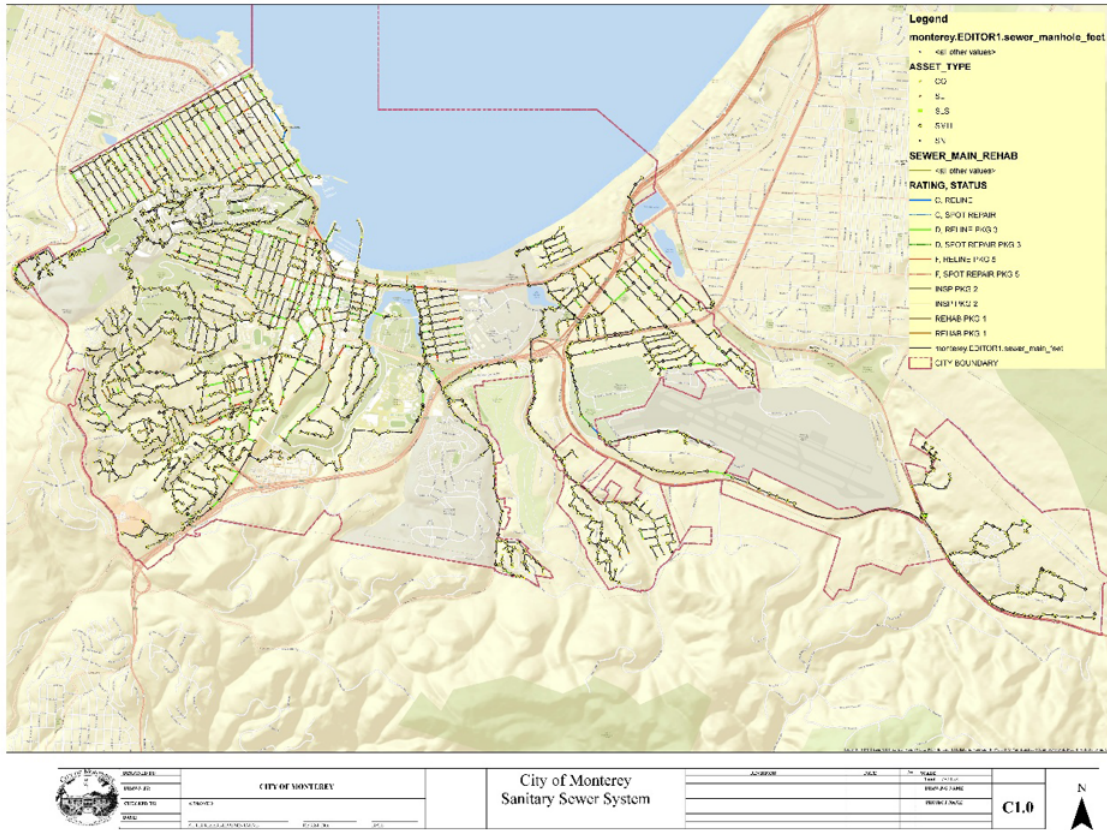
Figure 5.6. City of Monterey sewer system map. Source: [19].

In the graphic above, there are two important features to note. The black lines represent sewage lines and the yellow circles with black outline are manhole covers.
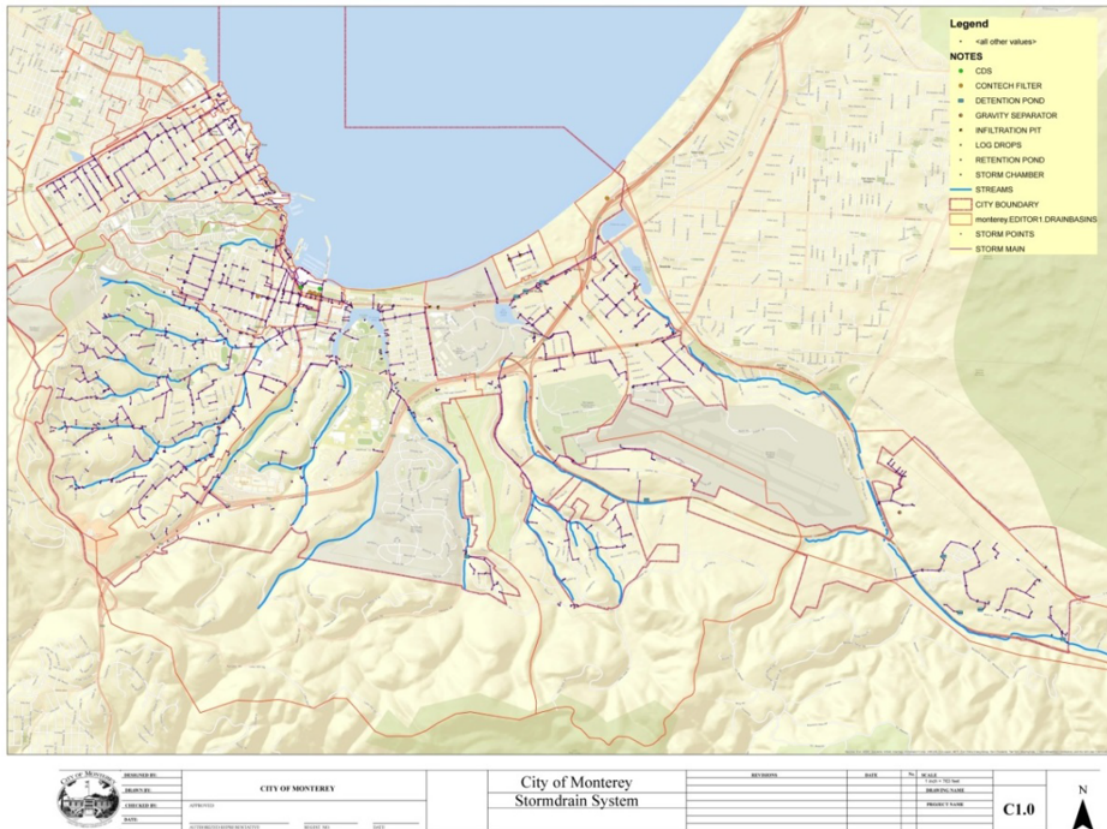
Figure 5.7. City of Monterey stormwater system map. Source: [19].

In the graphic above, there are two additional important features to highlight. The purple lines represent storm drainage lines and the purple dots along the storm drainage lines are storm points.

Building upon previous models, a limited number of Layer 1a sensors are placed in the UMI. We assume emplacement is hasty without perfect knowledge of UMI. The model uses Layer 1a and Layer 1b sensors to compare probabilities of detection. Figure 5.8 depicts the situation template when one enemy force attacking a defending force.
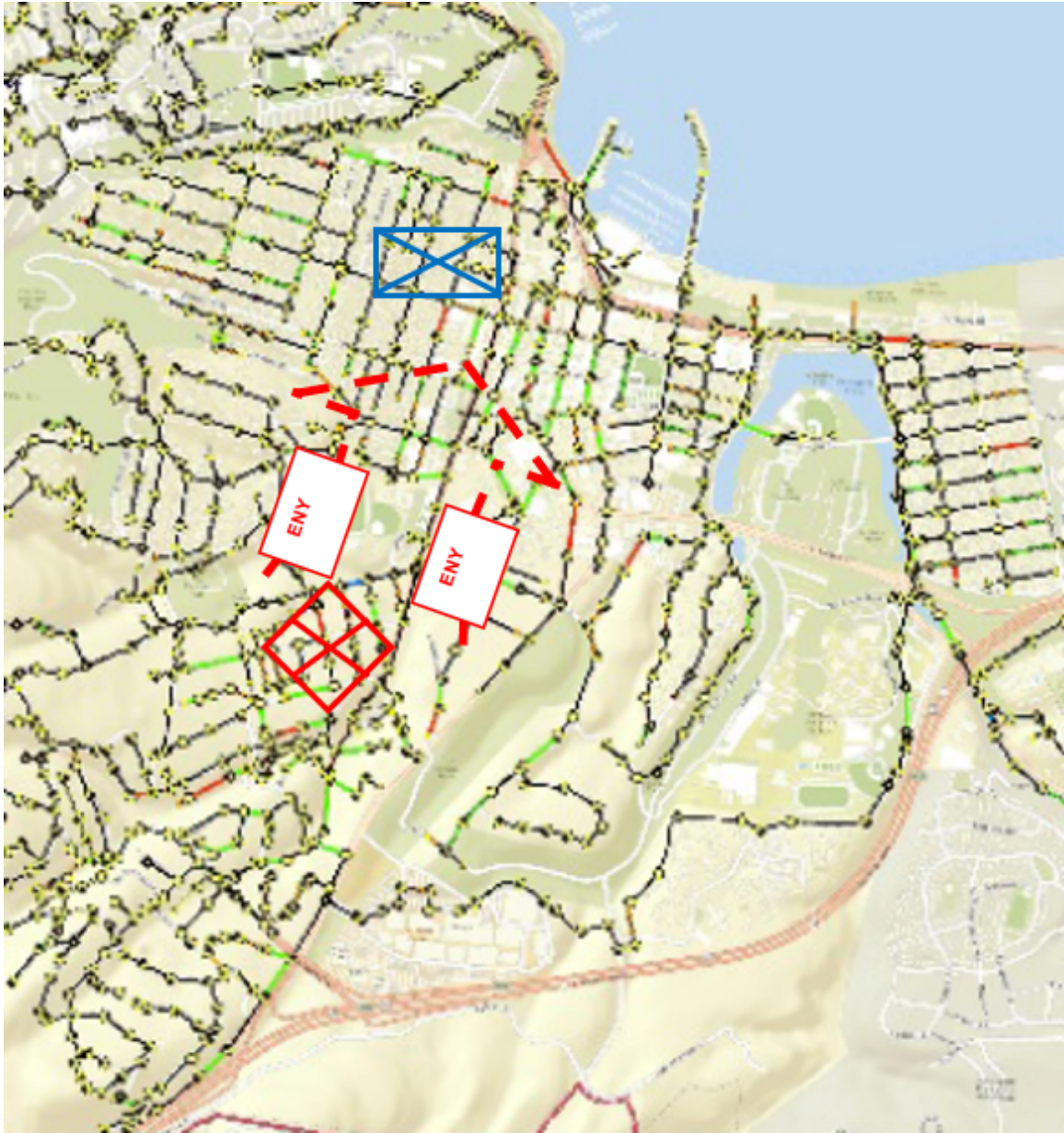
Figure 5.8. A situation template of an enemy force's movement toward a friendly force

Suppose the city block highlighted in Figure 5.9 has twelve UMI entry points to the operating area, eleven sewer system entry points, and one stormwater drainage entry point.

Figure 5.9. A diagram of the UMI underneath a city block in Monterey, CA.

As shown in Figure 5.10, the first model evaluates the probability of detection of four sensors placed on each block corner.

Figure 5.10. The purple circles are possible locations of sensors to detect targets.

The situation template graphic above is translated into a Markov chain diagram in Figure 5.11.

Twelve Routes, One Sensor on each Block Corner
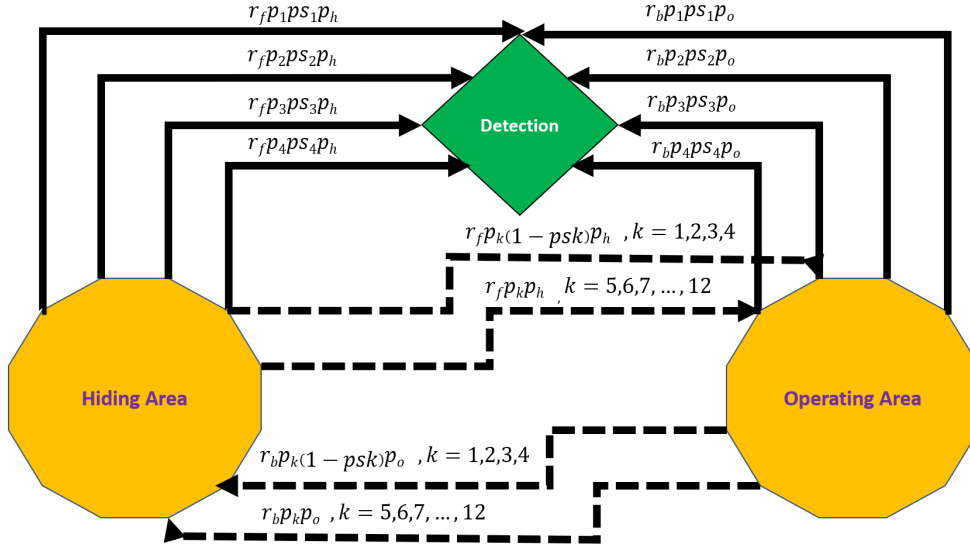
Figure 5.11. Diagram of Markov chain representing Twelves Routes, One Sensor on Each Block Corner

The equation reflects additional sensors and routes.

$$\frac{dp_h}{dt} = -r_f p_h + r_b[p_1(1-ps_1) + p_2(1-ps_2) + p_3(1-ps_3) + p_4(1-ps_4)$$
$$+ p_5 + p_6 + p_7 + p_8 + p_9 + p_{10} + p_{11} + p_{12}]p_o \tag{5.46}$$

$$\frac{dp_0}{dt} = -r_b p_o + r_f[p_1(1-ps_1) + p_2(1-ps_2) + p_3(1-ps_3) + p_4(1-ps_4)$$
$$+ p_5 + p_6 + p_7 + p_8 + p_9 + p_{10} + p_{11} + p_{12}]p_h \tag{5.47}$$

5.10 Twelve Routes, One Sensor on Eight Routes

The next model adds one Layer 1b sensor to four UMI intersection. Given the most recent model where a target's probability of selecting routes 1, 2, 3, and 4 is .120,

1.

and the probability of selecting the remaining routes is .065. All other parameters remain constant.

In the Figure 5.12 map, the additional sensors are highlighted by green circles.

Figure 5.12. The green circles are additional locations of sensors

With the addition of Layer 1b sensors, the model can detect all targets traveling into and out of the operating area.

$$
\begin{aligned}
\frac{dp_h}{dt} = {} & -r_f p_h + r_b [p_1(1 - ps_1) + p_2(1 - ps_2) + p_3(1 - ps_3) + p_4(1 - ps_4) \\
& + p_5(1 - ps_5) + p_6(1 - ps_6) + p_7(1 - ps_1) + p_8(1 - ps_2) + p_9 \\
& + p_{10} + p_{11} + p_{12}] p_o
\end{aligned}
\tag{5.48}
$$

Note, the ps_i value resets after ps_6 because there are only six defined sensors in the model.

$$\frac{dp_0}{dt} = -r_b p_o + r_f[p_1(1 - ps_1) + p_2(1 - ps_2) + p_3(1 - ps_3) + p_4(1 - ps_4)$$
$$+p_5(1 - ps_5) + p_6(1 - ps_6) + p_7(1 - ps_1) + p_8(1 - ps_2) + p_9 \qquad (5.49)$$
$$+p_{10} + p_{11} + p_{12}]p_h$$

A model that covers all routes will result in similar outcomes to Two Routes covered by one sensor each.

5.11 Multiple Hiding Areas, Routes, Entering a Single Operating Area

Finally, the AB^3C model adds additional hiding areas. The new models, A^2B^6C, $A^3B^{12}C$, represents multiple enemy hiding areas and model the sensors' ability to work as a network. An overview of the UMI precedes an updated Markov chain and system of equations.

Doctrinally, shown in Figure 5.13, the models attempt to replicate a unit conducting a hasty defense with an approximate 2:1 enemy to friendly ratio (Doctrinally, Hasty Defense is considered 2.5:1).

Friendly Mission	Position	Friendly : Enemy
Delay		1:6
Defend	Prepared or fortified	1:3
Defend	Hasty	1:2.5
Attack	Prepared or fortified	3:1
Attack	Hasty	2.5:1
Counterattack	Flank	1:1

Figure 5.13. FM 6-0 Historical Planning Force Ratio Table [20]

This situation may arise during initial entry into an urban area. Doctrinally, the situation looks like the following graphic, Figure 5.14.
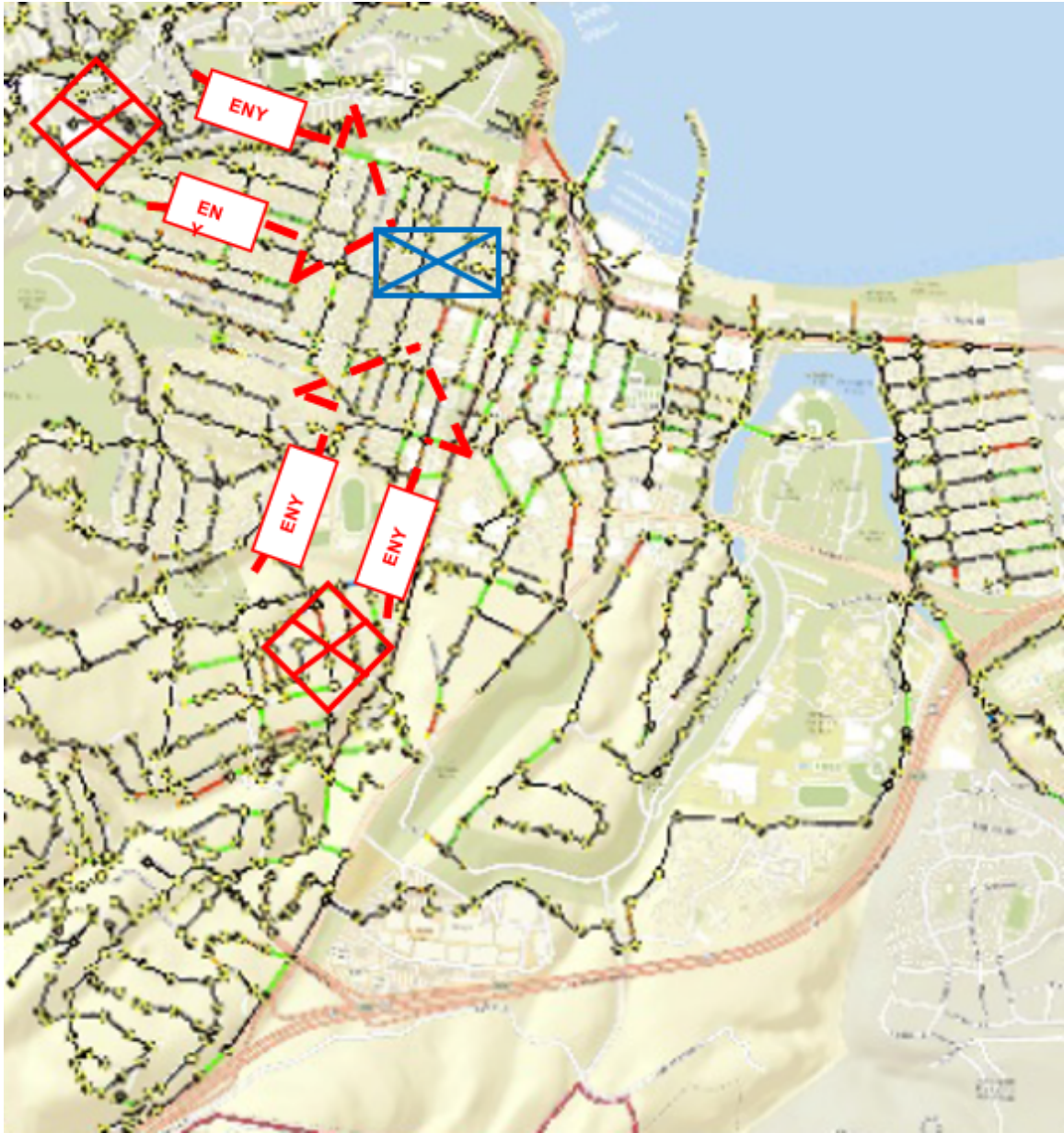
Figure 5.14. Situational template representing two hiding areas, one operating area and six routes

The situation template graphic above is translated into a Markov chain diagram in Figure 5.15 and Figure 5.16 where attacking enemy units coming into contact with one another on routes p_3 and p_4. There is also a probability of detect on each route.

Two Hiding Areas, Six Routes, One Sensor on each Route Overview
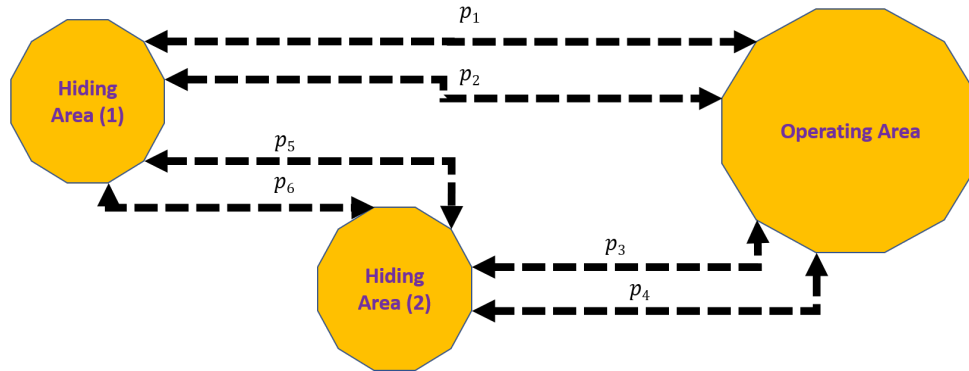
Figure 5.15. Diagram of Markov Chain representing Two Hiding Areas, One Operating Area and twelve Routes.

Two Hiding areas, Six Routes, One Sensor on each Route
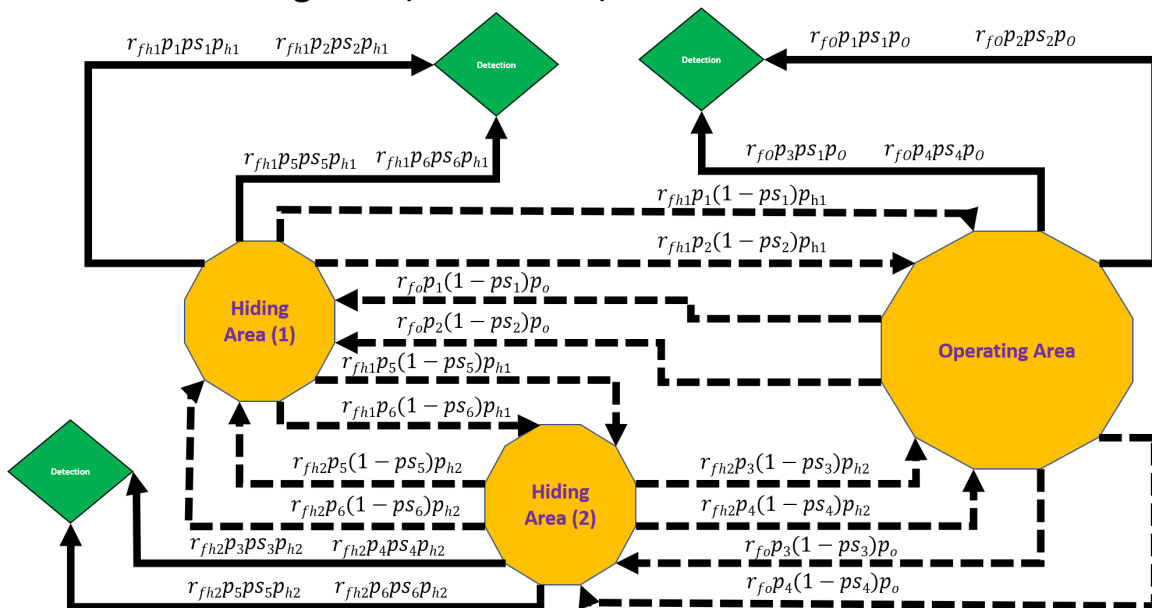
Figure 5.16. An expanded diagram of Markov chain representing two hiding areas, one operating area and six routes

.

The model can analyze two coordinated attacking units, but unlike Figure 5.15 and Figure 5.16 there is no probability of detection between hiding areas.

$$\frac{dp_{h1}}{dt} = -r_{fh1}p_{h1} + r_{fh2}[p_5(1 - ps_5) + p_6(1 - ps_6)]p_{h2} + r_{fo}[p_1(1 - ps_1) + p_2(1 - ps_2)]p_o$$

$$(5.50)$$

$$\frac{dp_{h2}}{dt} = -r_{fh2}p_{h2} + r_{fh1}[p_5(1 - ps_5) + p_6(1 - ps_6)]p_{h1} + r_{fo}[p_3(1 - ps_3) + p_4(1 - ps_4)]p_o$$

$$(5.51)$$

$$\frac{dp_o}{dt} = -r_{fo}p_o + r_{fph1}[p_1(1 - ps_1) + p_2(1 - ps_2)]p_{h1} + r_{fh2}[p_3(1 - ps_3) + p_4(1 - ps_4)]p_{h2}$$

$$(5.52)$$

The next model adds another hiding area. Doctrinally, the model replicates a unit conducting a deliberate defense with a 3:1 enemy to friendly ratio. Three hiding areas represent three company target assault positions ready to attack a friendly company defensive position in an urban environment. This situation is likely to arise after initial entry into an urban area. The three attacking units' movement may be coordinated, but they do not come into contact with one another. Doctrinally, the situation looks like the following graphic, Figure 5.17.
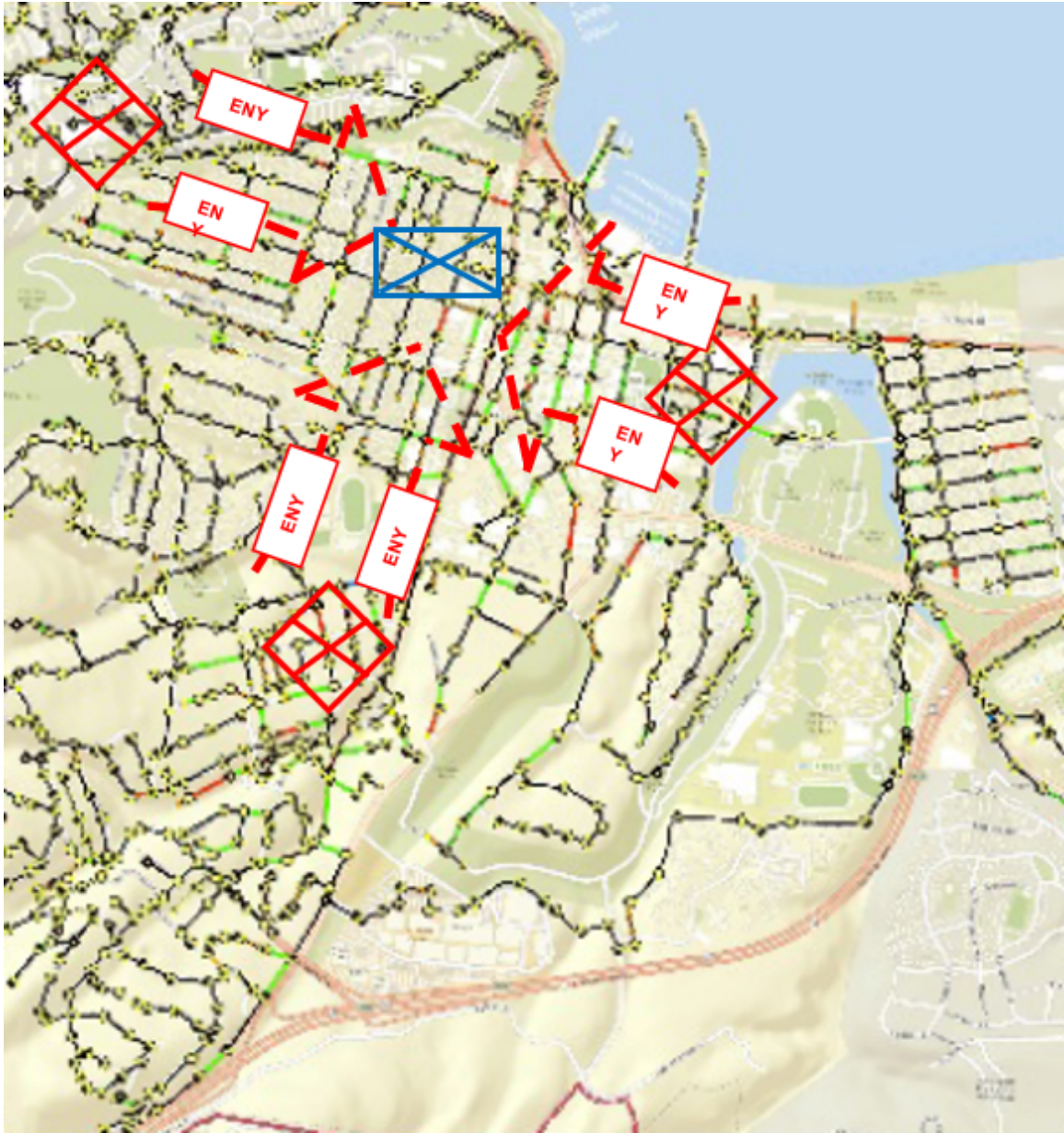
Figure 5.17. Situational Template representing three hiding areas, one operating area and twelve routes.

The situation template graphic above is translated into a Markov chain diagram illustrated in Figure 5.18 followed by the system of equations.

Three Hiding areas, Twelve Routes, One Sensor on each Route Overview
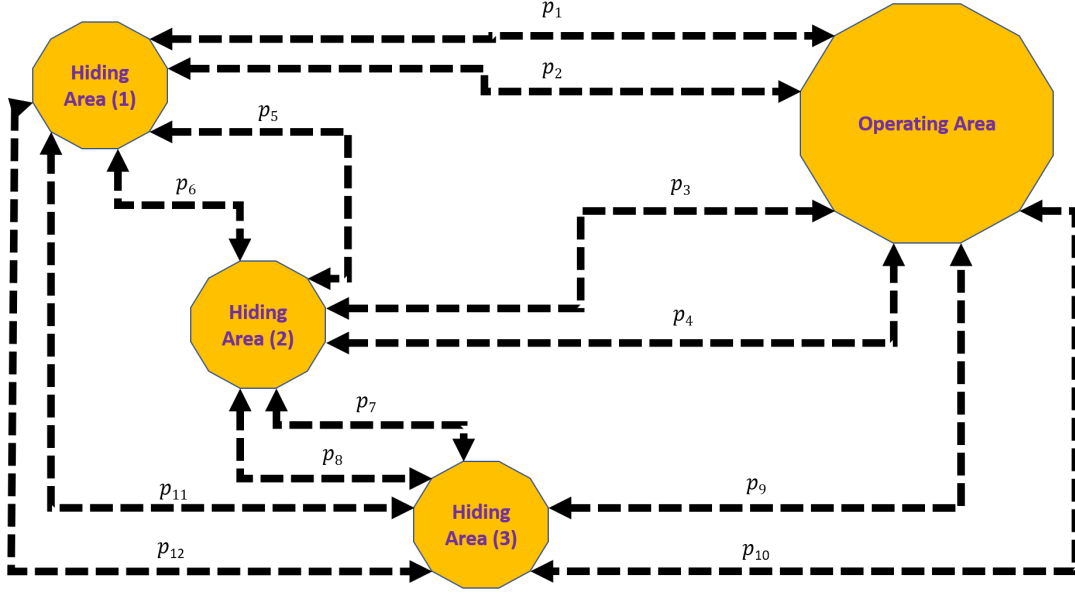
Figure 5.18. Diagram of Markov chain representing three hiding areas, one operating area and twelve routes

.

$$\frac{dp_{h1}}{dt} = -r_{fh1}p_{h1} + r_{fh2}[p_5(1 - ps_5) + p_6(1 - ps_6)]p_{h2} + r_{fh3}[p_{11}(1 - ps_5)$$
$$+ p_{12}(1 - ps_6)]p_{h3} + r_{fo}[p_1(1 - ps_1) + p_2(1 - ps_2)]p_o$$
(5.53)

$$\frac{dp_{h2}}{dt} = -r_{fh2}p_{h2} + r_{fh1}[p_5(1 - ps_5) + p_6(1 - ps_6)]p_{h1} + r_{fh3}[p_7(1 - ps_1)$$
$$+ p_8(1 - ps_2)]p_{h3} + r_{fo}[p_3(1 - ps_3) + p_4(1 - ps_4)]p_o$$
(5.54)

$$\frac{dp_{h3}}{dt} = -r_{fh3}p_{h3} + r_{fh1}[p_{11}(1 - ps_5) + p_{12}(1 - ps_6)]p_{h1} + r_{fh2}[p_7(1 - ps_1)$$
$$+ p_8(1 - ps_2)]p_{h2} + r_{fo}[p_9(1 - ps_3) + p_{10}(1 - ps_4)]p_o$$
(5.55)

$$\frac{dp_0}{dt} = -r_{fo}p_o + r_{fh1}[p_1(1 - ps_1) + p_2(1 - ps_2)]p_{h1} + r_{fh2}[p_3(1 - ps_3)$$
$$+ p_4(1 - ps_4)]p_{h2} + r_{fh3}[p_9(1 - ps_3) + p_{10}(1 - ps_4)]p_{h3}$$
(5.56)

48

The three attacking units' movement may be coordinated, but there is no probability of detection between hiding areas. Unlike all previous models which have a uniform travel rate from each area, the next model, seen in Figure 5.19, incorporates unique rates for each route. This enhances the model's ability to replicate each obstacle effect.

Three Hiding areas, Twelve Routes, One Sensor on each Route Overview
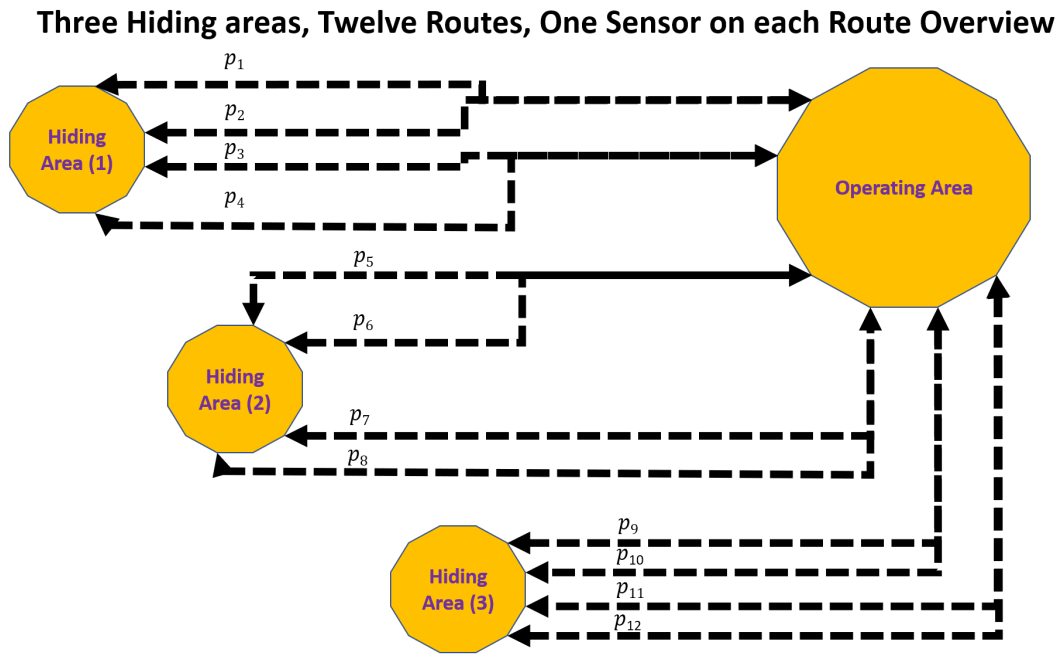
Figure 5.19. Diagram of Markov chain representing three hiding areas, one operating area and twelve routes

.

Chapter 6 shows the results from MATLAB's ODE45 solver program and analyzes the performance of each model.

THIS PAGE INTENTIONALLY LEFT BLANK

CHAPTER 6:
Results and Analysis

The models in this chapter incrementally build from one model to the next. Depending on the reader's understanding of Markov chains and differential equations, it may be advantageous to bypass the simpler mathematical models and proceed to Section 6.6. When a model produces a significant result, subsequent models will use that result in order to test other parameters. By the last section, the models aim to analyze impactful results for the U.S. military and lead to a thought provoking conclusion.

6.1 One Route without Sensor on Route

Recall the original ABC model consisting of one hiding area, one route representing a sewage or drainage line running from a hidden area into an operating area. Since no sensors are present, the probability of detection does not exist resulting in the system achieving a steady state. The results of steady state probabilities of P_h and P_o are shown in Figure 6.1
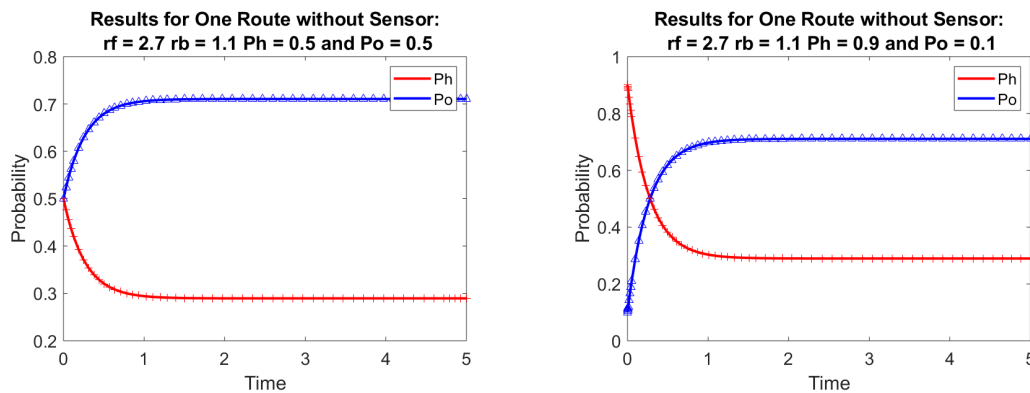
Figure 6.1. The graph shows probability of target location over time while P_h and P_o values change from .50/.50 on the left graph to .90/.10 on the right graph. The rates values, r_f and r_b, are held constant at 2.7 and 1.1, respectively.

The steady state general equation yields the steady state probabilities of P_h and P_o given $r_f = 2.7$ and $r_b = 1.1$.

The probability a target is in the hiding area at steady state:

$$P_h^{(S)} = \frac{r_b}{r_f + r_b} \tag{6.1}$$

$$P_h^{(S)} = \frac{1.1}{3.8} = 0.289. \tag{6.2}$$

The probability a target is in the operating area at steady state:

$$P_o^{(S)} = \frac{r_f}{r_b + r_f} \tag{6.3}$$

$$P_o^{(S)} = \frac{2.7}{3.8} = 0.711. \tag{6.4}$$

Both graphs in Figure 6.1 achieve the steady state of $P_h^{(S)} = 0.289$ and $P_o^{(S)} = 0.711$. While this model yields no significant results, the steady state solutions are independent of a target's initial location. The target's rates, r_f and r_b parameters, are more important to the target's behavior and model's performance. The next model validates MATLAB ODE45 program solver's solution against the analytical and numerical solutions.

6.2   One Route with Sensor on Route

With the addition of a sensor, the probability of detection changes over time when the parameter values change. The resulting probabilities of $P_h(t)$ and $P_o(t)$ are shown in Figure 6.2 and probabilities of detection are shown in Figure 6.3.
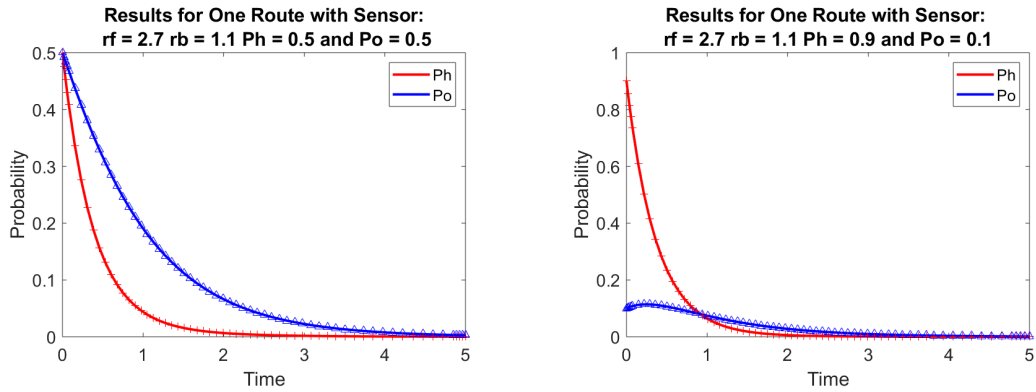
Figure 6.2. The graph shows probability of target location over time with the addition of a sensor with a probability of detection ps_i, P_h and P_o values change from .50/.50 on the left graph to .90/.10 on the right graph , r_f and r_b values are held constant at 2.7 and 1.1, respectively.
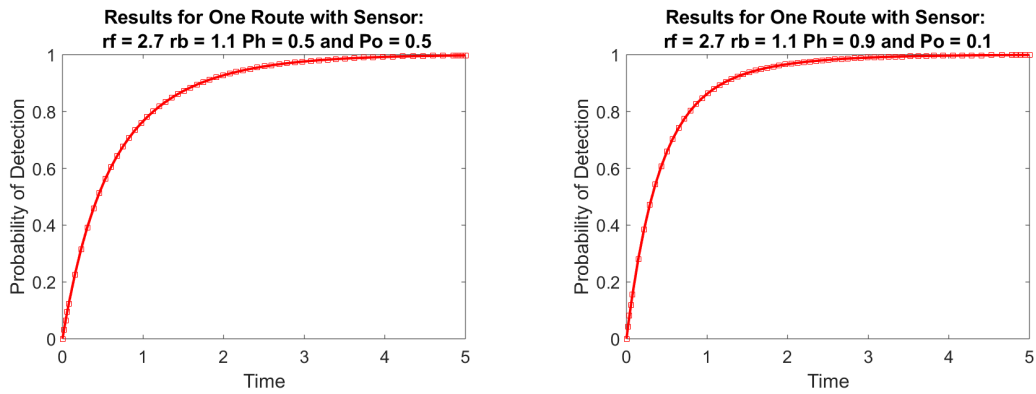
Figure 6.3. The graph depicts the probability of detection results over time depicted graphically for an addition of a sensor with a probability of detection ps_i, P_h and P_o values change from .50/.50 on the left graph to .90/.10 on the right graph , r_f and r_b values are held constant at 2.7 and 1.1, respectively.

The discrete results from the figures above are shown in Tables 6.1 and 6.2.

Table 6.1. Time versus Probability when $P_h = 0.5$ and $P_o = 0.5$ values change, $r_f = 2.7$ and $r_b = 1.1$

t	P(t)
0	0
1.00	0.7658
2.00	0.9275
3.00	0.9759
4.00	0.9919
5.00	0.9972

Table 6.2. Time versus Probability when $P_h = 0.9$ and $P_o = 0.1$ values change, $r_f = 2.7$ and $r_b = 1.1$

t	P(t)
0	0
1.00	0.8619
2.00	0.9664
3.00	0.9895
4.00	0.9965
5.00	0.9988

With constant rates forward and backward, the more drastic differences in a target's initial location yield higher probabilities of detection at each time interval. A comparison of the results in Tables 6.1 and 6.2 are shown in Table 6.3.

Table 6.3. Difference of Probabilities of Detection Figure 6.3's left-side and right-side results.

t	Difference in P(t)
0	0
1.00	0.0961
2.00	0.0389
3.00	0.0134
4.00	0.0041
5.00	0.0016

54

Analyzing results in from Figure 6.3 and Table 6.3, after one interval of time, the probability of detection increase by 9.61% from after varying P_h and P_o values.

Next, the rate forward value, r_f, increases to 3.7. The resulting probabilities of $P_h(t)$ and $P_o(t)$ are shown in Figure 6.4 and probabilities of detection are shown in Figure 6.5.

Figure 6.4. The graph shows probability of target location over time with the addition of a sensor with a probability of detection ps_i, P_h and P_o values change from .50/.50 on the left graph to .90/.10 on the right graph , r_f and r_b values are held constant at 3.7 and 1.1, respectively.

Figure 6.5. The graph depicts the probability of detection results over time depicted graphically for an addition of a sensor with a probability of detection ps_i, P_h and P_o values change from .50/.50 on the left graph to .90/.10 on the right graph , r_f and r_b values are held constant at 3.7 and 1.1, respectively.

The discrete results from the figures above are shown in Tables 6.4 and 6.5.

Table 6.4. Time versus Probability when $P_h = 0.5$ and $P_o = 0.5$ values change, $r_f = 3.7$ and $r_b = 1.1$

t	P(t)
0	0
1.00	0.7902
2.00	0.9322
3.00	0.9771
4.00	0.9923
5.00	0.9974

Table 6.5. Time versus Probability when $P_h = 0.9$ and $Po = 0.1$ values change, $r_f = 3.7$ and $r_b = 1.1$

t	P(t)
0	0
1.00	0.9018
2.00	0.9726
3.00	0.9909
4.00	0.9969
5.00	0.9990

After comparing Figure 6.3, and Figure 6.5 and corresponding Table 6.4 and Table 6.5, the increase in rates forward by 1.0 improves the probabilities of detection seen in Table 6.6 .

Table 6.6. Difference of Probabilities of Detection Figure 6.5's left-side and right-side results.

t	Difference in P(t)
0	0
1.00	0.1116
2.00	0.0404
3.00	0.0138
4.00	0.0046
5.00	0.0016

Increasing the rate forward from 2.7 in Figures 6.2 and 6.3 to 3.7 in Figures 6.4 and Figure 6.5 resulted in a increase from 9.61% to 11.16% after 1 interval of time.

The target's rate forward and rate backward influence the model's behavior more than the target's initial condition.

MATLAB's ODE45 program solver validates the following analytical solution and subsequent results for the remain 2x2 system of equations. The rate of change over time in the hiding area A is

$$\frac{dp_h}{dt} = ap_h + bp_o, \tag{6.5}$$

while the rate of change over time in the operating area is

$$\frac{dp_o}{dt} = dp_h + cp_o. \tag{6.6}$$

Together, a 2x2 matrix represents the rate of change over A and C over time t, when $P_h = 0.5$ and $P_o = 0.5$ values change, $r_f = 2.7$ and $r_b = 1.1$ and assume $ps_1 = .90$ is

$$\frac{d}{dt}\begin{bmatrix} p_h \\ p_o \end{bmatrix} = A \begin{bmatrix} p_h \\ p_o \end{bmatrix} = \begin{bmatrix} -2.7000 & .1100 \\ .2700 & -1.1000 \end{bmatrix} \begin{bmatrix} p_h \\ p_o \end{bmatrix}. \tag{6.7}$$

To solve for the eigenvalues, take the determinant of the following transposed matrix and set it equal to 0.

$$det(\lambda I - A) = \begin{bmatrix} \lambda - (2.7000) & -.1100 \\ -.2700 & \lambda - (1.1000) \end{bmatrix} = 0 \tag{6.8}$$

Taking determinant results in the following quadratic equations.

$$\lambda^2 - (3.800)\lambda + 2.9403 = 0 \tag{6.9}$$

The quadratic formula solves our roots, λ_1 and λ_2.

$$\lambda_{1,2} = \frac{-(3.800) \pm \sqrt{(3.800)^2 - 4(2.9403)}}{2}, \lambda_1 \neq \lambda_2, \tag{6.10}$$

The eigenvalues, λ_1 and λ_2, are

$$\lambda_1 = -2.7184, \lambda_2 = -1.0816. \tag{6.11}$$

Solve for the constant coefficients C_1 and C_2 using Equations 5.18 and 5.21.

$$C_1 = 0.5878 \tag{6.12}$$

$$C_2 = 0.3877 \tag{6.13}$$

The explicit solution is for the escape probability is

$$p_h(t) + p_o(t) = 0.5878e^{-2.7184t} + 0.3877e^{-1.0816t} \tag{6.14}$$

The probability of detection at $t = 5$ is

$$p_h(5) + p_o(5) = 0.0026, 1 - 0.0026 = 0.9974 \tag{6.15}$$

Figure 6.6 graphically compares the ODE45's solver solution to the analytical solution.
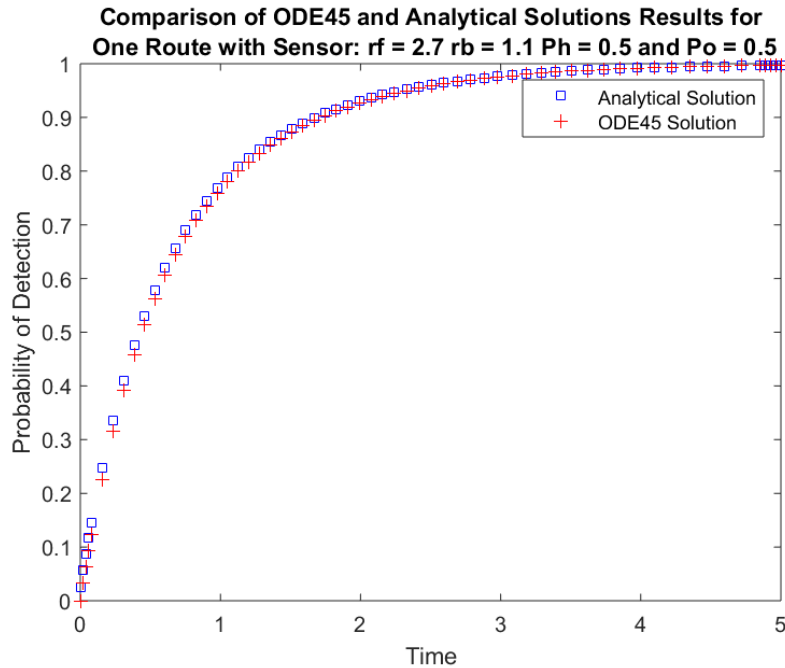
Figure 6.6. MATLAB ODE45 and Analytical Solution Comparison when $Ph = .50$, $P0 = .50$, $r_f = 2.7$ and $r_b = 1.1$

For a 2x2 system, MATLAB's ODE45 results are nearly identical when compared to the analytical solution.

6.3 Two Routes, One Sensor placed on Route 1

As explained in Chapter 5, this Section's models have two routes, but only route 1 has a sensor detecting targets. Section shows "how costly" uncovered routes are to operations.

Unless noted otherwise, the target has a 50% chance of selecting Route 1 or Route 2 to move between the hiding area and operating area. Knowing how difficult and resource extensive covering each route may be, units may choose to cover one route over another based on intelligence or variety of other factors. Since greater rf, rb values yield a higher probability of detection, models focus on the results of changing initial conditions but reinforce our results from the previous section. The resulting probabilities of $P_h(t)$ and $P_o(t)$ are shown in Figure 6.7 and probabilities of detection are shown in Figure 6.8.
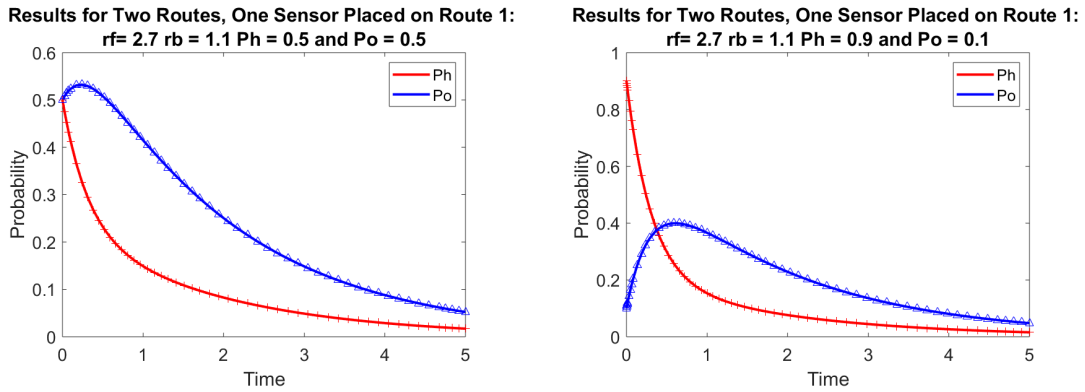
Figure 6.7. The graph shows probability of target location over time with the addition of a sensor with a probability of detection ps_i, P_h and P_o are .50/.50 , r_f and r_b values are held constant at 2.7 and 1.1, respectively.
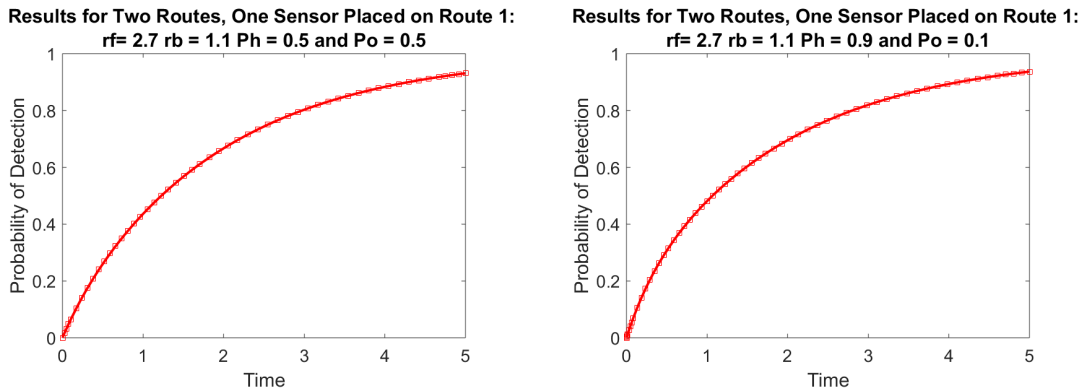
Figure 6.8. The graph depicts the probability of detection results over time depicted graphically for a sensor with a probability of detection ps_i covering one of two routes, P_h and P_o are .50/.50 , r_f and r_b values are held constant at 2.7 and 1.1, respectively.

The discrete results from the figures above are shown in Tables 6.7 and 6.8.

Table 6.7. Time versus Probability when $Ph = 0.5$ and $Po = 0.5$ values change, $r_f = 2.7$ and $r_b = 1.1$

t	P(t)
0	0
1.00	0.4361
2.00	0.6670
3.00	0.8027
4.00	0.8831
5.00	0.9308

Table 6.8. Time versus Probability when $P_h = 0.9$ and $Po = 0.1$ values change, $r_f = 2.7$ and $r_b = 1.1$

t	P(t)
0	0
1.00	0.4812
2.00	0.6954
3.00	0.8196
4.00	0.8932
5.00	0.9367

Obviously, the probability of detection decreases with the addition of an uncovered route when comparing results from Figure 6.5, the previous model of one sensor on covering a single route, to Figure 6.8 above. In short, adding an uncovered route significantly decreases the probability of detection no matter the performance of a sensor.

A comparison of the results in Tables 6.7 and 6.8 are shown in Table 6.9.

Table 6.9. Difference of Probabilities of Detection Figure 6.8's left-side and right-side results.

t	Difference in P(t)
0	0
1.00	0.0451
2.00	0.0284
3.00	0.0169
4.00	0.0101
5.00	0.0059

With constant forward and backward rates, adjusting the initial conditions, the target's initial location, results in higher probabilities of detection after one interval of time. The probability of detection after one interval of time increased from 43.61% in 48.12% in Figure 6.8.

Next, the following models analyzes increasing rf to 3.7 and compare its results. The resulting probabilities of $P_h(t)$ and $P_o(t)$ are shown in Figure 6.9 and probabilities of detection are shown in Figure 6.10.

Figure 6.9. The graph shows probability of target location over time with the addition of a sensor with a probability of detection ps_i, P_h and P_o are .50/.50 , r_f and r_b values are held constant at 3.7 and 1.1, respectively.

Results for Two Routes, One Sensor Placed on Route 1:
rf= 3.7 rb = 1.1 Ph = 0.5 and Po = 0.5

Results for Two Routes, One Sensor Placed on Route 1:
rf= 3.7 rb = 1.1 Ph = 0.9 and Po = 0.1

Figure 6.10. The graph depicts the probability of detection results over time depicted graphically for a sensor with a probability of detection ps_i covering one of two routes, P_h and P_o are .50/.50 , r_f and r_b values are held constant at 3.7 and 1.1, respectively.

The discrete results from the figures above are shown in Tables 6.10 and 6.11.

Table 6.10. Time versus Probability when $P_h = 0.5$ and $P_o = 0.5$ values change, $r_f = 3.7$ and $r_b = 1.1$

t	P(t)
0	0
1.00	0.4686
2.00	0.6951
3.00	0.8247
4.00	0.8992
5.00	0.9421

Table 6.11. Time versus Probability when $P_h = 0.9$ and $P_o = 0.1$ values change, $r_f = 3.7$ and $r_b = 1.1$

t	P(t)
0	0
1.00	0.5238
2.00	0.7276
3.00	0.8434
4.00	0.9100
5.00	0.9482

The increase in r_f by 1.0 increases the probabilities of detection to about 50% (Figure 6.10), but is low due to the uncovered route. A comparison of the results in Tables 6.10 and 6.11 are shown in Table 6.12.

Table 6.12. Difference of Probabilities of Detection Figure 6.10's left-side and right-side results.

t	Difference in P(t)
0	0
1.00	0.0552
2.00	0.0325
3.00	0.0187
4.00	0.0108
5.00	0.0061

Increasing the rate forward from 2.7 in Figure 6.8 to 3.7 in Figure 6.10 resulted in an increase from 4.51% to 5.52% after one interval of time. The 1.01% increase in early warning is moderate and Commanders may not warrant employing unique capabilities to obtain the desired effect to increased movement rate of targets through a certain UMI is worth the risk.

However, after adjusting the initial conditions from $P_h = 0.5$ and $P_h = 0.5$ to $P_h = 0.9$ and $P_h = 0.1$ in Figure 6.9 and Figure 6.10 the probability of detection is increased by 5.52%. The 5.52% is significant and may motivate a commander to employ unique capabilities to

obtain the desired effect. Although the increase would help provide early warning to units, the enemy does get a say in the fight.

Until this point, the models offer targets a 50% probability of selecting Route 1 and Route 2 when moving between a hiding area to an operating area. On the first run, model introduces a 75% probability of selecting Route 1 and a 25% probability of selecting Route 2 when moving from a hiding area to an operating area. On the return from the operating area to the hiding area, targets had a 25% probability of selecting Route 1 and a 75% probability of selecting Route 2. The percentages are flipped during the model's second run. The resulting probabilities of $P_h(t)$ and $P_o(t)$ are shown in Figure 6.11 and probabilities of detection are shown in Figure 6.12.

Figure 6.11. The graph shows probability of target location over time with the addition of a sensor with a probability of detection ps_i, P_h and P_o are .50/.50, r_f and r_b values are held constant at 3.7 and 1.1, respectively. However, the probability of selecting route p_k changes between .75 and .25 depending on the direction of travel.

Figure 6.12. The graph depicts the probability of detection results over time depicted graphically for a sensor with a probability of detection ps_i covering one of two routes, P_h and P_o are .50/.50, r_f and r_b values are held constant at 3.7 and 1.1, respectively. However, the probability of selecting route p_k changes between .75 and .25 depending on the direction of travel.

The discrete results from the figures above are shown in Tables 6.13 and 6.14.

Table 6.13. Time versus Probability when P_{k1} = .75, P_{k2} = .25, P_{k3} = .25, P_{k4} = .75, P_h = 0.5 and P_o = 0.5, r_f = 3.7 and r_b = 1.1

t	P(t)
0	0
1.00	0.5159
2.00	0.7321
3.00	0.8511
4.00	0.9173
5.00	0.9540

66

Table 6.14. Time versus Probability when $P_{k1} = .25$, $P_{k2} = .75$, $P_{k3} = .75$, $P_{k4} = .25$, $P_h = 0.5$ and $P_o = 0.5$, $r_f = 3.7$ and $r_b = 1.1$

t	P(t)
0	0
1.00	0.4480
2.00	0.6933
3.00	0.8296
4.00	0.9053
5.00	0.9474

While holding the rates constant, results above show adjusting initial conditions impacts the probability of detection. A comparison of the results in Tables 6.10 and 6.11 are shown in Table 6.15.

Table 6.15. Time versus Probability Comparison between Figure 6.12's left-side and right-side results.

t	Difference in P(t)
0	0
1.00	0.0679
2.00	0.0388
3.00	0.0215
4.00	0.0120
5.00	0.0066

Influencing the probability of route selection increased probability of detection from 46.86% from Figures 6.9 and 6.10 to 51.59% in Figure 6.11 and Figure 6.12 resulting in an increase of 4.73% after one interval of time. However, negative influences can have the opposite effect and decrease the probability of detection by 2.06%. In this case, the reward outweighs the risk.

Lastly, the model introduces a 90% probability of selecting Route 1 and a 10% probability of selecting Route 2 when moving from a hiding area to an operating area. On the return from the operating area to the hiding area targets had a 10% probability of selecting Route

1 and a 90% probability of selecting Route 2. The resulting probabilities of $P_h(t)$ and $P_o(t)$ are shown in Figure 6.13 and probabilities of detection are shown in Figure 6.14.

Results for Two Routes, One Sensor Placed on Route 1:
rf= 3.7 rb = 1.1 Ph = 0.5 and Po = 0.5

Figure 6.13. The graph shows probability of target location over time with the addition of a sensor with a probability of detection ps_i, P_h and P_o are .50/.50, r_f and r_b values are held constant at 3.7 and 1.1, respectively. However, the probability of selecting route p_k varies between .90 and .10 depending on the direction of travel.

.

Figure 6.14. The graph depicts the probability of detection results over time depicted graphically for a sensor with a probability of detection ps_i covering one of two routes, P_h and P_o are .50/.50, r_f and r_b values are held constant at 3.7 and 1.1, respectively. However, the probability of selecting route p_k varies between .75 and .25 depending on the direction of travel.

.

The discrete results from the figures above are shown in Tables 6.16.

Table 6.16. Time versus Probability when $P_{k1} = .90$, $P_{k2} = .10$, $P_{k3} = .10$, $P_{k4} = .90$, $P_h = 0.5$ and $P_o = 0.5$, $r_f = 3.7$ and $r_b = 1.1$

t	P(t)
0	0
1.00	0.5554
2.00	0.7673
3.00	0.8776
4.00	0.9356
5.00	0.9661

Lastly, after increasing probability of a target selecting Route 1 to 90%, the probability of detection increased to 3.95% in Figure 6.14.

Although increasing the hiding area's initial condition helps provide early warning to units,

69

the enemy does get a say in the fight. As much as commanders would like to dictate enemy movements, it is unreasonable to expect. Conversely, if the operating area's initial condition is greater than the hiding area, then the probability of detection decreases.

In the next model, commanders have the ability to influence targets to use or avoid certain UMI, which is promising to increase the probability of detection, especially if units are unable to cover all possible routes with sensors. Unless otherwise noted, the rf, rb values of 2.7 and 1.1, respectively, will be used exclusively. This allows for a better understanding of how other factors increase or decrease models' probability of detection.

6.4 Two Routes, Two Sensors on Route 1

With additional time, units are able to place an additional sensor on Route 1. First, a unit places a Layer 1a sensor on Route 1. After some time, the units add a Layer 1b sensor to the same route to provide redundancy. This model analyzes if multiple sensors on a single route significantly improve probability of detection and early warning. Route 2 remains uncovered.

Recall the probability of detection of Layer 1a sensors is significantly less than the probability of detection of Layer 1b sensors.

The resulting probabilities of $P_h(t)$ and $P_o(t)$ are shown in Figure 6.15 and probabilities of detection are shown in Figure 6.16.

Results for Two Routes, One Sensor Placed on Route 1:
rf= 2.7 rb = 1.1 Ph = 0.5 and Po = 0.5
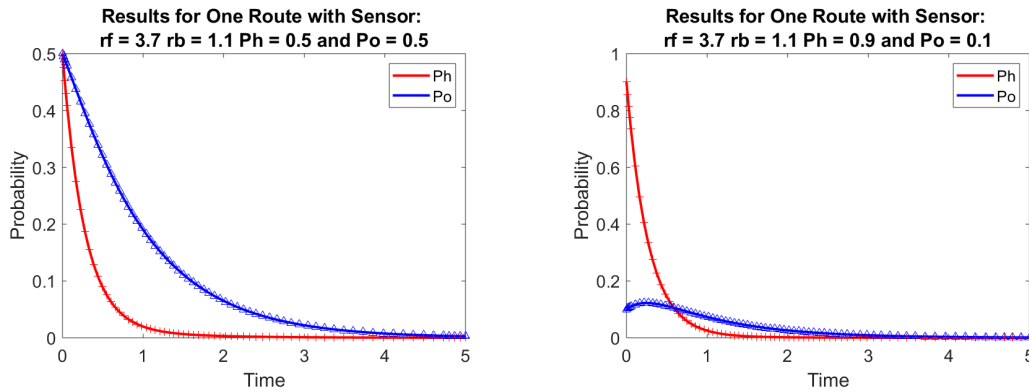
Figure 6.15. The graph shows probability of target location over time with two Layer 1a sensors with a probability of detection ps_i covering one of two routes, P_h and P_o are .50/.50, r_f and r_b values are held constant at 2.7 and 1.1, respectively. However, the probability of selecting route p_k varies between .90 and .10 depending on the direction of travel.

.

Results for Two Routes, One Sensor Placed on Route 1:
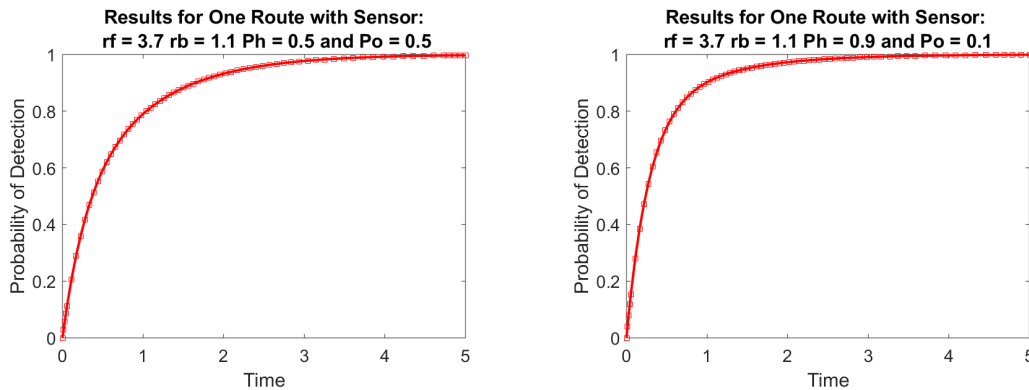**rf= 2.7 rb = 1.1 Ph = 0.5 and Po = 0.5**

Figure 6.16. The graph depicts the probability of detection results over time depicted graphically for two Layer 1a sensors with a probability of detection ps_i covering one of two routes, P_h and P_o are .50/.50, r_f and r_b values are held constant at 2.7 and 1.1, respectively.

.

71

The discrete results from the figures above are shown in Tables 6.17.

Table 6.17. Time versus Probability when P_h = 0.5 and P_o = 0.5 values change, r_f = 2.7 and r_b = 1.1

t	P(t)
0	0
1.00	0.3883
2.00	0.6118
3.00	0.7531
4.00	0.8430
5.00	0.9001

After one interval of time the probability of detection is 38.83%. However, with the addition of the second, Layer 1b, the results follow in Figure 6.17 and Figure 6.18.

Figure 6.17. The graph shows probability of target location over time with two Layer 1b sensors with a probability of detection ps_i covering one of two routes, P_h and P_o are .50/.50, r_f and r_b values are held constant at 2.7 and 1.1, respectively. However, the probability of selecting route p_k varies between .90 and .10 depending on the direction of travel.

.

Figure 6.18. The graph depicts the probability of detection results over time depicted graphically for two Layer 1b sensors with a probability of detection ps_i covering one of two routes, P_h and P_o are .50/.50, r_f and r_b values are held constant at 2.7 and 1.1, respectively.

.

The discrete results from the figures above are shown in Tables 6.18.

Table 6.18. Time versus Probability when $P_h = 0.5$ and $P_o = 0.5$ values change, $r_f = 2.7$ and $r_b = 1.1$

t	P(t)
0	0
1.00	0.5355
2.00	0.7678
3.00	0.8831
4.00	0.9411
5.00	0.9703

After running the models, there is a significant improvement in the probability of detection between Figure 6.15 and Figure 6.16 versus Figure 6.17 and Figure 6.18. However, the underwhelming performance of the Layer 1a probability of detection questions employing them in the first place.

Although emplacement of Layer 1b sensors is theoretically more cumbersome, the increased probability of detection seems to be worth the time and expense for emplacement, at least mathematically. Commanders must decide whether the additional time requirement and additional risk are worth an increased probability of detection.

6.5   Two Routes, One Sensor on each Route

Suppose sensors cover each route. It is the best option to provide the best chances of early warning. The following models will analyze pairing of Layer 1a and Layer 1b sensors across two routes.

First, units place a Layer 1a sensor on Route 1 and with another Layer 1a sensor on Route 2. The resulting probabilities of $P_h(t)$ and $P_o(t)$ are shown in Figure 6.19 and probabilities of detection are shown in Figure 6.20.

Figure 6.19. The graph shows probability of target location over time with two Layer 1a sensors with a probability of detection ps_i each covering one route, P_h and P_o are .50/.50, r_f and r_b values are held constant at 2.7 and 1.1, respectively.

Figure 6.20. The graph depicts the probability of detection results over time depicted graphically for two Layer 1a sensors with a probability of detection ps_i each covering one route, P_h and P_o are .50/.50, r_f and r_b values are held constant at 2.7 and 1.1, respectively.

The discrete results from the figures above are shown in Tables 6.19.

Table 6.19. Time versus Probability when $P_h = 0.5$ and $P_o = 0.5$ values change, $r_f = 2.7$ and $r_b = 1.1$

t	P(t)
0	0
1.00	0.6519
2.00	0.8615
3.00	0.9741
4.00	0.9911
5.00	0.9907

Next, units place a Layer 1a sensor on Route 1 and Layer 1b sensor on Route 2. The resulting probabilities of $P_h(t)$ and $P_o(t)$ are shown in Figure 6.21 and probabilities of detection are shown in Figure 6.22.

Results for Two Routes, One Sensor Placed on each Route:
rf= 2.7 rb = 1.1 Ph = 0.5 and Po = 0.5

Figure 6.21. The graph shows probability of target location over time with one Layer 1a sensor and Layer 1b sensor with a probability of detection ps_i and ps_j each covering one route, P_h and P_o are .50/.50, r_f and r_b values are held constant at 2.7 and 1.1, respectively.

Results for Two Routes, One Sensor Placed on each Route:
rf= 2.7 rb = 1.1 Ph = 0.5 and Po = 0.5

Figure 6.22. The graph depicts the probability of detection results over time depicted graphically for one Layer 1a sensor and one Layer 1b sensor with a probability of detection ps_i and ps_j each covering one route, P_h and P_o are .50/.50, r_f and r_b values are held constant at 2.7 and 1.1, respectively.

.

The discrete results from the figures above are shown in Tables 6.20.

Table 6.20. Time versus Probability when $P_h = 0.5$ and $P_o = 0.5$ values change, $r_f = 2.7$ and $r_b = 1.1$

t	P(t)
0	0
1.00	0.7031
2.00	0.8943
3.00	0.9610
4.00	0.9856
5.00	0.9946

The probability of detection difference between two Layer 1a sensor results shown in Figure 6.20 and Layer 1b sensor results shown in Figure 6.22 is about 5.0%.

Finally, two Layer 1b sensors cover both routes. The resulting probabilities of $P_h(t)$ and $P_o(t)$ are shown in Figure 6.23 and probabilities of detection are shown in Figure 6.24.

Results for Two Routes, One Sensor Placed on each Route:
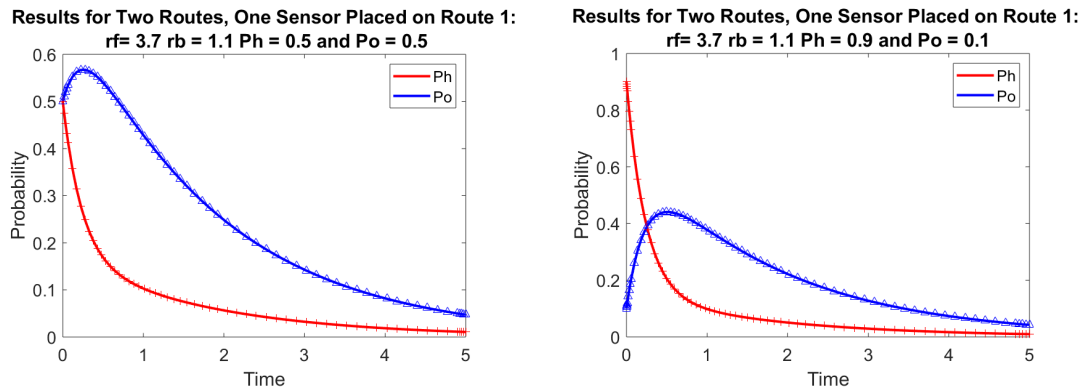**rf= 2.7 rb = 1.1 Ph = 0.5 and Po = 0.5**

Figure 6.23. The graph shows probability of target location over time with two Layer 1b sensors with a probability of detection ps_i each covering one route, P_h and P_o are .50/.50, r_f and r_b values are held constant at 2.7 and 1.1, respectively.
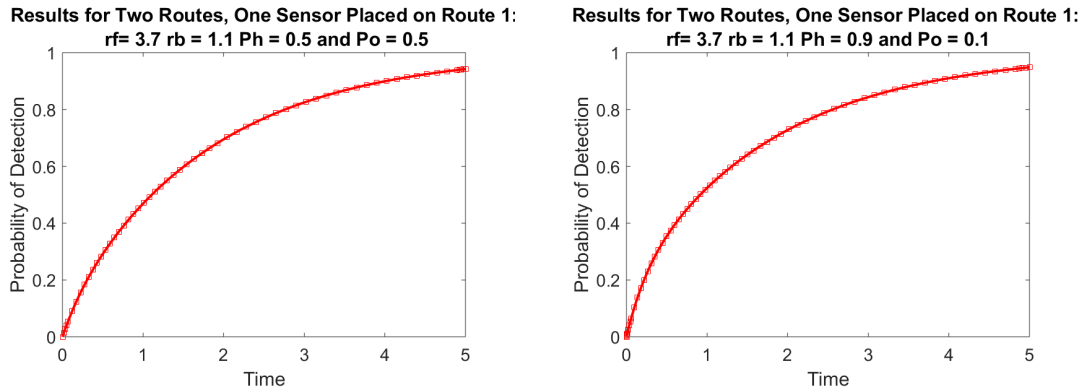
77
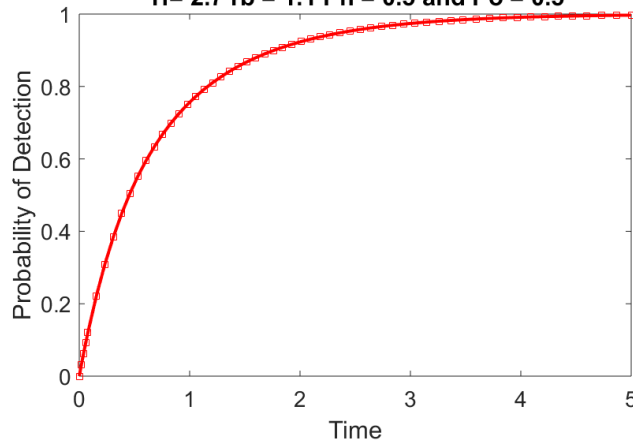
Figure 6.24. The graph depicts the probability of detection results over time depicted graphically for two Layer 1a sensors with a probability of detection ps_i each covering one route, P_h and P_o are .50/.50, r_f and r_b values are held constant at 2.7 and 1.1, respectively.

The discrete results from the figures above are shown in Tables 6.21.

Table 6.21. Time versus Probability when $P_h = 0.5$ and $P_o = 0.5$ values change, $r_f = 2.7$ and $r_b = 1.1$

t	P(t)
0	0
1.00	0.7563
2.00	0.9230
3.00	0.9741
4.00	0.9911
5.00	0.9970

The probability of detection difference between two Layer 1a sensor results shown in Figure 6.22 and Layer 1b sensor results shown in Figure 6.24 is about 5.0%.

The next models aim to simulate platoon's probability of detection given different situations in an urban subterranean environment.

6.6 Twelve Routes, One Sensor on each Block Corner

Based on feasible parameters and characteristics of previous models, the next models are the results analysis UMI underneath an actual city block.

First, the model compares the probability of detection of employing Layer 1a sensors and Layer 1b sensors. With a Layer 1a sensor, the results are discouraging. The resulting probabilities of $P_h(t)$ and $P_o(t)$ are shown in Figure 6.25 and probabilities of detection are shown in Figure 6.26.

Figure 6.25. The graph shows probability of target location over time with four Layer 1a sensors with a probability of detection ps_i each covering routes 1, 2, 3, and 4, P_h and P_o are .50/.50, r_f and r_b values are held constant at 2.7 and 1.1, respectively. A target's probability of selecting routes 1, 2, 3, and 4 is .834. The probability of selecting the remaining routes is .833.

**Results for Twelve Routes,
One Sensor Placed on each Block Corner:
rf= 2.7 rb = 1.1 Ph = 0.5 and Po = 0.5**

Figure 6.26. The graph depicts the probability of detection results over time depicted graphically for four Layer 1a sensors with a probability of detection ps_i covering routes 1, 2, 3, and 4, P_h and P_o are .50/.50, r_f and r_b values are held constant at 2.7 and 1.1, respectively. A target's probability of selecting routes 1, 2, 3, and 4 is .834. The probability of selecting the remaining routes is .833.

The discrete results from the figures above are shown in Tables 6.22.

Table 6.22. Time versus Probability when $P_h = 0.5$ and $P_o = 0.5$ values change, $r_f = 2.7$ and $r_b = 1.1$

t	P(t)
0	0
1.00	0.2802
2.00	0.4706
3.00	0.6103
4.00	0.7131
5.00	0.7888

After one interval of time, the probability of detection from Figure 6.27, Figure 6.28 and Figure 6.22 is 28.02%, and the probability of detection over a long period of time is only 78.88%.

Layer 1b sensors result in the following probabilities of $P_h(t)$ and $P_o(t)$ are shown in Figure 6.25 and probabilities of detection are shown in Figure 6.26.
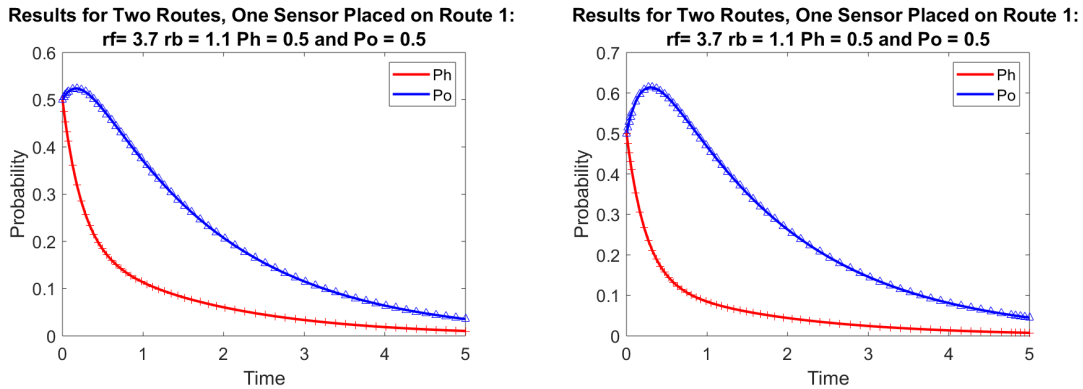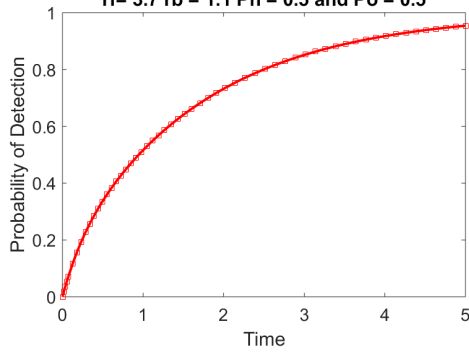
Results for Twelve Routes,
One Sensor Placed on each Block Corner:
rf= 2.7 rb = 1.1 Ph = 0.5 and Po = 0.5

Figure 6.27. The graph shows probability of target location over time with four Layer 1b sensors with a probability of detection ps_i each covering routes 1, 2, 3, and 4, P_h and P_o are .50/.50, r_f and r_b values are held constant at 2.7 and 1.1, respectively. A target's probability of selecting routes 1, 2, 3, and 4 is .834. The probability of selecting the remaining routes is .833.

**Results for Twelve Routes,
One Sensor Placed on each Block Corner:
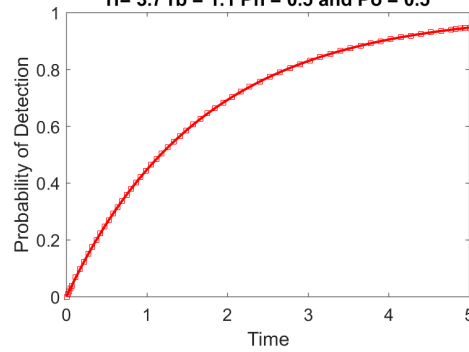rf= 2.7 rb = 1.1 Ph = 0.5 and Po = 0.5**

Figure 6.28. The graph depicts the probability of detection results over time depicted graphically for four Layer 1b sensors with a probability of detection ps_i covering routes 1, 2, 3, and 4, P_h and P_o are .50/.50, r_f and r_b values are held constant at 2.7 and 1.1, respectively. A target's probability of selecting routes 1, 2, 3, and 4 is .834. The probability of selecting the remaining routes is .833.

The discrete results from the figures above are shown in Tables 6.23.

Table 6.23. Time versus Probability when P_h = 0.5 and P_o = 0.5 values change, r_f = 2.7 and r_b = 1.1

t	P(t)
0	0
1.00	0.3886
2.00	0.6121
3.00	0.7534
4.00	0.8432
5.00	0.9003

After one interval of time, the probability of detection from Figure 6.27, Figure 6.28 and Table 6.23 is 38.86%, and the probability of detection over a long period of time is only 90.03%.

While the 10.0% increase is promising, the uncovered routes significantly hamper the performance of sensitive Layer 1b sensors.

As mentioned before, commanders attempt to influence the targets in selecting one route over another. When successful, the next models measure how much the probability of detection increases.

The next four models use the same Layer 1a and Layer 1b sensors used in the previous models in this section. The next model increases the target's probability of selecting routes 1, 2, 3, or 4 by .64% to 9.00% and decreases the remaining probabilities by .33% to 8.00%. The resulting probabilities of $P_h(t)$ and $P_o(t)$ are shown in Figure 6.29 and probabilities of detection are shown in Figure 6.30.

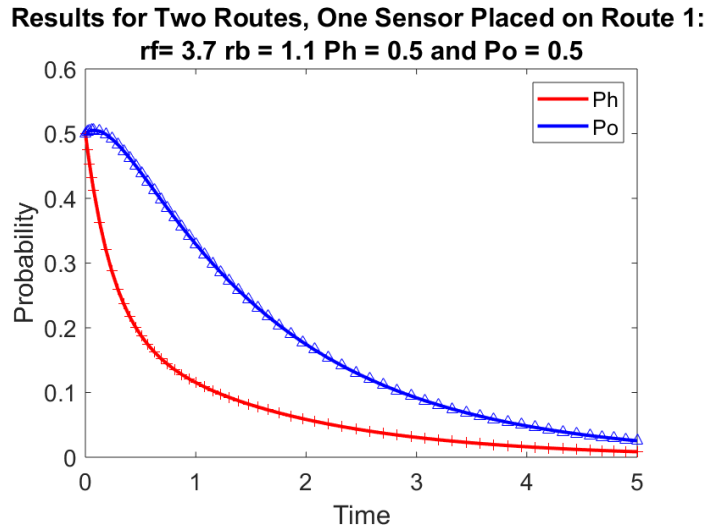**Results for Twelve Routes,
One Sensor Placed on each Block Corner:
rf= 2.7 rb = 1.1 Ph = 0.5 and Po = 0.5**

Figure 6.29. The graph shows probability of target location over time with four Layer 1a sensors with a probability of detection ps_i each covering routes 1, 2, 3, and 4, P_h and P_o are .50/.50, r_f and r_b values are held constant at 2.7 and 1.1, respectively. A target's probability of selecting routes 1, 2, 3, and 4 is .090. The probability of selecting the remaining routes is .080.
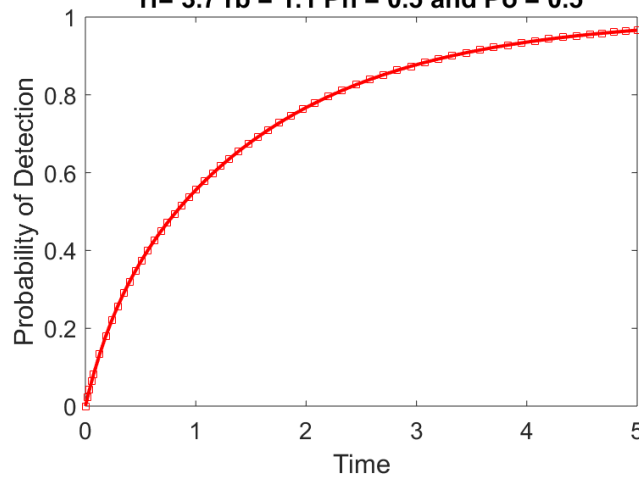
Figure 6.30. The graph depicts the probability of detection results over time depicted graphically for four Layer 1a sensors with a probability of detection ps_i covering routes 1, 2, 3, and 4, P_h and P_o are .50/.50, r_f and r_b values are held constant at 2.7 and 1.1, respectively. A target's probability of selecting routes 1, 2, 3, and 4 is .090. The probability of selecting the remaining routes is .080.

The discrete results from the figures above are shown in Table 6.24.

Table 6.24. Time versus Probability when $P_h = 0.5$ and $P_o = 0.5$ values change, $r_f = 2.7$ and $r_b = 1.1$

t	P(t)
0	0
1.00	0.2986
2.00	0.4962
3.00	0.6377
4.00	0.7395
5.00	0.8127

After one interval of time, the probability of detection from Figure 6.29, Figure 6.30 and 6.24 is 29.86%, and the probability of detection over a long period of time is only 81.27%. The resulting probabilities of $P_h(t)$ and $P_o(t)$ are shown in Figure 6.31 and probabilities of

detection are shown in Figure 6.32.

**Results for Twelve Routes,
One Sensor Placed on each Block Corner:
rf= 2.7 rb = 1.1 Ph = 0.5 and Po = 0.5**

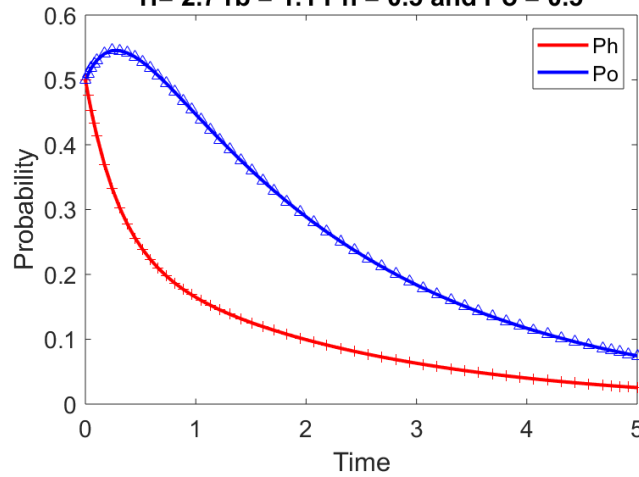Figure 6.31. The graph shows probability of target location over time with four Layer 1b sensors with a probability of detection ps_i each covering routes 1, 2, 3, and 4, P_h and P_o are .50/.50, r_f and r_b values are held constant at 2.7 and 1.1, respectively. A target's probability of selecting routes 1, 2, 3, and 4 is .090. The probability of selecting the remaining routes is .080.

**Results for Twelve Routes,
One Sensor Placed on each Block Corner:
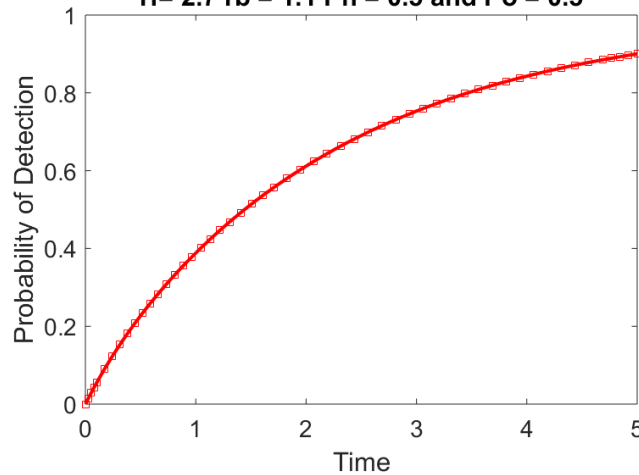rf= 2.7 rb = 1.1 Ph = 0.5 and Po = 0.5**

Figure 6.32. The graph depicts the probability of detection results over time depicted graphically for four Layer 1b sensors with a probability of detection ps_i covering routes 1, 2, 3, and 4, P_h and P_o are .50/.50, r_f and r_b values are held constant at 2.7 and 1.1, respectively. A target's probability of selecting routes 1, 2, 3, and 4 is .090. The probability of selecting the remaining routes is .080.

The discrete results from the figures above are shown in Table 6.25.

Table 6.25. Time versus Probability when $P_h = 0.5$ and $P_o = 0.5$ values change, $r_f = 2.7$ and $r_b = 1.1$

t	P(t)
0	0
1.00	0.4117
2.00	0.6394
3.00	0.7784
4.00	0.8638
5.00	0.9163

After one interval of time, the probability of detection from Figure 6.31, Figure 6.32 and 6.25 is 41.17%, and the probability of detection over a long period of time is 96.14%.

When compared to the Layer 1a performance from Figure 6.29, Figure 6.30 the Layer 1b

increases the probability of detection by 11.0%. Finally, the following model increases the target's probability of selecting routes 1, 2, 3, or 4 by 3.00% to 12.00% and decreases the remaining probabilities by 1.50% to 6.50%. The resulting probabilities of $P_h(t)$ and $P_o(t)$ are shown in Figure 6.33 and probabilities of detection are shown in Figure 6.34.
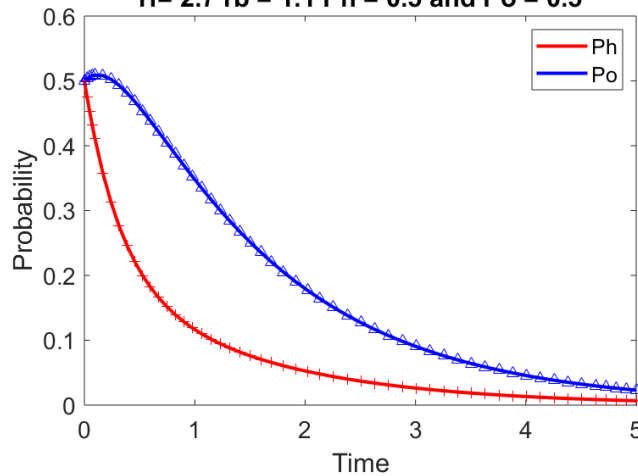

Figure 6.33. The graph shows probability of target location over time with four Layer 1a sensors with a probability of detection ps_i each covering routes 1, 2, 3, and 4, P_h and P_o are .50/.50, r_f and r_b values are held constant at 2.7 and 1.1, respectively. A target's probability of selecting routes 1, 2, 3, and 4 is .120. The probability of selecting the remaining routes is .065.

**Results for Twelve Routes,
One Sensor Placed on each Block Corner:
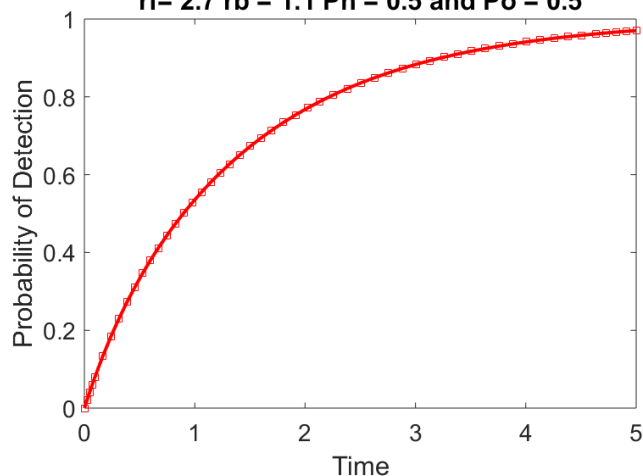rf= 2.7 rb = 1.1 Ph = 0.5 and Po = 0.5**
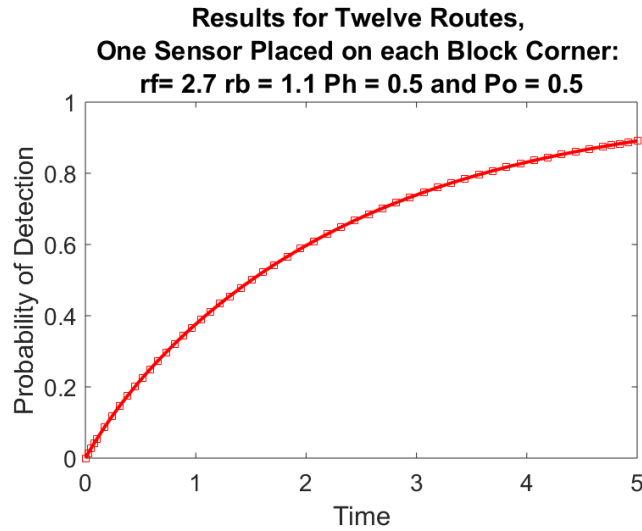
Figure 6.34. The graph depicts the probability of detection results over time depicted graphically for four Layer 1a sensors with a probability of detection ps_i covering routes 1, 2, 3, and 4, P_h and P_o are .50/.50, r_f and r_b values are held constant at 2.7 and 1.1, respectively. A target's probability of selecting routes 1, 2, 3, and 4 is .120. The probability of selecting the remaining routes is .065.

The discrete results from the figures above are shown in Table 6.26.

Table 6.26. Time versus Probability when P_h = 0.5 and P_o = 0.5 values change, r_f = 2.7 and r_b = 1.1

t	P(t)
0	0
1.00	0.3763
2.00	0.5972
3.00	0.7394
4.00	0.8313
5.00	0.8908

After one interval of time, the probability of detection from Figure 6.33, Figure 6.34 and Figure 6.26 is 37.63%, and the probability of detection over a long period of time is 89.08%. The resulting probabilities of $P_h(t)$ and $P_o(t)$ are shown in Figure 6.35 and probabilities of

detection are shown in Figure 6.36.

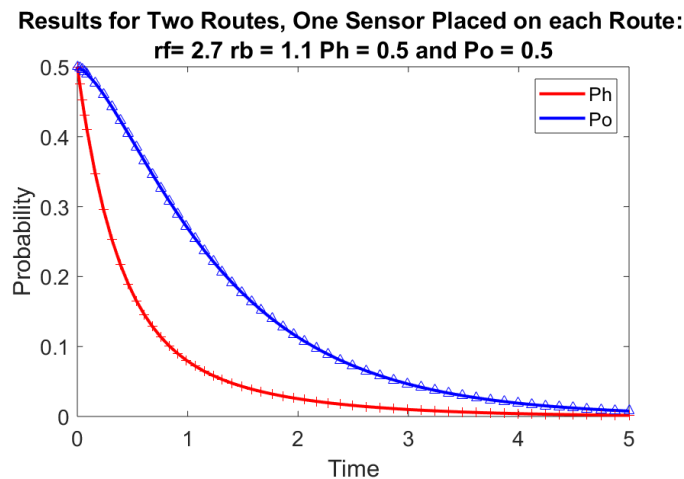Figure 6.35. The graph shows probability of target location over time with four Layer 1b sensors with a probability of detection ps_i each covering routes 1, 2, 3, and 4, P_h and P_o are .50/.50, r_f and r_b values are held constant at 2.7 and 1.1, respectively. A target's probability of selecting routes 1, 2, 3, and 4 is .120. The probability of selecting the remaining routes is .065.
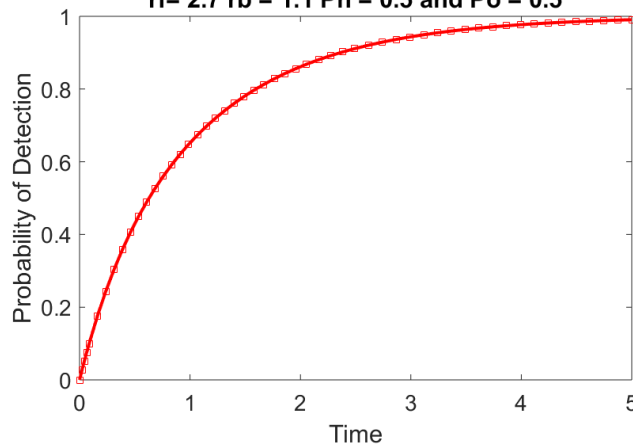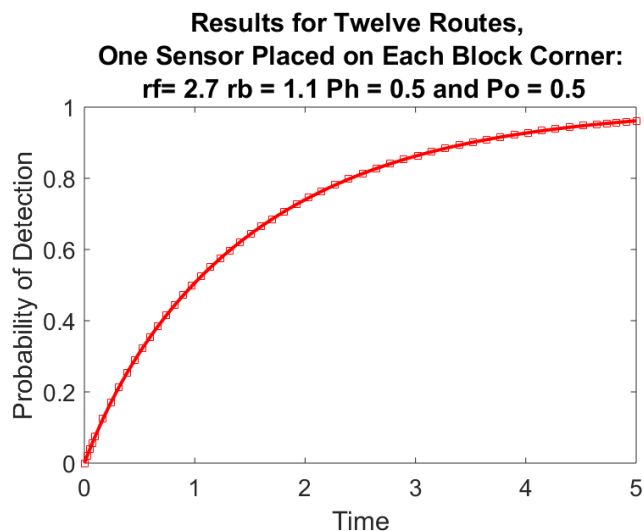
Figure 6.36. The graph depicts the probability of detection results over time depicted graphically for four Layer 1b sensors with a probability of detection ps_i covering routes 1, 2, 3, and 4, P_h and P_o are .50/.50, r_f and r_b values are held constant at 2.7 and 1.1, respectively. A target's probability of selecting routes 1, 2, 3, and 4 is .120. The probability of selecting the remaining routes is .065.

The discrete results from the figures above are shown in Table 6.27.

Table 6.27. Time versus Probability when P_h = 0.5 and P_o = 0.5 values change, r_f = 2.7 and r_b = 1.1

t	P(t)
0	0
1.00	0.5061
2.00	0.7400
3.00	0.8624
4.00	0.9271
5.00	0.9614

After one interval of time, the probability of detection from Figure 6.35, Figure 6.36 and Figure 6.27 is 50.61%, and the probability of detection over a long period of time is 96.14%.

When compared to the Layer 1a performance from Figure 6.29, Figure 6.30 the Layer 1b

increases the probability of detection by nearly 13.0%.

Of course, if sensors cover every route then the models behave like previous models.

6.7 Twelve Routes, One Sensor on Eight UMI Intersections

The next model adds one Layer 1b sensor to four additional UMI intersections. Given the most recent model where a target's probability of selecting routes 1, 2, 3, and 4 is .120 and the probability of selecting the remaining routes is .065, all other parameters remain constant. The resulting probabilities of $P_h(t)$ and $P_o(t)$ are shown in Figure 6.37 and probabilities of detection are shown in Figure 6.38.

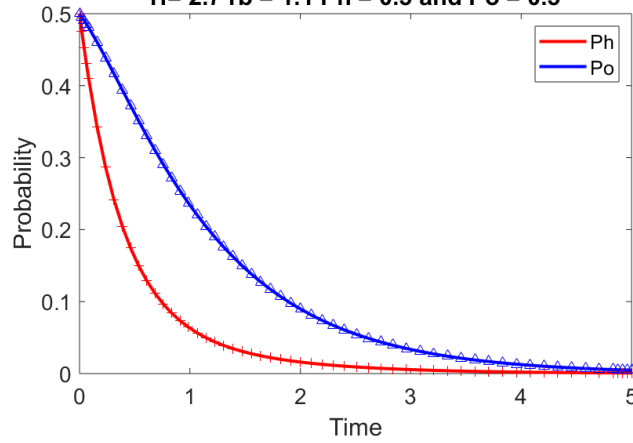Figure 6.37. The graph shows probability of target location over time with four Layer 1b sensors with a probability of detection ps_i each covering routes 1, 2, 3, 4, 5, 6, 7, and 8, P_h and P_o are .50/.50 , r_f and r_b values are held constant at 2.7 and 1.1, respectively. A target's probability of selecting routes 1, 2, 3, 4, 5, 6, 7, and 8 is .120. The probability of selecting the remaining routes is .065.
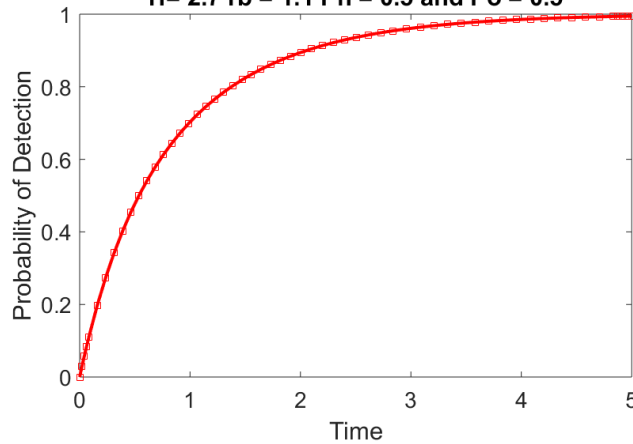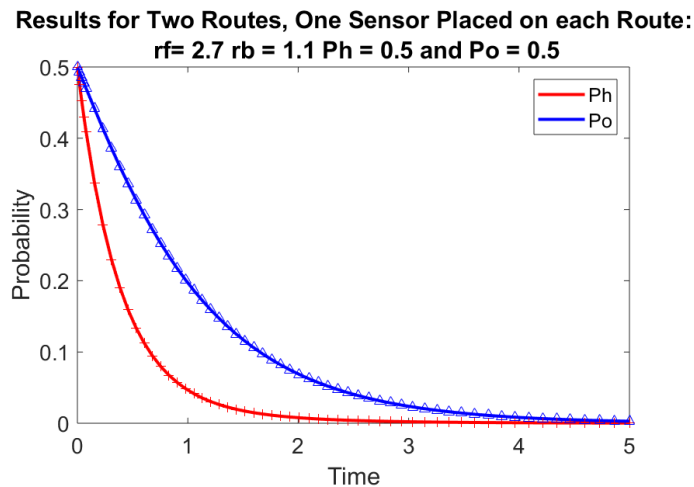
Figure 6.38. The graph depicts the probability of detection results over time depicted graphically for eight Layer 1b sensors with a probability of detection ps_i covering routes 1, 2, 3, 4, 5, 6, 7, and 8, P_h and P_o are .50/.50, r_f and r_b values are held constant at 2.7 and 1.1, respectively. A target's probability of selecting routes 1, 2, 3, 4, 5, 6, 7, and 8, is .120. The probability of selecting the remaining routes is .065.

The discrete results from the figures above are shown in Table 6.28.

Table 6.28. Time versus Probability when $P_h = 0.5$ and $P_o = 0.5$ values change, $r_f = 2.7$ and $r_b = 1.1$

t	P(t)
0	0
1.00	0.6485
2.00	0.8591
3.00	0.9424
4.00	0.9764
5.00	0.9903

Adding four Layer 1b sensors to detect targets moving in the UMI increase the probability of detection over 14.00%.

Covering all routes would result in probabilities of detection similar to Figure 6.20, Figure

6.22 or Figure 6.24.

In theory, given a platoon's space responsibility in an urban environment, emplacement of eight sensors is feasible.

6.8 Multiple Hiding Areas, Routes, Entering a Single Operating Area

6.8.1 Two Hiding Areas, Six Routes, One Sensor on each Route

The final two models represent targets leaving their hiding areas, and moving along UMI into their operation area. This model attempts to capture a subterranean attack by a force in the offense.

In the next model, the probability of selecting a route is equal.

The two attacking units' movements may be coordinated, and enemy units can come into contact with one another. Doctrinally, the models attempt to replicate a unit conducting a hasty defense with a 2:1 enemy to friendly ratio. This situation may arise during initial entry into a urban area with Layer 1a sensors. The resulting probabilities of $P_{h1}(t)$, $P_{h2}(t)$ and $P_o(t)$ are shown in Figure 6.39 and probabilities of detection are shown in Figure 6.40.
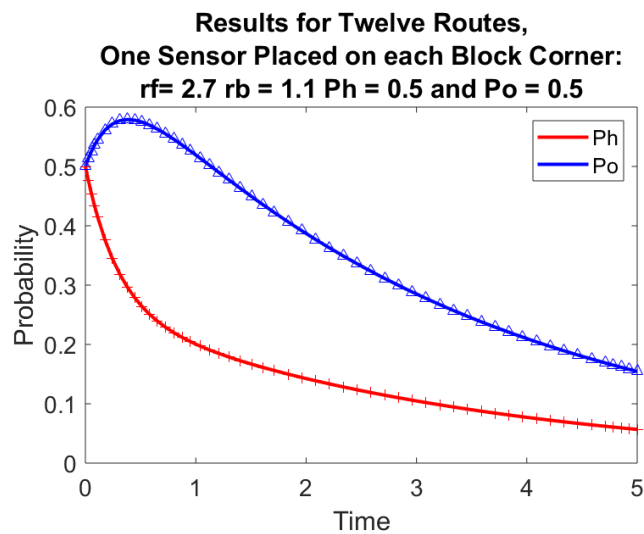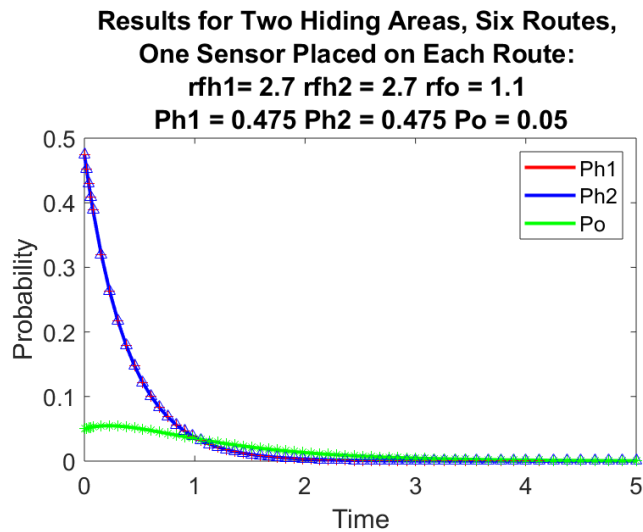
Figure 6.39. The graph shows probability of target location over time for six Layer 1b sensors with a probability of detection ps_i covering each route, P_{h1}, P_{h2} and P_o are .475, .475 and .05, respectively, r_{fh1}, r_{fh2} and r_0 values are held constant at 2.7, 2.7 and 1.1, respectively. A target's probability of selecting each route is .1666.
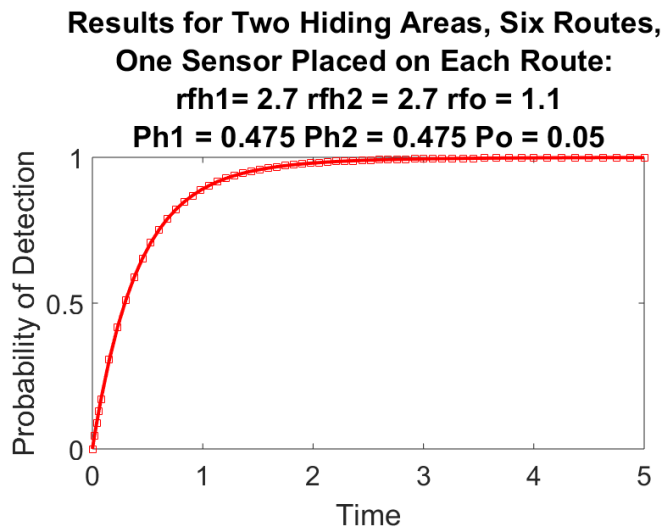
Figure 6.40. The graph depicts the probability of detection results over time depicted graphically for six Layer 1b sensors with a probability of detection ps_i cover each route, P_{h1}, P_{h2} and P_o are .475, .475 and .05, respectively, r_{fh1}, r_{fh2} and r_0 values are held constant at 2.7, 2.7 and 1.1, respectively. A target's probability of selecting each route is .1667.

The discrete results from the figures above are shown in Table 6.29.

Table 6.29. Time versus Probability when $P_{h1} = 0.475$,$P_{h2} = 0.475$ and $P_o = 0.05$ values change, $r_{fh1} = 2.7$, $r_{fh2} = 2.7$ and $r_{fo} = 1.1$

t	P(t)
0	0
1.00	0.8916
2.00	0.9805
3.00	0.9947
4.00	0.9983
5.00	0.9994

The resulting probabilities of $P_{h1}(t)$, $P_{h2}(t)$ and $P_o(t)$ are shown in Figure 6.41 and probabilities of detection are shown in Figure 6.42.

Figure 6.41. The graph shows probability of target location over time for six Layer 1b sensors with a probability of detection ps_i covering each route, P_{h1}, P_{h2} and P_o are .45, .45 and .10, respectively, r_{fh1}, r_{fh2} and r_0 values are held constant at 2.7, 2.7 and 1.1, respectively. A target's probability of selecting each route is .1666.

**Results for Two Hiding Areas, Six Routes,
One Sensor Placed on Each Route:
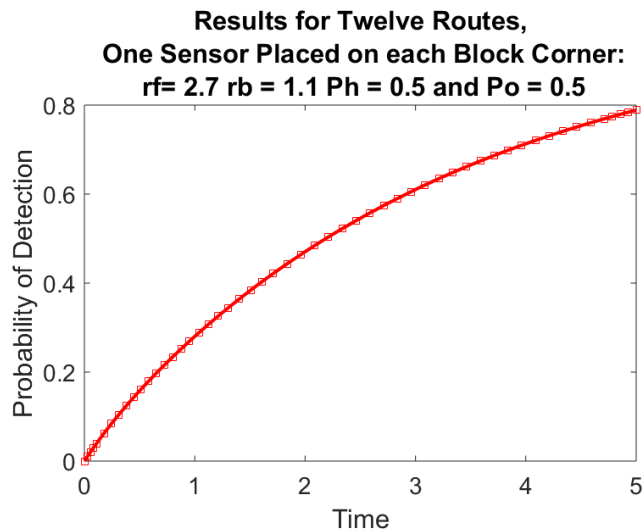rfh1= 2.7 rfh2 = 2.7 rfo = 1.1
Ph1 = 0.45 Ph2 = 0.45 Po = 0.1**

Figure 6.42. The graph depicts the probability of detection results over time depicted graphically for six Layer 1b sensors with a probability of detection ps_i cover each route, P_{h1}, P_{h2} and P_o are .45, .45 and .10, respectively, r_{fh1}, r_{fh2} and r_0 values are held constant at 2.7, 2.7 and 1.1, respectively. A target's probability of selecting each route is .1666.

The discrete results from the figures above are shown in Table 6.30.

Table 6.30. Time versus Probability when P_{h1} = 0.45 ,P_{h2} = 0.45 and P_o = 0.1 values change, r_{fh1} = 2.7, r_{fh2} = 2.7 and r_{fo} = 1.1

t	P(t)
0	0
1.00	0.8786
2.00	0.9752
3.00	0.9929
4.00	0.9977
5.00	0.9992

The resulting probabilities of $P_{h1}(t)$, $P_{h2}(t)$ and $P_o(t)$ are shown in Figure 6.43 and probabilities of detection are shown in Figure 6.44.
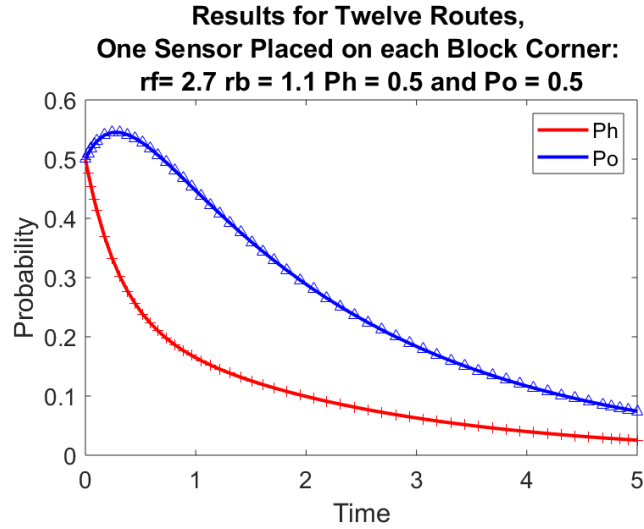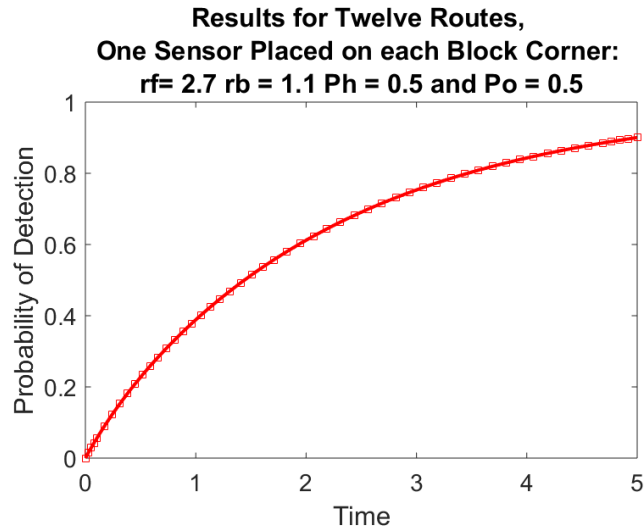
96

Figure 6.43. The graph shows probability of target location over time for six Layer 1b sensors with a probability of detection ps_i covering each route, P_{h1}, P_{h2} and P_o are .40, .40 and .20, respectively, r_{fh1}, r_{fh2} and r_0 values are held constant at 2.7, 2.7 and 1.1, respectively. A target's probability of selecting each route is .1666.

.
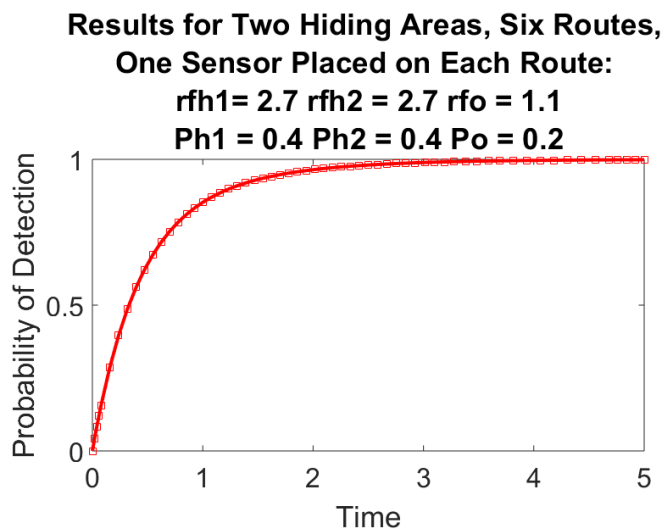
Figure 6.44. The graph depicts the probability of detection results over time depicted graphically for six Layer 1b sensors with a probability of detection ps_i cover each route, P_{h1}, P_{h2} and P_o are .40, .40 and .20, respectively, r_{fh1}, r_{fh2} and r_0 values are held constant at 2.7, 2.7 and 1.1, respectively. A target's probability of selecting each route is .1666.

97

The discrete results from the figures above are shown in Table 6.31.

Table 6.31. Time versus Probability when $P_{h1} = 0.4$,$P_{h2} = 0.4$ and $P_o = 0.2$ values change, $r_{fh1} = 2.7$, $r_{fh2} = 2.7$ and $r_{fo} = 1.1$

t	P(t)
0	0
1.00	0.7911
2.00	0.9376
3.00	0.9786
4.00	0.9924
5.00	0.9973

Even with the addition of multiple hiding areas, the difference of Figure 6.40, Figure 6.42, and Figure 6.44's initial conditions do not affect the overall probability of detection.

In the next model, the probability of selecting a route is adjusted.

The two attacking units' movements may be coordinated, but they do not come into contact with one another. The resulting probabilities of $P_{h1}(t)$, $P_{h2}(t)$ and $P_o(t)$ are shown in Figure 6.45 and probabilities of detection are shown in Figure 6.46.

Results for Two Hiding Areas, Six Routes,
One Sensor Placed on Each Route:
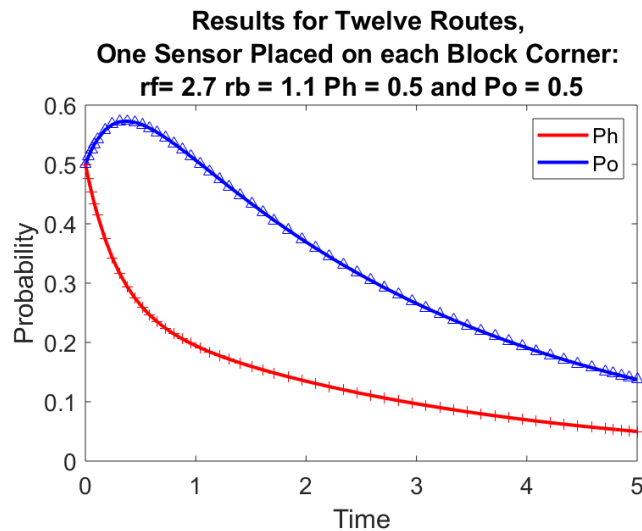**rfh1= 2.7 rfh2 = 2.7 rfo = 1.1**
Ph1 = 0.475 Ph2 = 0.475 Po = 0.05

Figure 6.45. The graph shows probability of target location over time for four Layer 1b sensors with a probability of detection ps_i covering each route, P_{h1}, P_{h2} and P_o are .475, .475 and .05, respectively, r_{fh1}, r_{fh2} and r_0 values are held constant at 2.7, 2.7 and 1.1, respectively. A target's probability of selecting each route is .25.

Results for Two Hiding Areas, Six Routes,
One Sensor Placed on Each Route:
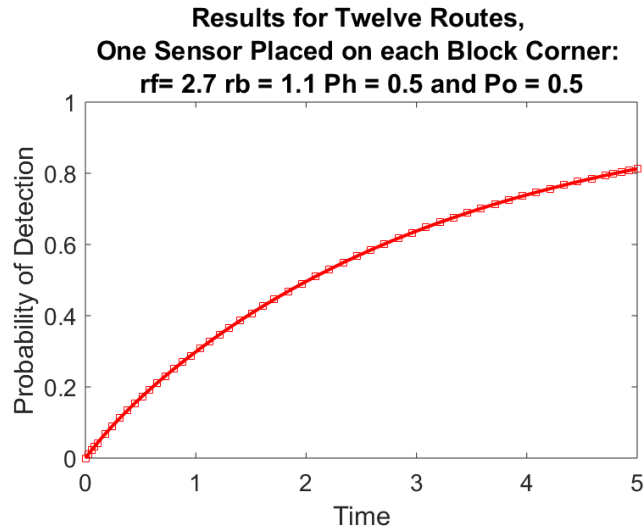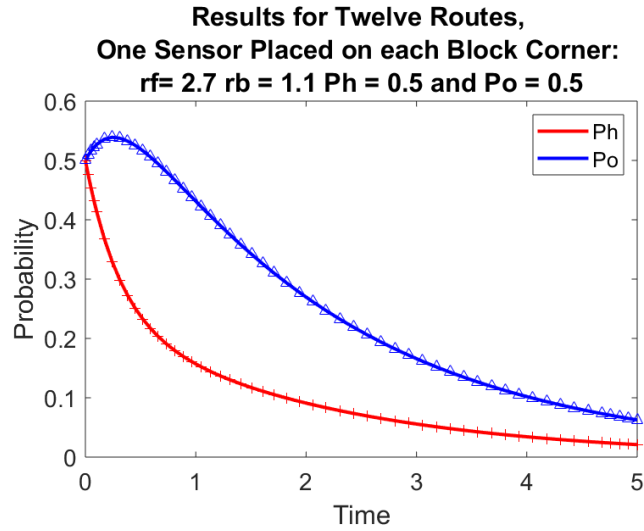**rfh1= 2.7 rfh2 = 2.7 rfo = 1.1**
Ph1 = 0.475 Ph2 = 0.475 Po = 0.05

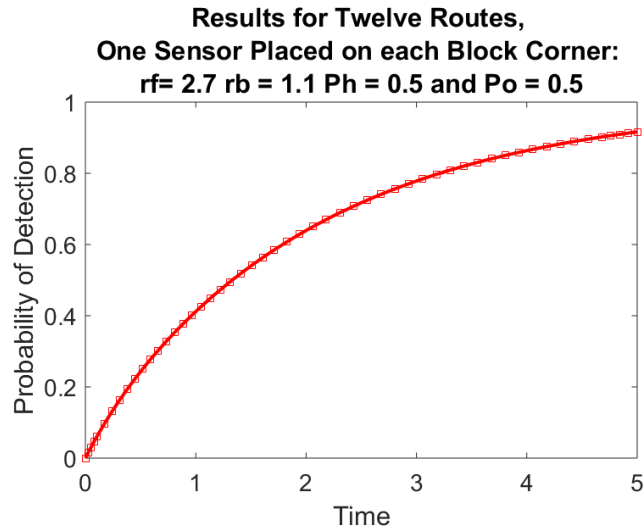Figure 6.46. The graph depicts the probability of detection results over time depicted graphically for six Layer 1b sensors with a probability of detection ps_i cover each route, P_{h1}, P_{h2} and P_o are .475, .475 and .05, respectively, r_{fh1}, r_{fh2} and r_0 values are held constant at 2.7, 2.7 and 1.1, respectively. A target's probability of selecting each route is .25.

99

The discrete results from the figures above are shown in Table 6.32.

Table 6.32. Time versus Probability when $P_{h1} = 0.4$, $P_{h2} = 0.5$ and $P_o = 0.1$ values change, $r_{fh1} = 2.7$, $r_{fh2} = 2.7$ and $r_{fo} = 1.1$

t	P(t)
0	0
1.00	0.8895
2.00	0.9776
3.00	0.9934
4.00	0.9978
5.00	0.9993

When compared to Figure 6.40's results after one interval of time, the probability of detection from Figure 6.46's results is 7.10% greater, and the probability of detection difference over a long period of time is 9.88% more.

This model can expand and encompass multiple routes as well. The final model addresses route expansion.

Assuming the sensor probability is 50%, the explicit numerical solution to model is

$$
\begin{bmatrix} p_{h1}(t) \\ p_{h2}(t) \\ p_o(t) \end{bmatrix} = -0.3652 \begin{bmatrix} -0.1257 \\ -0.1257 \\ -0.9841 \end{bmatrix} e^{-1.0213t} - 0.000 \begin{bmatrix} -0.7071 \\ 0.7071 \\ -0.0000 \end{bmatrix} e^{-3.0084t} - 0.5255 \begin{bmatrix} -0.6738 \\ -0.6738 \\ 0.3032 \end{bmatrix} e^{-2.4703t}.
$$

(6.16)

MATLAB's ODE45 solver solution validates the numerical solution. Figure 6.47 graphically compares the ODE45's solver solution to the numerical solution.
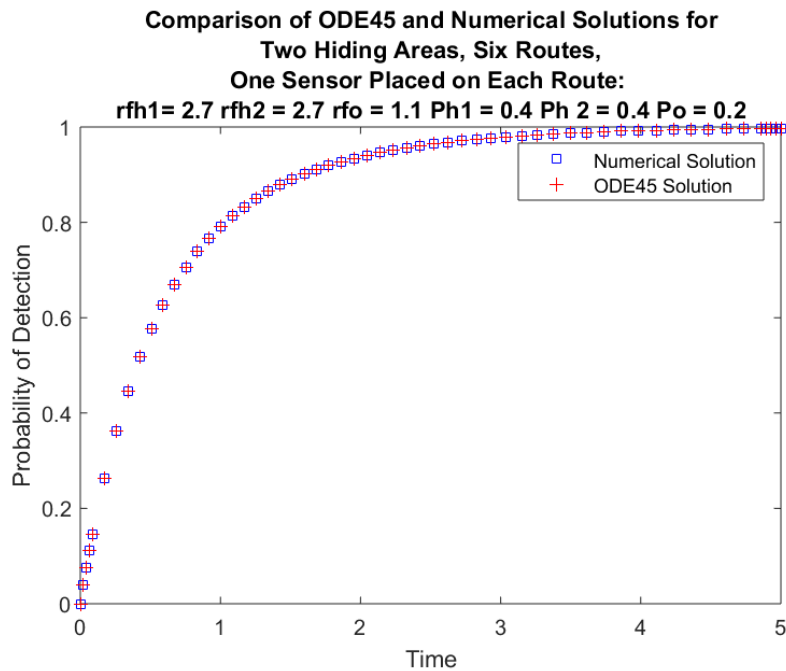
Figure 6.47. MATLAB ODE45 and Numerical Solution Comparison for a 3x3 System of Equations when $Ph1 = .40$, $Ph2 = .40$, $P_0 = .20$, $r_f1 = 2.7$, $r_f2 = 2.7$ and $r_b = 1.1$, and $p_{s1}=.50$. A target's probability of selecting each route is .1666.

6.8.2 Three Hiding areas, Twelve Routes, One Senors on each Route

The next model adds a hiding area area. Doctrinally, the models attempt to replicate a unit conducting a deliberate defense with a 3:1 enemy to friendly ratio. This situation may arise during defensive operations in an urban area.

The attacking units' movement may be coordinated, and targets may come into contact with one another. The resulting probabilities of $P_{h1}(t)$, $P_{h2}(t)$, $P_{h3}(t)$ and $P_o(t)$ are shown in Figure 6.48 and probabilities of detection are shown in Figure 6.49.
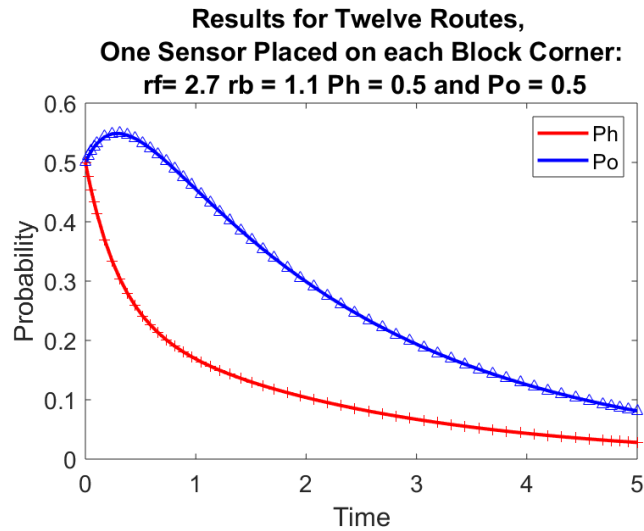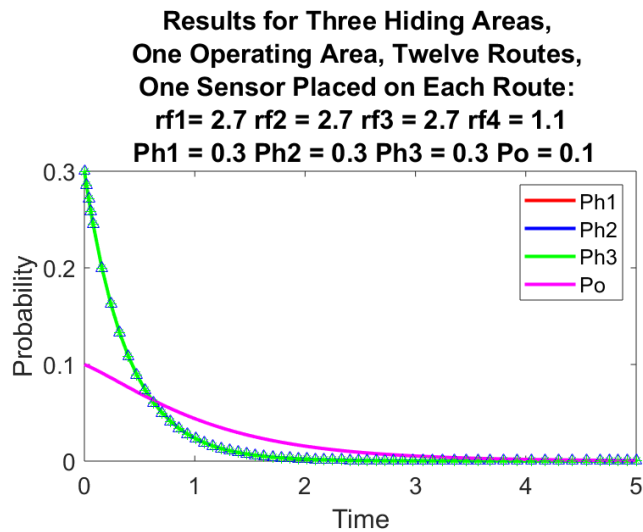
Figure 6.48. The graph shows probability of target location over time for four Layer 1b sensors with a probability of detection ps_i covering each route, P_{h1}, P_{h2}, P_{h3} and P_o are .30, .30, .30, and .10, respectively, r_{fh1}, r_{fh2}, r_{fh3} and r_0 values are held constant at 2.7, 2.7, 2.7, and 1.1, respectively. A target's probability of selecting a route is .0833.
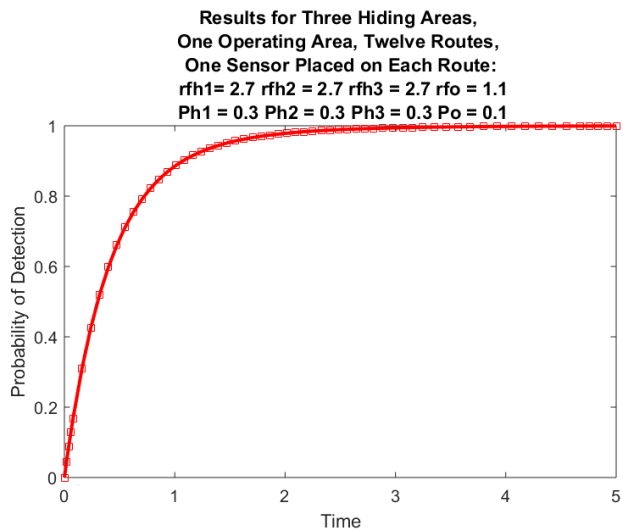
Figure 6.49. The graph depicts the probability of detection results over time depicted graphically for six Layer 1b sensors with a probability of detection ps_i cover each route, P_{h1}, P_{h2}, P_{h3} and P_o are .30, .30, .30, and .10, respectively, r_{fh1}, r_{fh2}, r_{fh3} and r_0 values are held constant at 2.7, 2.7, 2.7, and 1.1, respectively. A target's probability of selecting each route is .834.

The discrete results from the figures above are shown in Table 6.33.

Table 6.33. Time versus Probability when $P_{h1} = 0.3$ $P_{h2} = 0.3$, $P_{h3} = 0.3$ and $P_o = 0.1$ values change, $r_{fh1} = 2.7$, $r_{fh2} = 2.7$, $r_{fh3} = 2.7$ and $r_{fo} = 1.1$

t	P(t)
0	0
1.00	0.8850
2.00	0.9784
3.00	0.9941
4.00	0.9981
5.00	0.9994

After one interval of time, the probability of detection from Figure 6.49's results is 88.50%

The next model expands to four routes between the operating area and each hiding area to replicate multiple effects commanders may employ to increase the probability of detection. Tactically, this parameter change intends to mimic a "block" effect. Unlike the first model in this section, the targets cannot travel between hiding areas.

The models below have unique probabilities of detection and rates for each route. This change accurately models target behavior to depict a "block" or "disrupt" effect. Of the four possible routes from each hiding area to an operating area, two are blocked forcing targets to select from two routes instead of four. The resulting probabilities of $P_{h1}(t)$, $P_{h2}(t)$, $P_{h3}(t)$ and $P_o(t)$ are shown in Figure 6.50 and probabilities of detection are shown in Figure 6.51.

**Results for Three Hiding Areas,
One Operating Area, Twelve Routes,
One Sensor Placed on Each Route:
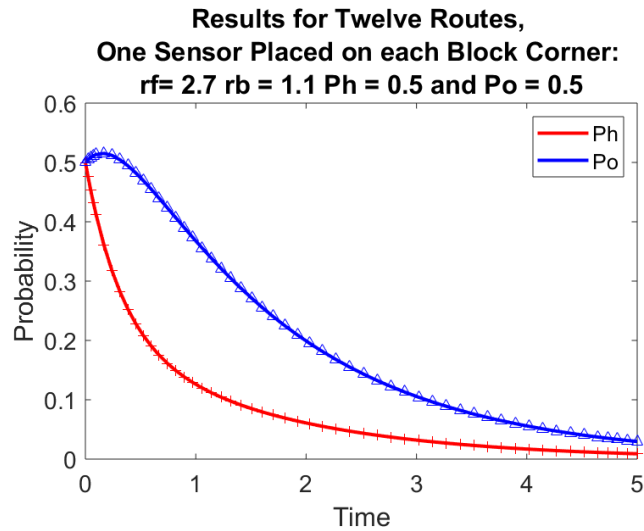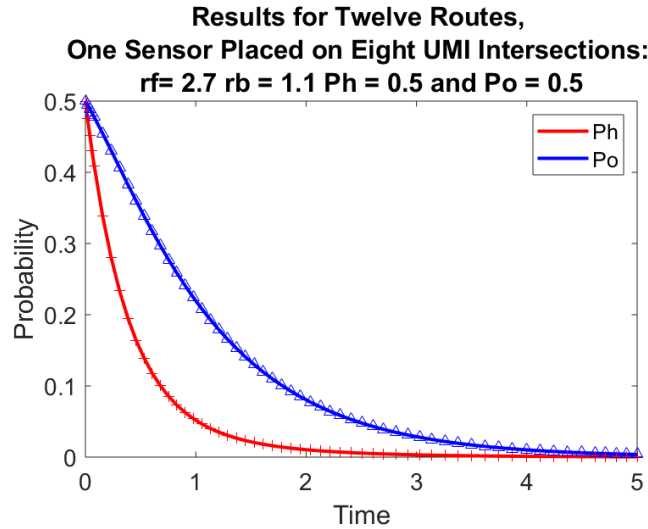rf1= 0 rf2 = 3.7 rf3 = 3.7 rf4 = 0
Ph1 = 0.3 Ph2 = 0.3 Ph3 = 0.3 Po = 0.1**
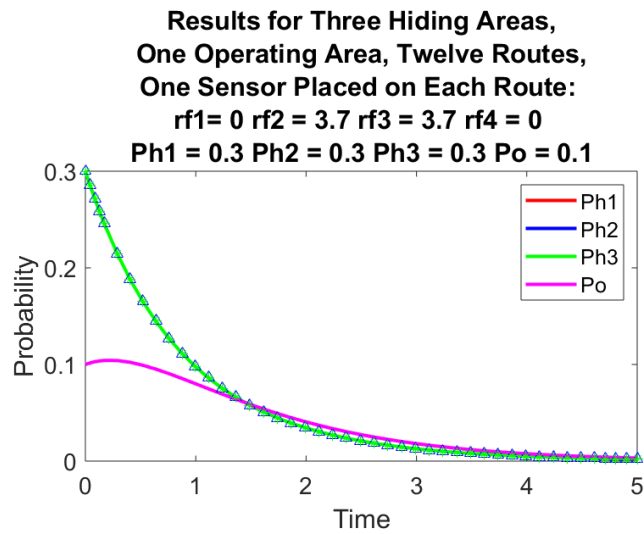
Figure 6.50. The graph shows probability of target location over time for four Layer 1b sensors with a probability of detection ps_i covering each route, P_{h1}, P_{h2}, P_{h3} and P_o are .30, .30, .30, and .10, respectively, r_{fh1}, r_{fh2}, r_{fh3} and r_{fh4} values are held constant at 0.0, 3.7, 3.7, and 0.0, respectively. Instead of four routes connecting each hiding area to the operating area, the model simulates a "block" with two open routes with target selection probability of .1666 for each open route.
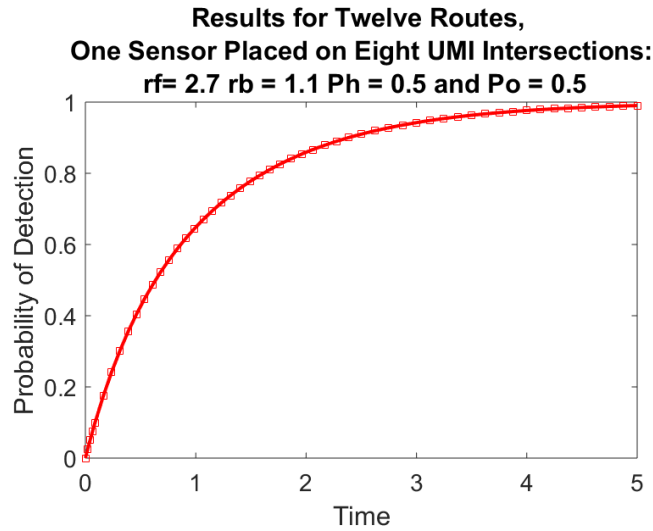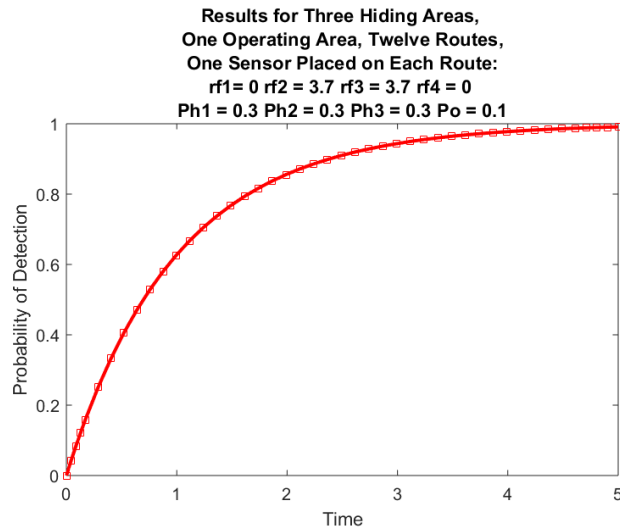
Figure 6.51. The graph depicts the probability of detection results over time depicted graphically for six Layer 1b sensors with a probability of detection ps_i cover each route, P_{h1}, P_{h2}, P_{h3} and P_o are .30, .30, .30, and .10, respectively, r_{fh1}, r_{fh2}, r_{fh3} and r_{fh4} values are held constant at 0.0, 3.7, 3.7, and 0.0, respectively. Instead of four routes connecting each hiding area to the operating area, the model simulates a "block" with two open routes with target selection probability of .1666 for each open route.

The discrete results from the figures above are shown in Table 6.34.

Table 6.34. Time versus Probability when $P_{h1} = 0.3$ $P_{h2} = 0.3$, $P_{h3} = 0.3$ and $P_o = 0.1$ values change, $r_{fh1} = 0.0$, $r_{fh2} = 3.7$, $r_{fh3} = 3.7$ and $r_{f4} = 0.0$

t	P(t)
0	0
1.00	0.6278
2.00	0.8767
3.00	0.9438
4.00	0.9777
5.00	0.9911

Of the four possible routes from each hiding area to an operating area, three are blocked forcing targets to select from a one route instead of four. The resulting probabilities of

105

$P_{h1}(t)$, $P_{h2}(t)$, $P_{h3}(t)$ and $P_o(t)$ are shown in Figure 6.52 and probabilities of detection are shown in Figure 6.53.
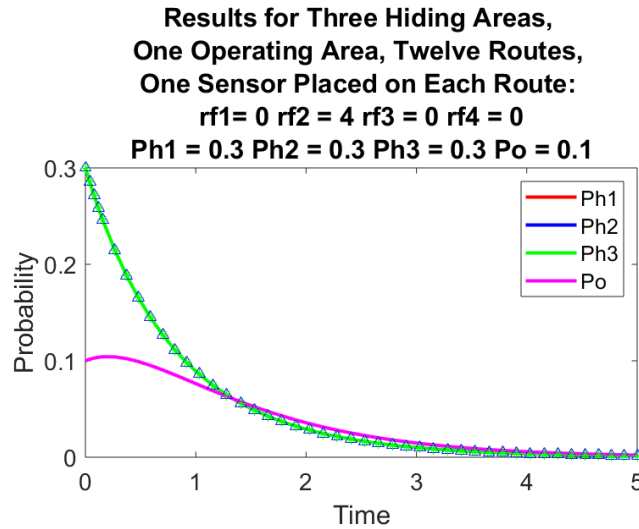
Figure 6.52. The graph shows probability of target location over time for four Layer 1b sensors with a probability of detection ps_i covering each route, P_{h1}, P_{h2}, P_{h3} and P_o are .30, .30, .30, and .10, respectively, r_{fh1}, r_{fh2}, r_{fh3} and r_{fh4} values are held constant at 0.0, 4.0, 0.0, and 0.0, respectively. Instead of four routes connecting each hiding area to the operating area, the model simulates a "block" with one open routes with target selection probability of .3333 for each open route.

Results for Three Hiding Areas,
One Operating Area, Twelve Routes,
One Sensor Placed on Each Route:
rf1= 0 rf2 = 4 rf3 = 0 rf4 = 0
Ph1 = 0.3 Ph2 = 0.3 Ph3 = 0.3 Po = 0.1
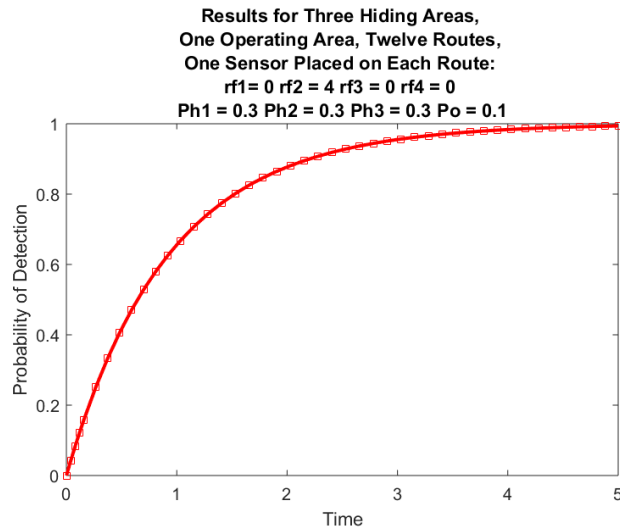
Figure 6.53. The graph depicts the probability of detection results over time depicted graphically for six Layer 1b sensors with a probability of detection ps_i cover each route, P_{h1}, P_{h2}, P_{h3} and P_o are .30, .30, .30, and .10, respectively, r_{fh1}, r_{fh2}, r_{fh3} and r_{fh4} values are held constant at 0.0, 4.0, 0.0, and 0.0, respectively. Instead of four routes connecting each hiding area to the operating area, the model simulates a "block" with two open routes with target selection probability of .3333 for each open route.

The discrete results from the figures above are shown in Table 6.35.

Table 6.35. Time versus Probability when P_{h1} = 0.3 P_{h2} = 0.3, P_{h3} = 0.3 and P_o = 0.1 values change, r_{fh1} = 0.0, r_{fh2} = 4.0, r_{fh3} = 0.0 and r_{fo} = 0.0

t	P(t)
0	0
1.00	0.6560
2.00	0.8771
3.00	0.9552
4.00	0.9835
5.00	0.9939

After one interval of time, blocking an additional route increases the probability to detect targets moving in the UMI by nearly 3.00%. Intuitively, this increase is unlikely to convince commanders to block single routes into operating areas.

107

The last model again restricts a target to select a certain route at a certain rate. This parameter change intents to mimic a "disrupt" effect. The resulting probabilities of $P_{h1}(t)$, $P_{h2}(t)$, $P_{h3}(t)$ and $P_o(t)$ are shown in Figure 6.54 and probabilities of detection are shown in Figure 6.55.


Results for Three Hiding Areas, One Operating Area, Twelve Routes, One Sensor Placed on Each Route: rf1= 0.7 rf2 = 3.7 rf3 = 3.7 rf4 = 0.7 Ph1 = 0.3 Ph2 = 0.3 Ph3 = 0.3 Po = 0.1
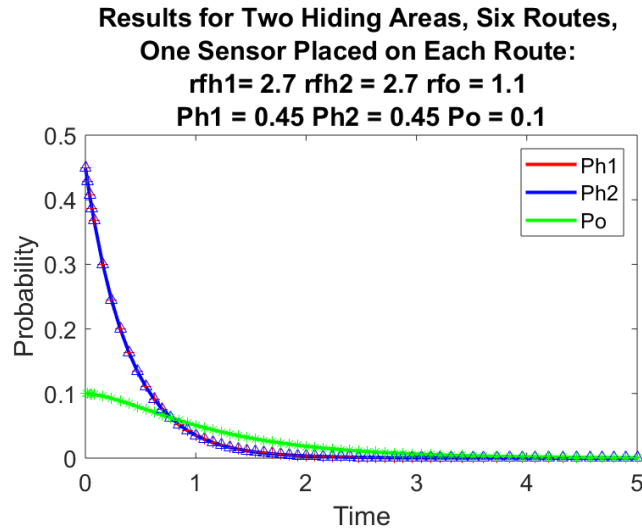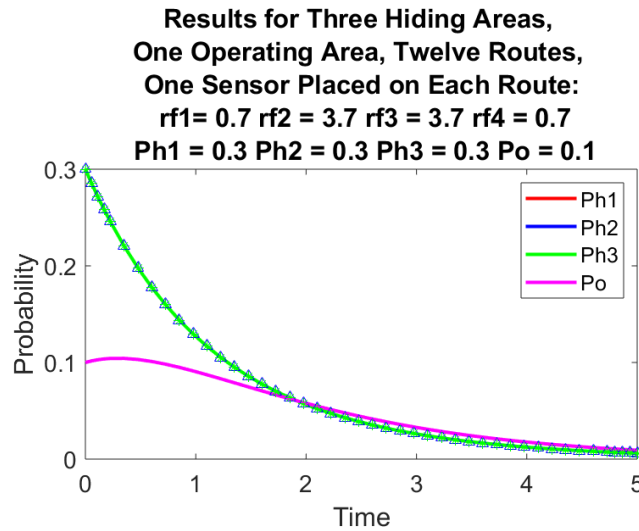
Figure 6.54. The graph shows probability of target location over time for four Layer 1b sensors with a probability of detection ps_i covering each route, P_{h1}, P_{h2}, P_{h3} and P_o are .30, .30, .30, and .10, respectively. Four routes connect each hiding area to the operating area, but the model simulates a "disrupt" with probabilities of selecting a route between hiding area and operating area for $pk_{1,5,9}$, $pk_{2,6,10}$, $pk_{3,7,11}$, $pk_{4,8,12}$, are .05, .1166, .1166, .05, consequently the routes with lower probability of selection are assumed to have lower rates r_{fh1}, r_{fh2}, r_{fh3} and r_{fh4}. The rates are values are 0.7, 3.7, 3.7, and 0.7, respectively.
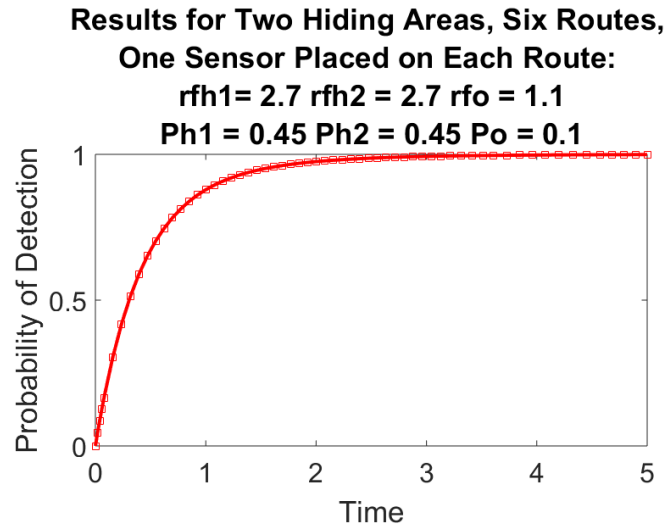
Figure 6.55. The graph depicts the probability of detection results over time depicted graphically for six Layer 1b sensors with a probability of detection ps_i cover each route,P_{h1}, P_{h2}, P_{h3} and P_o are .30, .30, .30, and .10, respectively. Four routes connect each hiding area to the operating area, but the model simulates a "disrupt" with probabilities of selecting a route between hiding area and operating area for $pk_{1,5,9}$, $pk_{2,6,10}$, $pk_{3,7,11}$, $pk_{4,8,12}$, are .05, .1166, .1166, .05, consequently the routes with lower probability of selection are assumed to have lower rates r_{fh1}, r_{fh2}, r_{fh3} and r_{fh4}. The rates are values are 0.7, 3.7, 3.7, and 0.7, respectively.

The discrete results from the figures above are shown in Table 6.36.

Table 6.36. Time versus Probability when $P_{h1} = 0.3$ $P_{h2} = 0.3$, $P_{h3} = 0.3$ and $P_o = 0.1$ values change, $r_{f1} = 1.1$, $r_{f2} = 2.7$, $r_{f3} = 2.7$ and $r_{f4} = 1.1$

t	P(t)
0	0
1.00	0.5285
2.00	0.7729
3.00	0.8890
4.00	0.9453
5.00	0.9728

The resulting probabilities of $P_{h1}(t)$, $P_{h2}(t)$, $P_{h3}(t)$ and $P_o(t)$ are shown in Figure 6.56 and

probabilities of detection are shown in Figure 6.57.

Results for Three Hiding Areas,
One Operating Area, Twelve Routes,
One Sensor Placed on Each Route:
rf1= 0.7 rf2 = 3.7 rf3 = 3.7 rf4 = 0.7
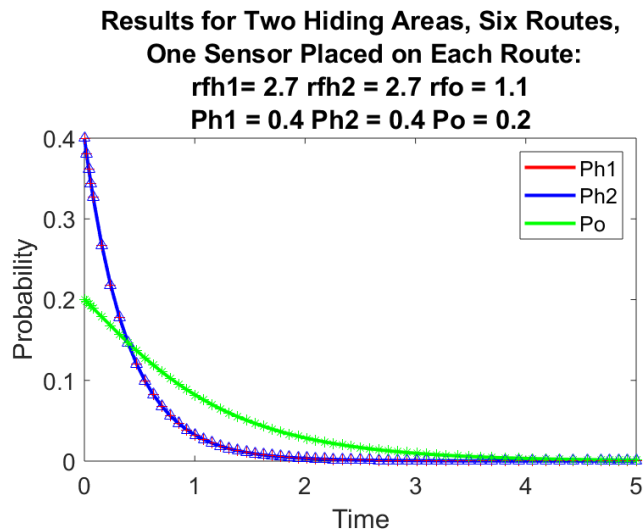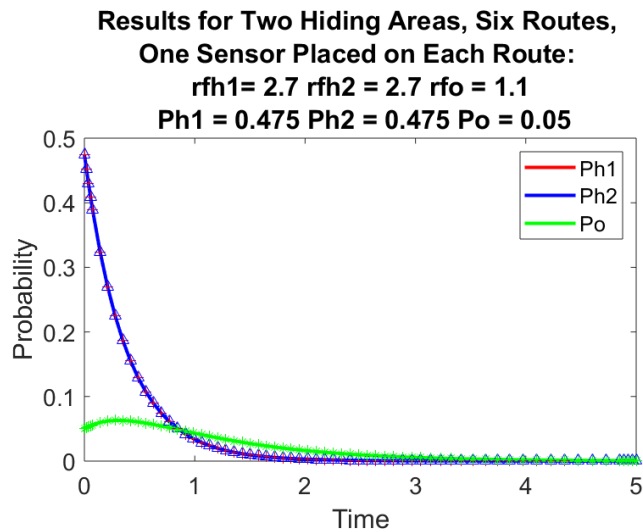**Ph1 = 0.3 Ph2 = 0.3 Ph3 = 0.3 Po = 0.1**
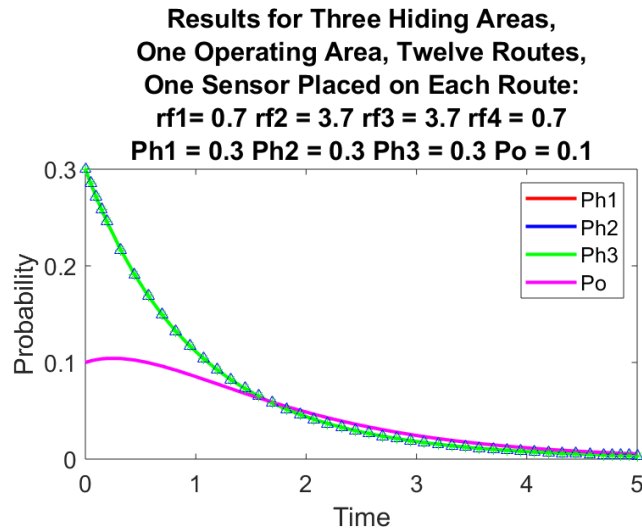
Figure 6.56. The graph shows probability of target location over time for four Layer 1b sensors with a probability of detection ps_i covering each route, P_{h1}, P_{h2}, P_{h3} and P_o are .30, .30, .30, and .10, respectively. Four routes connect each hiding area to the operating area, but the model simulates a "disrupt" with probabilities of selecting a route between hiding area and operating area for $pk_{1,5,9}$, $pk_{2,6,10}$, $pk_{3,7,11}$, $pk_{4,8,12}$, are .025, .1416, .1416, .025, consequently the routes with lower probability of selection are assumed to have lower rates r_{fh1}, r_{fh2}, r_{fh3} and r_{fh4}. The rates are values are 0.7, 3.7, 3.7, and 0.7, respectively.

**Results for Three Hiding Areas,
One Operating Area, Twelve Routes,
One Sensor Placed on Each Route:
rf1= 0.7 rf2 = 3.7 rf3 = 3.7 rf4 = 0.7
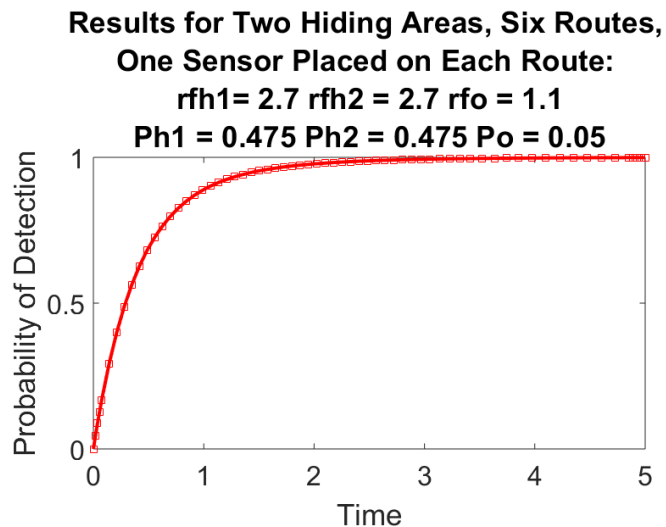Ph1 = 0.3 Ph2 = 0.3 Ph3 = 0.3 Po = 0.1**

Figure 6.57. The graph depicts the probability of detection results over time depicted graphically for six Layer 1b sensors with a probability of detection ps_i cover each route, P_{h1}, P_{h2}, P_{h3} and P_o are .30, .30, .30, and .10, respectively. Four routes connect each hiding area to the operating area, but the model simulates a "disrupt" with probabilities of selecting a route between hiding area and operating area for $pk_{1,5,9}$, $pk_{2,6,10}$, $pk_{3,7,11}$, $pk_{4,8,12}$, are .025, .1416, .1416, .025, consequently the routes with lower probability of selection are assumed to have lower rates r_{fh1}, r_{fh2}, r_{fh3} and r_{fh4}. The rates are values are 0.7, 3.7, 3.7, and 0.7, respectively.

The discrete results from the figures above are shown in Table 6.37.

Table 6.37. Time versus Probability when $P_{h1} = 0.3$ $P_{h2} = 0.3$, $P_{h3} = 0.3$ and $P_o = 0.1$ values change, $r_{f1} = 0.7$, $r_{f2} = 3.7$, $r_{f3} = 3.7$ and $r_{f4} = 0.7$

t	P(t)
0	0
1.00	0.5811
2.00	0.8197
3.00	0.9211
4.00	0.9651
5.00	0.9845

After one interval of time, the probability of targets selecting a route increases the probability

111

to detect targets moving in UMI by 5.26%. This increase may be enough to convince commanders to employ resource to achieve a similar result.

The overall performance of employing "disrupting" obstacles to increase the probability of detection is lower than employing "blocking" obstacles nearly 7.50%. Yet, comparing the results from Figure 6.49 to Figure 6.53 and Figure 6.57 covering each route yields the best change to detect target movement in UMI.

Assuming the sensor probability is 50%, the explicit numerical solution to model is

$$
\begin{bmatrix} p_{h1}(t) \\ p_{h2}(t) \\ p_{h3}(t) \\ p_o(t) \end{bmatrix} = 0.0001 \begin{bmatrix} 0.8166 \\ -0.4082 \\ -0.4082 \\ -0.0001 \end{bmatrix} e^{-2.9249t} - 0.5105 \begin{bmatrix} -0.5491 \\ -0.5492 \\ -0.5492 \\ 0.3085 \end{bmatrix} e^{-2.3016t}
$$

$$
+ 0.2597 \begin{bmatrix} 0.0756 \\ 0.0756 \\ 0.0756 \\ 0.9914 \end{bmatrix} e^{-1.0485t} - 0.000 \begin{bmatrix} 0.0000 \\ -0.7071 \\ 0.7071 \\ -0.0001 \end{bmatrix} e^{-2.9250t}. \tag{6.17}
$$

MATLAB's ODE45 solver solution validates the numerical solution. Figure 6.58 graphically compares the ODE45's solver solution to the numerical solution.

112
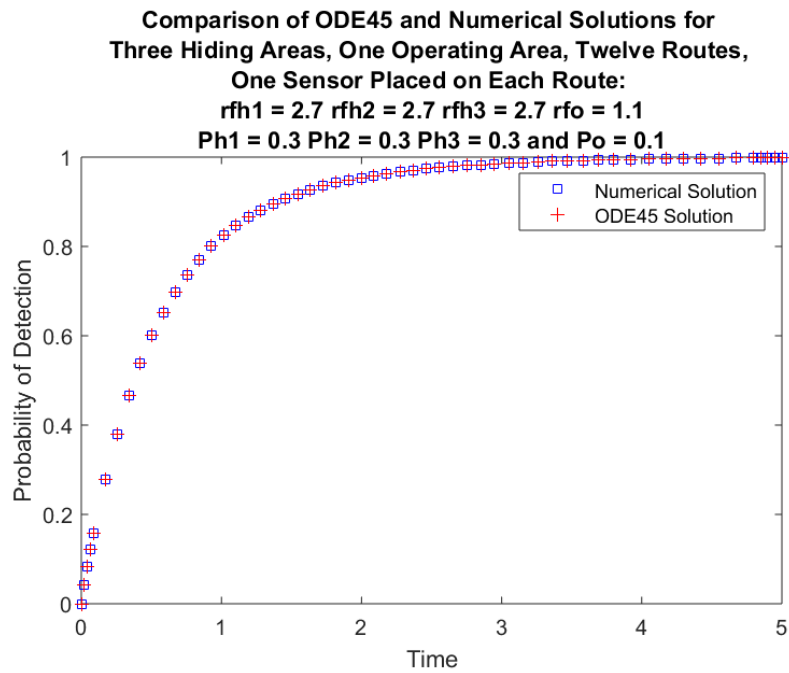
Figure 6.58. MATLAB ODE45 and Numerical Solution Comparison for a 3x3 System of Equations when $Ph1 = .30$, $Ph2 = .30$, $Ph3 = .30$ $P_0 = .10$, $r_f1 = 2.7$, $r_f2 = 2.7$, $r_f3 = 2.7$ and $r_b = 1.1$, and $p_{s1} = .50$. A target's probability of selecting each route is .834.

THIS PAGE INTENTIONALLY LEFT BLANK

CHAPTER 7:
Conclusion

7.1 Research Objectives

7.1.1 Assess Detectability

Commanders must decide where to place sensors and must accept prudent risk to expose troops to an unknown subterranean environment. They must weigh the risk and reward of expending resources in the subterranean space. Since there are so many factors that go into decision making, multiple commanders from the company to Joint Task Force level contributed their units' experience to a survey. The survey's trends and explanations are below.

(1) Experience in subterranean urban environments. Officers' experience in the subterranean did not occur in urban environments, reference Section A.2. This trend is understandable considering the concept of fighting in a dense urban metropolitan area is a newer concept. Moreover, experience in UMI in a dense urban environment is so rare that doctrine is currently under development. For example, of the officers that mentioned their units did have some subterranean exposure, only one dealt with UMI, a wadi.

(2) Adversary usage of subterranean environment. According to the survey, some units were concerned with entering cave systems, and rudimentary tunnels impacting force protection of Forward Observation Bases (FOBs) or nodes of transportation, reference Section A.2. Applying the situations above to the model, the location of a target's hiding area A is unknown, rudimentary tunnels or cave systems represent routes k, and FOBs or nodes of transportation as operating areas C. If the U.S. Military knew the tunnel location and had access to the routes, the ABC model is applicable. While the survey did not enhance modeling the urban subterranean environment, it did confirm the doctrine used to build the models is accurate.

(3) Subterranean training and Sensor Employment. Only one officer used sensors to detect enemy movement, and one other trained in subterranean operations while deployed to the

115

Republic of Korea, reference Section A.2. Due to the officers' limited experience with sensors, it is difficult to assess the model or sensor employment.

Future sensors must have a high probability of detection to be worth employing in a megacity's UMI. Finding the balance between speed of emplacement and performance is critical. However, based on the results of all models presented, the more sensors, the better. In the future, if Commanders are willing to use sensors in a megacity's UMI to provide early warning of target movement, units should place as many sensors as possible. Covering as many routes as possible with sensors will result in the highest probability of detection.

The difference between employing a Layer 1b sensor versus a Layer 1a sensor is 10.44% , as shown in Section 6.5.

According to the models, after one interval of time elapsed, covering each route yielded a probability of detection between 65.19% and 89.16%, as shown in Section 6.5 and Section 6.8.1.

Blocking Routes in order to canalized targets yielded a probability of detection between 62.78% and 65.60%, as shown in Section 6.8.2

Disrupting target movement along routes yielded a probability of detection between 52.85% and 58.11%, as shown in Section 6.8.2.

The probability of target detection for models with covered and uncovered routes was between 43.61% and 66.07%, as shown in Section 6.3 and Section 6.6.

7.1.2 Improve Readiness

The model results significantly affect the Department of Defense and the Department of Homeland Security's current and future subterranean operations efforts. Non-mathematical findings or qualitative recommendations encapsulate important points to consider when approaching the urban subterranean environment through a military perspective. Mathematical results support the importance of factors that should be considered in future urban subterranean operations when effective sensor technology exists to aid in the subterranean fight.

The most important recommendation drawn from this research emphasizes knowledge of the

operating environment before entering an urban environment. Open-source documentation provides immensely beneficial information when researching a megacity's UMI. In addition, the most effective way to increase the probability of detection with minimal physical impact on the environment is to influence an enemy's selection of which route they are most likely to select from the hiding area to operating area.

The research concludes some of the tactics and principles executed by the U.S. military's fight on land are not a practical approach to engaging adversaries in UMI.

According to the mathematical model results, obstacle effects of fixing and disrupting enemy movement lowers the probability of detection because each obstacle effect slows the target's rate of travel between the hiding and operating areas. Employing the obstacle effects of fix and disrupt are not recommended tactics in UMI.

While block/turn effect model is the best performing model in the subterranean environment for obstacle effects, the principle of obstacle over-watch is severely limited and the obstacle can be breached without resistance. Blocking UMI corridors for an extended period time may have negative effects on the population's public service. Moreover, targets can reduce obstacles with no resistance, assuming the route is completely blocked in both directions of travel. Extended use of the block and turn obstacle effects is not a recommended in UMI. Figure 7.1 recalls each obstacle effect from Chapter 4.

Figure 7.1. ATP 3-90.8 Combined Arms Countermobility Operations' Obstacle Effects. Source: [17].

7.2 Future Work

Three areas of future work may enhance the finding of this paper. First, given the increased attention to subterranean operations in the past few years, intelligence communities must begin to gather information on megacities' UMI blue prints. Second, modeling rates of travel r_f and r_b, and probability of taking a route k using UMI size (diameter of UMI) may improve the realism of the model. Third, modeling UMI as a complex network may significantly speed up the process of identifying the most important areas to employ sensors. By effectively utilizing intelligence data and improving the flow rates and probability of route selection the U.S. Army can mathematically determine the most effective area to place sensors.

7.2.1 Intelligence Gathering

Data from building blueprints, subway systems, UMI, road networks, communication lines, and maintenance corridors are considered routes that targets may use to conduct invasive operation in a subterranean environment. Current building codes, if available, or open-source

transportation maps also help conceptualize the complexity of urban subterranean. From megacity data, the Intelligence Preparation of the Battlefield (U.S. Army) or Joint Intelligence Preparation of the Operating Environment process turns data into useful knowledge before entering a megacity. Commands are better prepared for subterranean operations. Education and preparation save time and treasure during the conflict.

7.2.2 Improving ABC Model's Rate Forward/Back Values and Route Selection Probability

Although each model used educated assumptions to represent different rates of travel between areas, and probabilities that targets would choose one route over another, there is a significant opportunity for improvement. Future work in the area of subterranean warfare includes enhancing the subterranean model with real-life data, such as the actual size and measurements of sewer and storm water systems. Using the actual size of UMI aids in determining the flow rate of target along a route and the probability of the target's route selection when moving between areas. One would imagine the diameter of the sewer and stormwater lines is directly proportional to the opportunity of flow rate for the target and the target's probability of route selection. Moreover, additional research may uncover additional urban zones (core, industry, commercial, peripheral, residential, and high rise) that have unique subterranean characteristics to exploit or deny during subterranean operations.

7.2.3 Complex Network Centralities

When determining where to employ sensors in megacities' UMI, using network centrality metrics may significantly aid in identifying the most important intersections (vertices/nodes) highly connected to a large number of UMI voids (edges/arcs) such as pipes, culverts, tunnels,...etc. One way to decide where to place sensors is to calculate vertex centralities.

Future work may model a megacity's subterranean environment as a complex network and run different centrality tests to aid in sensor placement decision making.

Calculating Degree Centrality, the number of connected edges to a signal vertex [21] is important if a sensor is able to detect target movement in multiple directions. The Degree Centrality essentially determines what node provides the 'best value' criteria for commanders to enter the subterranean space simply by determining all its connections.

Eigenvector Centrality measures the strength of a vertex's neighbors and ranks the importance of all vertices [21]. Calculating Eigenvector centrality gives commanders a list of vertex's of greatest and least importance. The list may aid in deciding where to focus efforts. Eigenvector Centrality provides mathematical criteria for commanders to either bypass or enter [15] the subterranean space.

Distance Centrality "identifies how much influence a given vertex has over graph structure by calculating the amount of neighbor matrix change resulting from vertex removal" [21]. In other words, utilizing Distance Centrality in a complex UMI network gives insight to important vertex to place a sensor to detect movement, or to block an important route.

All centrality results provide a unique way to prioritize sensor locations.

7.2.4   Layer 2 Sensors

Layer 2, non-UMI sensor technology, is the next layer of defense. These sensors detect the construction and utilization of non-UMI voids. Non-UMI voids may connect UMI to other UMI, building foundations, underground parking lots, etc. While Layer 2 sensors utilization is interesting and as well as important, modeling its probability of detection is outside the scope of this research and should be considered for future work.

7.2.5   Using Sensors in the Offense

The transition from defense to offense is rapid. Once the initiative is achieved, it must be retained. While defense is reactive, offense dictates the battle's tempo. Layer 1a and Layer 1b sensors assist in setting conditions to transition from defensive operations to offensive operations. As units patrol deeper into the subterranean environment, sensors are employed. Like in the defense, these sensors can detect target activity.

Consider a scenario where troops unknowingly approach an enemy subterranean hiding space A. Troops place sensors in routes and return to there assembly area. Over the next hours, days, or weeks the network of sensors detects large amounts of target activity. Whether the enemy is staging a counterattack or conducting its defensive patrols near its hiding area, sensors provide the unit leadership the ability to locate enemy positions without direct contact.

While it is important to address sensors' abilities in the offense, modeling this scenario is difficult. Our ABC model does not accurately depict enemy behavior so close to hiding area and modeling sensors in the offense is a great topic for future work.

THIS PAGE INTENTIONALLY LEFT BLANK

APPENDIX: MATLAB Code and Survey Questions and Results

A.1 MATLAB Code

A.1.1 "One Route with Sensor on Route"

MATLAB Sytem of Equations:

```
1 function output=gm1(t,x,rf,rb,ps1)
2 output=[-rf*x(1)+rb*(1-ps1)*x(2);...
3     -rb*x(2)+rf*(1-ps1)*x(1)];
```

MATLAB Code :

```
1 %% Model 1 Master
2 x0=[0.50 0.50];%initial condition for x(1), x(2), where x(1)
    +x(2)+... = 1
3 rf=2.7;%rate forward to operating area
4 rb=1.1;%rate backward to hidding area
5 %ps1 =0.0;% no sensor, the solution converges to a steady
    state solution
6 ps1 = 0.9;% Probability of Detection, Introduction of a
    sensor to Route 1
7 tfinal = 5.0;%Time Max
8 [t,x]=ode45(@(t,x) gm1(t,x,rf,rb,ps1),[0 tfinal],x0);
9 clf;
10 figure(1)
11 plot(t,x(:,1),'r', t, x(:,2),'b','linewidth',2)
12 hold on
13 plot(t,x(:,1),'r+', t, x(:,2),'b^')
14 title(['Results for One Route with Sensor: rf = ', num2str(
    rf),' rb = '...
```

```matlab
15        , num2str ( rb ) , ' Ph = ' , num2str ( x0 ( 1 ) ) , ' and Po = ' , ...
              num2str ( x0 ( 2 ) ) ] )
16 xlabel ( ' Time ' )
17 ylabel ( ' Probability ' )
18 legend ( ' Ph ' , ' Po ' )
19 set ( gca , ' fontsize ' ,14)
20 %% Model 1 Cumulative Probability of Detection
21 figure (2)
22 p_nd = x ( : ,1)+x ( : ,2) ; % escape or non−detection probability
23 plot ( t ,1−p_nd , ' r ' , ' linewidth ' ,2)%Plot Probabilty of
       Detection from t =[0 ,5]
24 hold on
25 plot ( t ,1−p_nd , ' rs ' )
26 title ([ ' Results for One Route with Sensor : rf = ' , num2str (
       rf ) , ' rb = ' ...
27       , num2str ( rb ) , ' Ph = ' , num2str ( x0 ( 1 ) ) , ' and Po = ' , ...
              num2str ( x0 ( 2 ) ) ] )
28 xlabel ( ' Time ' )
29 ylabel ( ' Probability of Detection ' )
30 set ( gca , ' fontsize ' ,14)
31
32 t_desired =[1 ,2 ,3 ,4 ,5];
33 y_desired=spline ( t ,(1−p_nd) , t_desired ) ;
34 y_desired
35 %% Model 1 Numerical Solution Check
36 A=[−rf    rb∗(1−ps1 ) ;
37    rf∗(1−ps1 )  −rb ]
38
39 a=1
40 b=−trace (A)
41 c=A( 1 ,1)∗A( 2 ,2)−A( 2 ,1)∗A( 1 ,2)
42 lambda1 =(−b+sqrt ((b∗b)−4∗a∗c ) ) /(2∗a)
43 lambda2 =(−b−sqrt ((b∗b)−4∗a∗c ) ) /(2∗a)
```

```
44
45 c1 =((((A(1 ,1)+A(1 ,2))−lambda2)*x(1)+((A(2 ,1)+A(2 ,2))−lambda2)
       *x(2))./(lambda1−lambda2)
46
47 c2 =((((A(1 ,1)+A(1 ,2))−lambda1)*x(1)+((A(2 ,1)+A(2 ,2))−lambda1)
       *x(2))./(lambda2−lambda1)
48
49 tn=t
50
51 poph=c1*exp(lambda1*t)+c2*exp(lambda2*t)
52 plot(t,1−poph,'bs')
53 hold on
54 plot(t,1−p_nd,'r+')
55 title([ 'Comparison of ODE45 and Analytical Solutions Results
       for '...
56     ' One Route with Sensor: rf = ', num2str(rf),' rb = ',
           num2str(rb) ,...
57     ' Ph = ', num2str(x0(1)),' and Po = ', num2str(x0(2))])
58 legend('Analytical Solution','ODE45 Solution')
59 xlabel('Time')
60 ylabel('Probability of Detection')
61 hold off
```

A.1.2 "Two routes, One Sensor placed on Route 1"

MATLAB Sytem of Equations:

```
1 function output=gm2 (t ,x ,rf ,rb ,pk0 ,ps1)
2 output =[−rf*x(1)+ rb*(pk0(3)*(1−ps1)+pk0(4))*x(2) ;...
3     −rb*x(2)+ rf*(pk0(1)*(1−ps1)+pk0(2))*x(1)];
```

MATLAB Code :

```
1 %% Model 2 Master
```

```matlab
2  x0 = [0.50 0.50]; % initial condition for x(1), x(2), x(1) +
       x(2)+... = 1
3  pk0=[.75 .25 .25 .75];
4  rf = 3.7;
5  rb = 1.1;
6  ps1 = 0.0; % sensor probability of detection,
7  %the solution converges to a steady state solution
8          %  ph_s = rb/(rf+rb), po_0 = rf/(rf+rb)
9          %x0 =[ rb/(rf+rb) rf/(rf+rb)]; % reset the initial
              condition
10 tfinal = 5.0;
11 [t,x]=ode45(@(t,x) gm2(t,x,rf,rb,pk0,ps1),[0 tfinal],x0);
12 clf;
13 figure(1)
14 plot(t,x(:,1),'r', t, x(:,2),'b','linewidth',2)
15 hold on
16 plot(t,x(:,1),'r+', t, x(:,2),'b^')
17 title(['Results for Two Routes, One Sensor Placed on Route
       1: rf= ',...
18     num2str(rf), ' rb = ', num2str(rb),' Ph = ', num2str(x0
          (1)),...
19     ' and Po = ', num2str(x0(2))])
20 xlabel('Time')
21 ylabel('Probability')
22 legend('Ph','Po')
23 set(gca,'fontsize',14)
24 %% Model 2 Cumulative Probability of Detection
25 figure(2)
26 p_nd = x(:,1)+x(:,2); % escape or non-detection probability
27 plot(t,1-p_nd,'r','linewidth',2)
28 hold on
29 plot(t,1-p_nd,'rs')
30 title(['Results for Two Routes, One Sensor Placed on Route
```

```
      1:  rf=  ’...
31      ,  num2str(rf),  ’ rb = ’,  num2str(rb),’ Ph = ’,  num2str(
            x0(1)) ,...
32      ’ and Po = ’,  num2str(x0(2))])
33 xlabel(’Time’)
34 ylabel(’Probability of Detection’)
35 set(gca,’fontsize’,14)
36
37 t_desired=[1,2,3,4,5];
38 y_desired=spline(t,(1−p_nd),t_desired);
39 y_desired
```

A.1.3   "Two routes, Two Sensors on Route 1"

MATLAB Sytem of Equations:

```
1 function output=gm3 (t,x,rf,rb,pk0, ps0)
2 output=[−rf∗x(1)+ rb∗((pk0(4))+(pk0(3)∗(1−ps0(2))∗(1−ps0(1))
    ))∗x(2);...
3    −rb∗x(2)+ rf∗((pk0(2))+(pk0(1)∗(1−ps0(1))∗(1−ps0(2))))∗x
        (1)];
```

MATLAB Code :

```
1 %% Model 3 Master
2 x0 = [0.50 0.50]; % initial condition for x(1), x(2), where
    x(1) + x(2)+... = 1
3 pk0=[.50 .50 .50 .50];
4 rf = 2.7;
5 rb = 1.1;
6 ps0 = [0.00 0.0];% sensor probability of detection,
7 %the solution converges to a steady state solution
8        %   ph_s = rb/(rf+rb), po_0 = rf/(rf+rb)
9        %x0 =[ rb/(rf+rb) rf/(rf+rb)]; % reset the initial
            condition
```

```matlab
10  tfinal = 5.0;
11  [t,x]=ode45(@(t,x) gm3(t,x,rf,rb,pk0,ps0),[0 tfinal],x0);
12  clf;
13  figure(1)
14  plot(t,x(:,1),'r', t, x(:,2),'b','linewidth',2)
15  hold on
16  plot(t,x(:,1),'r+', t, x(:,2),'b^')
17  title(['Results for Two Routes, Two Sensors Placed on Route
       1: rf= '...
18      , num2str(rf), ' rb = ', num2str(rb),' Ph = ', num2str(
           x0(1)),...
19      ' and Po = ', num2str(x0(2))])
20  xlabel('Time')
21  ylabel('Probability')
22  legend('Ph','Po')
23  set(gca,'fontsize',14)
24  %% Model 3 Cumulative Probability of Detection
25  figure(2)
26  p_nd = x(:,1)+x(:,2); % escape or non-detection probability
27  plot(t,1-p_nd,'r','linewidth',2)
28  hold on
29  plot(t,1-p_nd,'rs')
30  title(['Results for Two Routes, Two Sensors Placed on Route
       1: rf= '...
31      , num2str(rf), ' rb = ', num2str(rb),' Ph = ', num2str(
           x0(1)),...
32      ' and Po = ', num2str(x0(2))])
33  xlabel('Time')
34  ylabel('Probability of Detection')
35  set(gca,'fontsize',14)
36  %Want Results for t=1,2,3,4,5
37  t_desired=[1,2,3,4,5];
38  y_desired=spline(t,(1-p_nd),t_desired);
```

```
39 y_desired
```

A.1.4   "Two routes, One Sensors on each Route"

MATLAB Sytem of Equations:

```
1 function output = gm4(t,x,rf,rb,pk0,ps0)
2 output = [−rf∗x(1)+ rb∗((pk0(1))∗(1−ps0(1))+pk0(2)∗(1−ps0(2)
    ))∗x(2);...
3    −rb∗x(2)+ rf ∗((pk0(1))∗(1−ps0(1))+pk0(2)∗(1−ps0(2)))∗x(1)
       ];
```

MATLAB Code :

```
1 %% Model 4 Master
2 x0 = [0.50 0.50]; % initial condition for x(1), x(2),x(1) +
    x(2)+... = 1
3 pk0 =[.50 .50 .50 .50];
4 rf = 2.7;
5 rb = 1.1;
6 ps0 = [0.0 0.0];% sensor probability of detection ,
7 %the solution converges to a steady state solution
8        %   ph_s = rb/(rf+rb), po_0 = rf/(rf+rb)
9        %x0 =[ rb/(rf+rb) rf/(rf+rb)]; % reset the initial
            condition
10 tfinal = 5.0;
11 [t,x]=ode45(@(t,x) gm4(t,x,rf,rb,pk0,ps0),[0 tfinal],x0);
12 clf;
13 figure(1)
14 plot(t,x(:,1),'r', t, x(:,2),'b','linewidth',2)
15 hold on
16 plot(t,x(:,1),'r+', t, x(:,2),'b^')
17 title(['Results for Two Routes, One Sensor Placed on each
    Route: rf= '...
```

```
18        , num2str(rf), ' rb = ', num2str(rb),' Ph = ', num2str(
             x0(1))...
19        ,' and Po = ', num2str(x0(2))])
20 xlabel('Time')
21 ylabel('Probability')
22 legend('Ph','Po')
23 set(gca,'fontsize',14)
24 %% Model 4 Cumulative Probability of Detection
25 figure(2)
26 p_nd = x(:,1)+x(:,2); % escape or non-detection probability
27 plot(t,1-p_nd,'r','linewidth',2)
28 hold on
29 plot(t,1-p_nd,'rs')
30 title(['Results for Two Routes, One Sensor Placed on each
        Route: rf= '...
31        , num2str(rf), ' rb = ', num2str(rb),' Ph = ', num2str(
             x0(1))...
32        ,' and Po = ', num2str(x0(2))])
33 xlabel('Time')
34 ylabel('Probability of Detection')
35 set(gca,'fontsize',14)
36 %Want Results for t=1,2,3,4,5
37 t_desired=[1,2,3,4,5];
38 y_desired=spline(t,(1-p_nd),t_desired);
39 y_desired
```

A.1.5 "Twelve routes, One Sensor on each Block Corner"

MATLAB Sytem of Equations:

```
1 function output = gm5(t,x,rf,rb,pk0,ps0)
2 output = [-rf*x(1)+ rb*((pk0(1)*(1-ps0(1)))+(pk0(2)*(1-ps0
      (1)))...
3    +(pk0(3)*(1-ps0(1)))+(pk0(4)*(1-ps0(1)))...
```

```
4        +pk0 ( 5 )+pk0 ( 6 )+pk0 ( 7 )+pk0 ( 8 )+pk0 ( 9 )+pk0 ( 1 0 )+pk0 ( 1 1 )+pk0
            ( 1 2 ) ) ∗x ( 2 ) ; . . .
5        −rb ∗x ( 2 )+  rf ∗ ( ( pk0 ( 1 ) ∗(1−ps0 ( 1 ) ) )+(pk0 ( 2 ) ∗(1−ps0 ( 1 ) ) ) . . .
6        +(pk0 ( 3 ) ∗(1−ps0 ( 1 ) ) )+(pk0 ( 4 ) ∗(1−ps0 ( 1 ) ) ) . . .
7        +pk0 ( 5 )+pk0 ( 6 )+pk0 ( 7 )+pk0 ( 8 )+pk0 ( 9 )+pk0 ( 1 0 )+pk0 ( 1 1 )+pk0
            ( 1 2 ) ) ∗x ( 1 ) ] ;
```

MATLAB Code :

```
 1 %% Model  5  Master
 2 x0  =  [ 0 . 5 0   0 . 5 0 ] ; %  i n i t i a l   c o n d i t i o n   f o r   x ( 1 ) ,   x ( 2 ) ,   x ( 1 )  +
        x ( 2 )+ . . .   =  1
 3 pk0 = [ . 0 8 3 4   . 0 8 3 4   . 0 8 3 4   . 0 8 3 4   . 0 8 3 3   . 0 8 3 3   . 0 8 3 3   . 0 8 3 3   . 0 8 3 3
        . 0 8 3 3   . 0 8 3 3 . . .
 4        . 0 8 3 3 ] ;
 5 %pk0 = [ . 0 9 0 0   . 0 9 0 0   . 0 9 0 0   . 0 9 0 0   . 0 8 0 0   . 0 8 0 0   . 0 8 0 0   . 0 8 0 0   . 0 8 0 0
        . 0 8 0 0   . 0 8 0 0 . . .
 6 % . 0 8 0 0 ] ;
 7 %pk0 = [ . 1 2 0 0   . 1 2 0 0   . 1 2 0 0   . 1 2 0 0   . 0 6 5 0   . 0 6 5 0   . 0 6 5 0   . 0 6 5 0   . 0 6 5 0
        . 0 6 5 0   . 0 6 5 0 . . .
 8 %  . 0 6 5 0 ] ;
 9 rf  =  2 . 7 ;
10 rb  =  1 . 1 ;
11 ps0  =  [ 0 . 0   0 . 0   0 . 0   0 . 0   0 . 0   0 . 0 ]  ; %  s e n s o r   p r o b a b i l i t y   o f
        d e t e c t i o n ,
12 %the   s o l u t i o n   c o n v e r g e s   t o   a   s t e a d y   s t a t e   s o l u t i o n
13            %    ph_s  =  rb / ( rf+rb ) ,   po_0  =   rf / ( rf+rb )
14            %x0  = [  rb / ( rf+rb )   rf / ( rf+rb ) ] ; %  r e s e t   t h e   i n i t i a l
                c o n d i t i o n
15 t f i n a l  =  5 . 0 ;
16 [ t , x ]=ode45 (@( t , x )  gm5( t , x , rf , rb , pk0 , ps0 ) , [ 0   t f i n a l ] , x0 ) ;
17 clf ;
18 figure ( 1 )
19 plot ( t , x ( : , 1 ) , ' r ' ,  t ,  x ( : , 2 ) , ' b ' , ' l i n e w i d t h ' , 2 )
```

```
20 hold on
21 plot(t,x(:,1),'r+', t, x(:,2),'b^')
22 title(['Results for Twelve Routes, One Sensor Placed on
      Eight UMI'...
23     'Intersections: rf= ', num2str(rf), ' rb = ', num2str(rb
          ),...
24     ' Ph = ', num2str(x0(1)),' and Po = ', num2str(x0(2))])
25 xlabel('Time')
26 ylabel('Probability')
27 legend('Ph','Po')
28 set(gca,'fontsize',14)
29 %% Model 5 Cumulative Probability of Detection
30 figure(2)
31 p_nd = x(:,1)+x(:,2); % escape or non-detection probability
32 plot(t,1-p_nd,'r','linewidth',2)
33 hold on
34 plot(t,1-p_nd,'rs')
35 title(['Results for Twelve Routes, One Sensor Placed on
      Eight UMI'...
36     'Intersections: rf= ', num2str(rf), ' rb = ', num2str(rb
          ),...
37     ' Ph = ', num2str(x0(1)),' and Po = ', num2str(x0(2))])
38 xlabel('Time')
39 ylabel('Probability of Detection')
40 set(gca,'fontsize',14)
41 %Want Results for t=1,2,3,4,5
42 t_desired=[1,2,3,4,5];
43 y_desired=spline(t,(1-p_nd),t_desired);
44 y_desired
```

A.1.6   "Two Hiding Areas, Six Routes, One Senors on each Route"

MATLAB Sytem of Equations:

```
1 function output = gm7(t,x,rf0,pk0,ps0)
2 output=[-rf0(1)*x(1)+(rf0(2)*(pk0(5)*(1-ps0(5)))+(pk0(6)*(1-
      ps0(5))))*x(2)...
3    +(rf0(3)*(pk0(1)*(1-ps0(5)))+(pk0(2)*(1-ps0(5))))*x(3)
         ;...
4    (rf0(1)*(pk0(5)*(1-ps0(5)))+(pk0(6)*(1-ps0(5))))*x(1)-
         rf0(2)*x(2)...
5    +(rf0(3)*(pk0(3)*(1-ps0(3)))+(pk0(4)*(1-ps0(5))))*x(3)
         ;...
6    (rf0(1)*(pk0(1)*(1-ps0(5)))+(pk0(2)*(1-ps0(5))))*x(1)...
7    +(rf0(2)*(pk0(3)*(1-ps0(5)))+(pk0(4)*(1-ps0(5))))*x(2)-
         rf0(3)*x(3)];
```

MATLAB Code :

```
1 %% Model 7 Master
2 x0=[0.475 0.475 0.05];% initial condition for x(1),x(2), x
      (1)+x(2)+...= 1
3 pk0=[.1666 .1667 .1667 .1666 .1667 .1667];%Units can come
      into contact.
4 %pk0=[.25 .25 .25 .25 0 0]; %Units do not come into contact.
5 rf0 = [2.7 2.7 1.1];
6 ps0 = [0.0 0.0 0.0 0.0 0.0 0.0]; % sensor probability of
      detection
7         %   ph_s = rb/(rf+rb), po_0 = rf/(rf+rb)
8         %x0 =[ rb/(rf+rb) rf/(rf+rb)]; % reset the initial
             condition
9 tfinal = 5.0;
10 [t,x]=ode45(@(t,x) gm7(t,x,rf0,pk0,ps0),[0 tfinal],x0);
11 clf;
12 figure(1)
13 plot(t,x(:,1),'r', t,x(:,2),'b',t,x(:,3),'g','linewidth',2)
14 hold on
15 plot(t,x(:,1),'r+', t, x(:,2),'b^',t, x(:,3),'g*')
```

```matlab
16 title(['Results for Two Hiding Areas, Six Routes, One Sensor
       Placed on'...
17     'Each Route: rfh1= ', num2str(rf0(1)), ' rfh2 = ',
         num2str(rf0(2)),...
18     ' rfo = ', num2str(rf0(3)),' Ph1 = ', num2str(x0(1)),...
19     ' Ph2 = ', num2str(x0(2)),' Po = ', num2str(x0(3))])
20 xlabel('Time')
21 ylabel('Probability')
22 legend('Ph1','Ph2','Po')
23 set(gca,'fontsize',14)
24 %% Model 7 Cumulative Probability of Detection
25 figure(2)
26 p_nd = x(:,1)+x(:,2)+x(:,3); % escape or non-detection
       probability
27 plot(t,1-p_nd,'r','linewidth',2)
28 hold on
29 plot(t,1-p_nd,'rs')
30 title(['Results for Two Hiding Areas, Six Routes, One Sensor
       Placed on'...
31     'Each Route: rfh1= ', num2str(rf0(1)), ' rfh2 = ',
         num2str(rf0(2)),...
32     ' rfo = ', num2str(rf0(3)),' Ph1 = ', num2str(x0(1)),...
33     ' Ph2 = ', num2str(x0(2)),' Po = ', num2str(x0(3))])
34 xlabel('Time')
35 ylabel('Probability of Detection')
36 set(gca,'fontsize',14)
37 %Want Results for t=1,2,3,4,5
38 t_desired=[1,2,3,4,5];
39 y_desired=spline(t,(1-p_nd),t_desired);
40 y_desired
41 %% Model 7 Numerical Solution Check
42 A=[-rf0(1)  rf0(2)*(pk0(5)*(1-ps0(5)))+(pk0(6)*(1-ps0(5)))...
43     rf0(3)*(pk0(1)*(1-ps0(5)))+(pk0(2)*(1-ps0(5)));
```

134

```matlab
44        rf0 (1) *( pk0 (5) *(1−ps0 (5)))+(pk0 (6) *(1−ps0 (5))) ...
45        −rf0 (2)  rf0 (3) *( pk0 (3) *(1−ps0 (3)))+(pk0 (4) *(1−ps0 (5)));
46        rf0 (1) *( pk0 (1) *(1−ps0 (5)))+(pk0 (2) *(1−ps0 (5))) ...
47        rf0 (2) *( pk0 (3) *(1−ps0 (5)))+(pk0 (4) *(1−ps0 (5)))  −rf0 (3)]
48
49 [V,D]= eig (A)
50 %V are the Eigenvectors   Columns V(1), V(2)...
51 %D are the Eigenvalues or Lambda
52
53 c0=V\x0'
54
55 tn=t
56
57 poph=c0 (1) .* V(1:3) .* exp (D(1 ,1) *t )+c0 (2) .* V(4:6) .* exp (D(2 ,2) *
       t ) +...
58        c0 (3) .* V(7:9) .* exp (D(3 ,3) *t );
59 plot ( t ,1−poph (: ,1)−poph (: ,2)−poph (: ,3) , 'bs ')
60 hold on
61 plot ( t ,1−p_nd , 'r+')
62 title ([ 'Comparison of ODE45 and Numerical Solutions for '...
63        'Two Hiding Areas , Six Routes , One Sensor Placed on Each
            Route : '...
64        'rfh1= ', num2str ( rf0 (1)) , ' rfh2 = ', num2str ( rf0 (2)) ,'
            rfo = ' ,...
65        num2str ( rf0 (3)) ,'Ph1 = ', num2str (x0 (1)) ,' Ph2 = ',
            num2str (x0 (2)) ,...
66        'Po = ', num2str (x0 (3)) ])
67 legend ('Numerical Solution ','ODE45 Solution ')
68 xlabel ('Time ')
69 ylabel ('Probability of Detection ')
70 hold off
```

A.1.7 "Three Hiding areas, Twelve Routes, One Senors on each Route"

MATLAB Sytem of Equations:

```
1  function output = gm8(t,x,rf0,pk0,ps0)
2  dh12= rf0(2)*((pk0(5)*(1-ps0(5)))+(pk0(6)*(1-ps0(6))))*x(2);
3  dh13= rf0(3)*((pk0(11)*(1-ps0(5)))+(pk0(12)*(1-ps0(6))))*x
       (3);
4  dh14= rf0(4)*((pk0(1)*(1-ps0(1)))+(pk0(2)*(1-ps0(2))))*x(4);
5  dh21= rf0(1)*((pk0(5)*(1-ps0(5)))+(pk0(6)*(1-ps0(6))))*x(1);
6  dh23= rf0(3)*((pk0(7)*(1-ps0(1)))+(pk0(8)*(1-ps0(2))))*x(3);
7  dh24= rf0(4)*((pk0(3)*(1-ps0(3)))+(pk0(4)*(1-ps0(4))))*x(4);
8  dh31= rf0(1)*((pk0(11)*(1-ps0(5)))+(pk0(12)*(1-ps0(6))))*x
       (1);
9  dh32= rf0(2)*((pk0(7)*(1-ps0(1)))+(pk0(8)*(1-ps0(2))))*x(2);
10 dh34= rf0(4)*((pk0(9)*(1-ps0(3)))+(pk0(10)*(1-ps0(4))))*x(4)
       ;
11 dh41= rf0(1)*((pk0(1)*(1-ps0(1)))+(pk0(2)*(1-ps0(2))))*x(1);
12 dh42= rf0(2)*((pk0(5)*(1-ps0(5)))+(pk0(6)*(1-ps0(6))))*x(2);
13 dh43= rf0(3)*((pk0(9)*(1-ps0(3)))+(pk0(10)*(1-ps0(4))))*x(3)
       ;
14 output = [(-rf0(1)*x(1))+(dh12)+(dh13)+(dh14);...
15     (-rf0(2)*x(2))+(dh21)+(dh23)+(dh24);...
16     (-rf0(3)*x(3))+(dh31)+(dh32)+(dh34);...
17     (-rf0(4)*x(4))+(dh41)+(dh42)+(dh43)];
```

MATLAB Sytem of Equations with a different rate, route probability for each route:

```
1  function output = gm8c(t,x,rf0,pk0,ps0)
2  dh14a= rf0(1)*((pk0(1)*(1-ps0(5))))*x(1);
3  dh14b= rf0(2)*((pk0(2)*(1-ps0(5))))*x(1);
4  dh14c= rf0(3)*((pk0(3)*(1-ps0(5))))*x(1);
5  dh14d= rf0(4)*((pk0(4)*(1-ps0(5))))*x(1);
6
7  dh41a= rf0(1)*((pk0(1)*(1-ps0(5))))*x(4);
8  dh41b= rf0(2)*((pk0(2)*(1-ps0(5))))*x(4);
```

```
9  dh41c= rf0 (3)*((pk0 (3)*(1−ps0 (5))))*x(4);
10 dh41d= rf0 (4)*((pk0 (4)*(1−ps0 (5))))*x(4);
11
12
13 dh24a= rf0 (1)*((pk0 (5)*(1−ps0 (5))))*x(2);
14 dh24b= rf0 (2)*((pk0 (6)*(1−ps0 (5))))*x(2);
15 dh24c= rf0 (2)*((pk0 (7)*(1−ps0 (5))))*x(2);
16 dh24d= rf0 (4)*((pk0 (8)*(1−ps0 (5))))*x(2);
17
18 dh42a= rf0 (1)*((pk0 (5)*(1−ps0 (5))))*x(4);
19 dh42b= rf0 (2)*((pk0 (6)*(1−ps0 (5))))*x(4);
20 dh42c= rf0 (3)*((pk0 (7)*(1−ps0 (5))))*x(4);
21 dh42d= rf0 (4)*((pk0 (8)*(1−ps0 (5))))*x(4);
22
23 dh34a= rf0 (1)*((pk0 (9)*(1−ps0 (5))))*x(3);
24 dh34b= rf0 (2)*((pk0 (10)*(1−ps0 (5))))*x(3);
25 dh34c= rf0 (3)*((pk0 (11)*(1−ps0 (5))))*x(3);
26 dh34d= rf0 (4)*((pk0 (12)*(1−ps0 (5))))*x(3);
27
28 dh43a= rf0 (1)*((pk0 (9)*(1−ps0 (5))))*x(4);
29 dh43b= rf0 (2)*((pk0 (10)*(1−ps0 (5))))*x(4);
30 dh43c= rf0 (3)*((pk0 (11)*(1−ps0 (5))))*x(4);
31 dh43d= rf0 (4)*((pk0 (12)*(1−ps0 (5))))*x(4);
32
33 output = [(−rf0 (1)*pk0 (1)*x(1)−rf0 (2)*pk0 (2)*x(1)−rf0 (3)*pk0
       (3)*x(1) ...
34     −rf0 (4)*pk0 (4)*x(1))+(dh41a)+(dh41b)+(dh41c)+(dh41d);...
35     (−rf0 (1)*pk0 (1)*x(2)−rf0 (2)*pk0 (2)*x(2)−rf0 (3)*pk0 (3)*x
          (2) ...
36     −rf0 (4)*pk0 (4)*x(2))+(dh42a)+(dh42b)+(dh42c)+(dh42d);...
37     (−rf0 (1)*pk0 (1)*x(3)−rf0 (2)*pk0 (2)*x(3)−rf0 (3)*pk0 (3)*x
          (3) ...
38     −rf0 (4)*pk0 (4)*x(3))+(dh43a)+(dh43b)+(dh43c)+(dh43d);...
```

```
39    (−rf0(1)∗pk0(1)∗x(4)−rf0(2)∗pk0(2)∗x(4)−rf0(3)∗pk0(3)∗x
         (4)...
40    −rf0(4)∗pk0(4)∗x(4))+(dh14a)+(dh14b)+(dh14c)+(dh14d)+(
         dh24a)+(dh24b)...
41    +(dh24c)+(dh24d)+(dh34a)+(dh34b)+(dh34c)+(dh34d)];
```

MATLAB Code :

```
1 %% Model 8 Master
2 x0 = [0.30  0.30  0.30  0.10]; % initial condition for x(1), x
      (2)...,
3 %where x(1) + x(2)+... = 1
4 pk0=[.0834 .0833 .0833 .0834 .0833 .0833 .0834...
5      .0833 .0833 .0834 .0833 .0833];
6 %Probability of selecting pk route k={1,2,...,12}
7 %pk0 = [.0 .1667 .1666 .0 .0 .1667 .1667 .0 .0 .1667 .1666
       .0];
8 %Probability of selecting pk route k={1,2,...,12} for model
      8b
9 %pk0 = [.0 .3334 .0 .0 .0 .3333 .0   .0 .0 .3333 .0 .0 ];
10 %Probability of selecting pk route k={1,2,...,12} for model
      8b
11 %pk0 = [.05 .1167 .1167 .05 .05 .1167 .1166 .05 .05 .1167
      .1166 .05];
12 %Probability of selecting pk route k={1,2,...,12} for model
      8c
13 pk0 = [.025 .1416 .1417 .025 .025 .1417 .1416 .025 .025
      .1417 .1417 .025];
14 %Probability of selecting pk route k={1,2,...,12}
15 %rf0 = [2.7 2.7 2.7 1.1];
16 %Rate forward from Hiding Area 1 (rf0(1)), Hiding Area 2 (
      rf0(2)),...
17 %Hiding Area 3 (rf0(3)) and Operating Area (rf0(4))
18 %rf0 = [0.0 3.7 3.7 0.0]; %Block/Turn
```

```matlab
19 %rf0 = [0.0 5.0 0.0 0.0]; %Block/Turn
20 rf0 = [0.7 3.7 3.7 0.7]; %Disrupt
21 ps0 = [0.0 0.0 0.0 0.0 0.0 0.0]; % sensor probability of
     detection
22
23          %  ph_s = rb/(rf+rb), po_0 = rf/(rf+rb)rf
24          %x0 =[ rb/(rf+rb) rf/(rf+rb)]; % reset the initial
               condition
25 tfinal=5.0;
26 [t,x]=ode45(@(t,x) gm8c(t,x,rf0,pk0,ps0),[0 tfinal],x0);
27 clf;
28 figure(1)
29 plot(t,x(:,1),'r', t,x(:,2),'b',t,x(:,3),'g',t,x(:,4),'m','
     linewidth',2)
30 hold on
31 plot(t,x(:,1),'r+', t,x(:,2),'b^',t,x(:,3),'g*',t,x(:,4),'m
     --')
32 title(['Results for Three Hiding Areas, One Operating Area,'
     ...
33     'Twelve Routes, One Sensor Placed on Each Route: rf1= '
         ...
34     , num2str(rf0(1)), ' rf2 = ', num2str(rf0(2)),' rf3 = '
         ,...
35   num2str(rf0(3)),' rf4 = ',num2str(rf0(4)),' Ph1 = ',...
36   num2str(x0(1)),' Ph2 = ', num2str(x0(2)),' Ph3 = ',...
37   num2str(x0(3)),' Po = ', num2str(x0(4))])
38 xlabel('Time')
39 ylabel('Probability')
40 legend('Ph1','Ph2','Ph3','Po')
41 set(gca,'fontsize',14)
42 %% Model 8 Cumulative Probability of Detection
43 figure(2)
44 p_nd = x(:,1)+x(:,2)+x(:,3)+x(:,4); % escape or non-
```

```matlab
                detection probability
45  plot(t,1-p_nd,'r','linewidth',2)
46  hold on
47  plot(t,1-p_nd,'rs')
48  title(['Results for Three Hiding Areas, One Operating Area,'
        ...
49      'Twelve Routes, One Sensor Placed on Each Route: rf1= '
            ...
50      , num2str(rf0(1)), ' rf2 = ', num2str(rf0(2)),' rf3 = '
            ,...
51      num2str(rf0(3)),' rf4 = ',num2str(rf0(4)),' Ph1 = ',...
52      num2str(x0(1)),' Ph2 = ', num2str(x0(2)),' Ph3 = ',...
53      num2str(x0(3)),' Po = ', num2str(x0(4))])
54  xlabel('Time')
55  ylabel('Probability of Detection')
56  set(gca,'fontsize',14)
57  %Want Results for t=1,2,3,4,5
58  t_desired=[1,2,3,4,5];
59  y_desired=spline(t,(1-p_nd),t_desired);
60  y_desired
61  %% Model 8 Numerical Solution Check
62  dh12b= rf0(2)*((pk0(5)*(1-ps0(5)))+(pk0(6)*(1-ps0(6))));
63  dh13b= rf0(3)*((pk0(11)*(1-ps0(5)))+(pk0(12)*(1-ps0(6))));
64  dh14b= rf0(4)*((pk0(1)*(1-ps0(1)))+(pk0(2)*(1-ps0(2))));
65  dh21b= rf0(1)*((pk0(5)*(1-ps0(5)))+(pk0(6)*(1-ps0(6))));
66  dh23b= rf0(3)*((pk0(7)*(1-ps0(1)))+(pk0(8)*(1-ps0(2))));
67  dh24b= rf0(4)*((pk0(3)*(1-ps0(3)))+(pk0(4)*(1-ps0(4))));
68  dh31b= rf0(1)*((pk0(11)*(1-ps0(5)))+(pk0(12)*(1-ps0(6))));
69  dh32b= rf0(2)*((pk0(7)*(1-ps0(1)))+(pk0(8)*(1-ps0(2))));
70  dh34b= rf0(4)*((pk0(9)*(1-ps0(3)))+(pk0(10)*(1-ps0(4))));
71  dh41b= rf0(1)*((pk0(1)*(1-ps0(1)))+(pk0(2)*(1-ps0(2))));
72  dh42b= rf0(2)*((pk0(5)*(1-ps0(5)))+(pk0(6)*(1-ps0(6))));
73  dh43b= rf0(3)*((pk0(9)*(1-ps0(3)))+(pk0(10)*(1-ps0(4))));
```

```matlab
74
75  A= [(-rf0(1)) (dh12b) (dh13b) (dh14b);
76      (dh21b) (-rf0(2)) (dh23b) (dh24b);
77      (dh31b) (dh32b) (-rf0(3)) (dh34b);
78      (dh41b) (dh42b) (dh43b) (-rf0(4))];
79
80  [V,D]= eig(A)
81  %V are the Eigenvectors   Columns V(1), V(2)...
82  %D are the Eigenvalues or Lambda
83
84  c0=V\x0'
85
86  tn=t
87
88  poph=c0(1).*V(1:4).*exp(D(1,1)*t)+c0(2).*V(5:8).*exp(D(2,2)*
        t)+...
89      c0(3).*V(9:12).*exp(D(3,3)*t)+c0(4)*t.*V(13:16).*exp(D
          (4,4)*t);
90  plot(t,1-poph(:,1)-poph(:,2)-poph(:,3)-poph(:,4),'bs')
91  hold on
92  plot(t,1-p_nd,'r+')
93  title(['Comparison of ODE45 and Numerical Solutions for'...
94      'Three Hiding Areas, One Operating Area, Twelve Routes,'
          ...
95      'One Sensor Placed on Each Route: rfh1 = ', num2str(rf0
          (1)),...
96      'rfh2 = ', num2str(rf0(2)),'rfh3 = ', num2str(rf0(3)),'
          rfo = ',...
97      num2str(rf0(4)) 'Ph1 = ', num2str(x0(1)),'Ph2 = ',
          num2str(x0(2))...
98      ,'Ph3 = ', num2str(x0(3)),'and Po = ', num2str(x0(4))])
99  legend('Numerical Solution','ODE45 Solution')
100 xlabel('Time')
```

```
101 ylabel ( ' Probability of Detection ' )
102 hold off
```

A.2   Subterranean Survey

A.2.1   Survey Questions

Name of Interviewee: US Army Branch:

When and where did your unit deploy to an urban environment?

How did your unit plan to enter and/or operate in an urban environment?

What doctrinal process(es) did your unit follow during Urban Operations?

During your unit operational deployment, did adversaries ever utilize subterranean voids (tunnels, pipes, transportation lines...etc.) to evade the US military pursuit? If so, when, where and how were they used.

Did your unit use Unattended Ground sensors (UGs)? UGs are sensors able to detect movement, sound, light, and magnetic signatures. . . etc. If so, please describe when, where and how they were used.

Did your unit train for subsurface/subterranean operations? If so, what doctrinal guide did your unit use?

A.2.2   Survey Responses

Name of Interviewee: Not Applicable

US Army Branch:

Response 1: Engineer

Response 2: Infantry

Response 3: Armor

Response 4: Engineer

When and where did your unit deploy to an urban environment?

Response 1: The 1st Infantry Division (1ID) staff served as the Combined Joint Force Land Component Command-Iraq (CJFLCC-I) during Operation Inherent Resolve (OIR) in 2015. We operated out of bases in Baghdad, Iraq.

Response 2: 2017-2018, 2ABCT/1CD deployed to the ROK, including some urban and some rural areas

Response 3: As a Division Plans Officer, deployed to Bosnia (June 1998 to Dec 98). As a battalion operations officer deployed to Kosovo from June 2000 to Dec 2000. As a Squadron Commander, deployed to OIF I (APR 2003 – March 2004) and OIF III Feb 2005 – Mar 2006).

Response 4: 2003-2004, Kirkuk, Iraq, 2005-2006, Kandahar, Afghanistan, 2011-2012, Farah, Afghanistan

How did your unit plan to enter and/or operate in an urban environment?

Response 1: It was a division level staff, so we did not conduct urban operations per se, but we were facilitating Build Partner Capacity (BPC) sites to train Iraqi units to conduct urban operations against Daesh fighters, to recapture Iraqi cities being held by them.

Response 2: We had to plan for both air assault/movement as well as mechanized (IFV) movement.

Response 3: ? Initially, entry into the urban environment, was forced entry. Once units began rotations into assigned zones, TTPs changed based on the location and time period of deployments. In operating in urban terrain, dismounted troops with support from armored platforms conducted area security operations to stabilize and improve living conditions of the population. In some cases, forces are positioned within the population to improve access and enhance security.

Response 4: In 2003, and 2005 we would try to operate at night as much as possible to limit the potential of interaction with unintended people and traffic. Our unit would typically use available MGRS maps, and recent significant activity reports to develop areas of interest where we would take extra precautions.

What doctrinal process(es) did your unit follow during Urban Operations?

Response 1: We were training Iraqi engineer units the principles of SOSRA (Suppress, Obscure, Secure, Reduce, Assault) to breach through the many obstacles that Daesh fighters had emplaced. The infantry units leading the BPC site training were instructing the Iraqi soldiers in room clearing techniques.

Response 2: TLPs, but mostly we did urban ops and the very initially published sub-T ops. We fleshed out a lot of TLPs that we used on our own, with some cooperation with AWG.

Response 3: We relied on aspects of FM 2.0 to conduct IPB; FM 5-0 for planning, and FM 3-0 for operational references.

Response 4: At the time, the doctrine for operating in urban terrain was the Infantry Battle Drills. "Enter and Clear a Room" or building. We would establish support by fire positions at intersections around city blocks to prevent targets from escaping. Then, one or two squads would enter and clear the block.

During your unit operational deployment, did adversaries ever utilize subterranean voids (tunnels, pipes, transportation lines...etc.) to evade the US military pursuit? If so, when, where and how were they used.

Response 1: Yes, Daesh fighters used tunnels to avoid our Intelligence, Surveillance, and Reconnaissance assets. Tunnels may have been used to bypass Iraqi fortifications to attack Iraqi Forward Operating Bases (FOBs).

Response 2: We didn't have "adversaries," per se, but when my platoons played OPFOR, we used all kinds of terrain.

Response 3: I know that culverts were used to hide contraband and move across major roads. Sub terrain was also used to store munitions, weapons and devices. Although I did not see any evidence of tunnels, I often worried about them as a means of penetrating operating bases and outposts – like the tunneling that occurred on Bagram Air Base.

Response 4: They did, In Farah Afghanistan, there were large wadi systems. Insurgents would enter the wadis to escape, sometimes on motorcycles. They would also emplace IEDs to slow our pursuit. In another instance, [my unit] chased two insurgents into a cave

complex in a mountain where they escaped. [My unit] was unable to follow them due to my equipment, and the height of the drop into the cave. My team leader used a rope to lower us into the cave, but they were long gone by the time we were able to secure and enter. Also, occasionally, snipers would make small holes in walls that we called "murder holes" to take shots at us while we moved around.

Did your unit use Unattended Ground sensors (UGs)? UGs are sensors able to detect movement, sound, light, and magnetic signatures... etc. If so, please describe when, where and how they were used.

Response 1: Our unit was not conducting Urban Operations directly but was training the Iraqi units to do so. I don't believe the Iraqi units were equipped with UGs.

Response 2: We did not use UGS.

Response 3: The Air Force dropped a series of UGs along the Syrian Iraq border in 2005 to record movements across the border via seismic measurements.

Response 4: We used ground-penetrating radar to detect objects placed in roads and buildings. Occasionally, we would place wires and grates over entrances. This would allow us to detect disturbances.

Did your unit train for subsurface/subterranean operations? If so, what doctrinal guide did your unit use?

Response 1: Not to my knowledge. There was a concern of Daesh fighters tunneling under the walls of US FOB's but I was not aware of any assets committed to counter this other than pushing the campaign forward and recapturing territory from Daesh. Daesh was known to use explosive booby traps in territory it was about to lose, so Iraqi units may have avoided tunnels as much as possible because of the deliberate Explosive Ordnance Disposal (EOD) efforts needed to clear them.

Response 2: We had drafts of the SubT doctrine, but primarily we used urban ops manuals with close attention to CBRNE stuff, etc.

Response 3: No subterranean training.

Response 4: In preparation for deployment, my unit trained in a man-made cave complex at JMRC, in Hoenfels Germany. Our training included entering and clearing the cave complex similar to shoot house training. The cave complex did not have a roof so that observers could critique our operation.

List of References

[1] P. J. R. Joshua S. Bowes, Mark T. Newdigate and D. D. Tindoll, "The enemy below: Preparing ground forces for subterranean warfare," M.S. thesis, Naval Postgraduate School, Monterey, California, 2013.

[2] M. Fredenburg, "The mother of all moab articles," *National Review*, May 16 2017. Available: https://www.nationalreview.com/2017/05/moab-mother-all-bombs-afghanistan-use-analysis/

[3] M. Janaszek-Seydiltz. (2008). Warsaw Sewers. [Online]. Available: http://www.sppw1944.org/powstanie/kanaly_eng.html. Translated by Jolanta Siestrzewitowska.

[4] J. Rossman. (1994). In the Warsaw Sewers. *Zeszyty Historyczne*. [Online]. Available: http://www.warsawuprising.com/paper/warsaw_sewers.htm. Translated by Łukasz Nogalski.

[5] M. Cox, "Army is spending half a billion to train soldiers to fight underground," *Military.com*, June 24 2018. Available: https://www.military.com/daily-news/2018/06/24/army-spending-half-billion-train-troops-fight-underground.html

[6] D. Richemond-Barak, *Underground Warfare*. New York, NY: Oxford University Press, 2018, ch. 7, sec. II, pp. 209–249.

[7] D. Richemond-Barak, *Underground Warfare*. New York, NY: Oxford University Press, 2018, ch. 4, sec. II, pp. 1–117.

[8] D. N. Farrell and D. M. Ward, "U.S. Army TRADOC G-2 mad scientist megacities and dense urban areas initiative: Data collection and analysis," Mitre, Hampton, Virginia, Tech. Rep. MP160330, 2016.

[9] G. G. et al., "Reimagining the character of urban operations for the U.S. Army: How the past can inform the present and future," Rand Corporation, Santa Monica, California, Tech. Rep. RR-1602-A, 2017.

[10] J. Spencer. (2019, February). My Underground Warfare Wish List. [Online]. Available: https://mwi.usma.edu/underground-warfare-wish-list/

[11] T. Smith, "The subterranean battlefield: Warfare is going underground, into dark, tight spaces," *Army Times*, March 4 2019.

[12] M. S. et al., "Sensor integration study for a shallow tunnel detection system," Sandia National Laboratories, Albuquerque, New Mexico, Tech. Rep. SAND2010-0901, 2010.

[13] H. Wang and H. Zhou. (2015, July). Searching for a Target Traveling between a Hiding Area and an Operating Area over Multiple Route. *American Journal of Operations Research*. [Online]. *5*(4). pp. 258–273.

[14] *Small Unit Training in Subterranean Environments*, Training Circular 3-21.50, U.S. Dept. of the Army, Washington, DC, 2017, '.

[15] *Subterranean Operations*, ATP 3-21.51, U.S. Dept. of the Army, Washington, DC, 2019, '.

[16] *Urban Operations*, ATP 3-06, U.S. Dept. of the Army, Washington, DC, 2017, 5-30–5-55.

[17] *Combined Arms Countermobility Operations*, ATP 3-90.8, U.S. Dept. of the Army, Washington, DC, 2017, 5-30–5-55.

[18] MATLAB, *version 9.6.0.1072779 (R2019a)*. Natick, Massachusetts: The MathWorks Inc., 2019.

[19] C. of Monterey, "City of monterey sewer system management plan," City of Monterey, Tech. Rep., November 2005, updated April 2018.

[20] *Command and Staff Organization and Operations*, FM 6-0, U.S. Dept. of the Army, Washington, DC, 2014, 9-103 Table 9-2 'Historical minimum planning ratios'.

[21] J. W. Roginski, "The distance centrality: Measuring structural disruption in a network," Ph.D. dissertation, Naval Postgraduate School, Monterey, CA, 2018.

Initial Distribution List

1. Defense Technical Information Center
   Ft. Belvoir, Virginia

2. Dudley Knox Library
   Naval Postgraduate School
   Monterey, California